UNIVERSITÀ DEGLI STUDI DI TRIESTE

XXVIII CICLO DEL DOTTORATO DI RICERCA IN

Scuola di Dottorato in Scienze e Tecnologie Chimiche e Farmaceutiche

INNOVATIVE ANTIBACTERIAL SYSTEMS FOR ORTHOPEDIC AND TRAUMATOLOGY APPLICATIONS

Settore scientifico-disciplinare: CHIM/09

DOTTORANDO
NOME COGNOME

Ph.D. student
Samuel Golob

COORDINATORE
PROF. NOME COGNOME

Coordinator/Director
Prof. Mauro Stener

SUPERVISORE DI TESI
PROF. NOME COGNOME

Thesis Supervisor
Prof. Dario Voinovich

ANNO ACCADEMICO 2014 / 2015

INDEX

ABSTRACT

Infections of orthopaedic prosthesis joints develop in *ca.* 2% of the total joint procedures. Although this is therefore not a frequent problem, when it does occur, it represents a devastating complication for the healthcare system, and more importantly, for the patient. Prosthesis joint infections result in at least one, and often all, of the following postoperative situations for the patient: multiple operations; multiway prolonged antibiotic therapies; extended disability; bad clinical outcome; and in the worst-case scenario, amputation of the limb. Moreover, this represents a tremendous economic risk that in the following decades will become unsustainable due to the almost exponential increases in medical costs.

As conventional antibiotic approaches have been shown not to be adequate for prevention and cure of this particular typology of infection, this PhD project on 'innovative antibacterial systems for orthopaedic and traumatology applications was initiated. This arose through a collaboration between the University of Trieste and Lima Corporate, a world-leading Italian prosthesis company. Thus, the principal aim of this PhD project was to design, create and test an alternative strategy to reduce prosthesis joint infections, with both preventive and curative purposes.

This innovative strategy was designed around the concept of a local biphasic antibiotic delivery system, comprising a thermosensitive hydrogel phase and a microparticle phase, with both being loaded with a model active antibiotic (vancomycin). The hydrogel phase was chosen as a Poloxamer polymer solution, while the microparticle phase was made from a poly-lactic-co-glycolic acid polymer that was processed using spray drying and solvent evaporation technologies. The properties of this mechanical biphasic system were defined through rheological investigations.

Further measures of the release of the active pharmaceutical agent were carried out using *in-vitro* dissolution kinetics, with *in-vitro* microbiological tests performed to demonstrate the antibacterial activity. To determine the feasibility of the technological transfer, the antibiotic release was defined through a mathematical model. Moreover, the model presented here provides a suitable numerical law orientated towards modifications of the variables of the main aspects, such as the molar fraction of the poloxamer in the hydrogel, and the mean dimensions of the microparticles, to be able to modulate the antibiotic release.

The proposed local release system shows adequate release of the active pharmaceutical agent compared to its reference minimal inhibitory concentration, and potent growth inhibition of the main bacterial strains that are commonly involved in prosthesis joint infections, with both investigated *in vitro*. With the aim to also bring the proposed biphasic system to the final pharma-formulations process, an appropriate system for this application has been individuated. This is a double-chamber syringe that can maintain the two phases of the system separated.

In conclusion, the proposed biphasic system has now been successfully tested *in vitro* against prosthesis infections, with a view to its preventive and curative purposes. Further studies are now being undertaken to demonstrate its functionality and tolerability *in vivo*.

RIASSUNTO

Le infezioni peri-protesiche a seguito di interventi chirurgici si sviluppano in circa il 2% delle procedure ortopediche totali. Pur manifestandosi come una complicanza a frequenza bassa, quando presente, risulta essere notevolmente onerosa per i Servizi Sanitari in termini di costi e, soprattutto, per i pazienti stessi. Negli ammalati che presentano infezione peri-protesiche, sono sempre presenti situazioni postintervento, quali: necessità di nuove procedure chirurgiche all'arto, terapia antibiotica multipla attraverso diverse vie di somministrazione, disabilità prolungata, riabilitazione motoria scarsamente efficace, e nei casi limite amputazione dell'arto interessato. Negli anni a venire, la problematica inerente le infezioni, potrebbe essere aggravata dall'aumentato fabbisogno di operazioni ortopediche, imputabili quest'ultime a una maggiore aspettativa di vita, con il conseguente aumento dei costi di gestione.

Considerando che la terapia convenzionale, con la somministrazione di antibiotici, si è dimostrata nettamente insufficiente nella prevenzione e cura delle infezioni peri protesiche, la presenti tesi di dottorato: "Innovative antibacterial systems for orthopedic and traumatology applications" è stata proposta quale metodo alternativo o complementare alla cura antibiotica. Tale progetto prende forma dalla collaborazione tra l'Università di Trieste e la Lima Corporate, azienda italiana fra i leader mondiali nella produzione di protesi ortopediche.

I principali obbiettivi della tesi di dottorato, si sono indirizzati alla progettazione ed alla creazione di una strategia innovativa, capace di risolvere le gravi infezioni peri protesiche curandole e, soprattutto, prevenendole. La strategia individuata è stata quella del rilascio locale di antibiotico (vancomicina) attraverso il suo caricamento, in un sistema bifasico basato su un idrogel termosensibile con micro particelle disperse all'interno, rispettivamente in tutte le due fasi del sistema. L'idrogel era costituito da una soluzione di polimero Poloxamer mentre le micro particelle erano formate da acido poli-lattico-co-glicolico, processato secondo diverse tecnologie come lo *spray drying* ed l'evaporazione del solvente. Le caratteristiche meccaniche del suddetto sistema sono state individuate tramite prove reologiche, successivamente testate con test dissolutivi, per verificare la cinetica di rilascio dell'antibiotico. Infine con esami microbiologici, *in vitro*, si è cercato di appurare l'efficacia antibatterica.

Al fine di verificare la fattibilità, su scala industriale, per il trasferimento tecnologico del sistema studiato, il fenomeno di rilascio è stato razionalizzato postulando un modello

matematico. Grazie a tale modello è stato inoltre possibile ottenere, una legge numerica utile alla descrizione delle variabili del sistema, quali: frazione molare di Poloxamer nel idrogel e classe dimensionale media delle micro-particelle e l'influenza che quest'ultime esercitano sul rilascio del principio attivo.

Nell'ottica di portare il sistema bifasico a livello di formulazione tecnologica finale, è stato individuato un metodo di applicazione sulla superfice protesica, per mezzo di una siringa a doppia camera, capace quest'ultima, di tenere separati le due fasi del sistema. In conclusione si può stabilire che il sistema, *in vitro*, possa essere utile nella cure e prevenzioni delle infezioni peri-protesiche e che ulteriori studi *in vivo* saranno necessari al fine di dimostrare funzionalità e tollerabilità del sistema.

COMMITTEE

Coordinator

Prof. Mauro Stener, Department of Chemistry, University of Trieste, Italy

Supervisor

Prof. Dario Voinovich, Department of Chemical and Pharmaceutical Sciences, University of Trieste, Italy

Reviewers

Prof. Jelena Filipović-Grčić, Department of Pharmaceutical Technology, University of Zagreb, Croatia

Prof. Iztok Grabnar, Faculty of Pharmacy, University of Ljubljana, Slovenia

Commission

Prof. Cynthia Ebert, Department of Chemical and Pharmaceutical Sciences, University of Trieste, Italy

Prof. Martin Albrecht, Department for Chemistry and Biochemistry, University of Berna, Switzerland

Prof. Sabrina Castellano, Department of Medicine and Surgery, University of Salerno, Italy

CONTENTS

LIST OF FIGURES

Figure 40. Representative scanning electron microscopy images of the microparticles obtained by spray drying (A) and by solvent evaporation (B).

Figure 41. Temperature sweep test of the Poloxamer 20% (w/w) solutions with the starting and finishing gelling processes highlighted (n = 3).

Figure 42. Variation of the sol–gel temperature as a function of the concentration of the Poloxamer polymer (n = 3).

Figure 43. Trends of G' according to the various Poloxamer concentrations (n = 3).

Figure 44. Time sweep function performed for the 20% (w/w) Poloxamer hydrogel matrix (n = 3).

Figure 45. Stress sweep test of the 20% (w/w) Poloxamer hydrogel matrix (n = 3).

Figure 46. Profiles for the G' modulus of the 20% (w/w) Poloxamer water solution (red), 0,9% NaCl solution (grey), and 0,9% NaCl with $NaHCO_3$ solution (black), according to temperature (n = 3).

Figure 47. Temperature sweep for the G' and G' modulus profiles of 20% (w/w) Poloxamer solution (red) and the autoclaved 20% (w/w) Poloxamer solution (green) (n = 3).

Figure 48. The G' and G" profiles for 20% (w/w) Poloxamer loaded with 1% (w/w) vancomycin according to temperature for the temperature-sweep protocol (n = 3).

Figure 49. The G' and G" profiles for 20% (w/w) Poloxamer loaded with 1% (w/v) vancomycin according to time for the time-sweep protocol (n = 3).

Figure 50. The G' and G" profiles for 20% (w/w) Poloxamer loaded with 2% (w/v) vancomycin plotted according to temperature for the temperature-sweep protocol (n = 3).

Figure 51. The G' and G" profiles for 20% (w/w) Poloxamer loaded with 2% (w/v) vancomycin according to time for the time-sweep protocol (n = 3).

Figure 52. Stress sweep protocol at 37 °C for 20% (w/w) Poloxamer with 1% vancomycin (n = 3).

Figure 53. Stress sweep protocol at 37 °C for 20% (w/w) Poloxamer with 2% vancomycin (n = 3).

Figure 54. G' and G" profiles of the different vancomycin formulations according to temperature (n = 3).

Figure 55. G' and G" profiles of the different vancomycin formulations according to time (n = 3).

Figure 56. G' and G" as functions of the 20% (w/w) Poloxamer hydrogel matrix with

microparticles of PLGA according to temperature during temperature sweep experiments (n = 3).

Figure 57. G' and G" as functions of 20% (w/w) Poloxamer hydrogel matrix with the 1% dispersion of microparticles according to time during temperature sweep experiments (n = 3).

Figure 58. Stress sweep protocol at 37 °C for 20% (w/w) Poloxamer hydrogel matrix with the PLGA microparticles (n = 3).

Figure 59. Release profile (over 24 h) of vancomycin HCl from the 20% (w/w) Poloxamer hydrogel matrix (n = 3, SD <4%).

Figure 60. *In-vitro* release profiles (over 24 h) of vancomycin from the 20% (w/w) Poloxamer hydrogel matrix (n = 3, SD <4%). This demonstrates complete release of the vancomycin HCl within the first 24 h.

Figure 61. Release profile of vancomycin HCl from the microparticles system for batches A1-A6 (n = 3).

Figure 62. Vancomycin HCl release profiles from batch A4 (spray dried), batch A5 (spray dried) and batch A6 (solvent evaporated) over 7 days (n = 3).

Figure 63. Release profile for vancomycin from batch A5 microparticles, from batch A5 microparticles in the 20% (w/w) Poloxamer hydrogel matrix, and from batch A5 microparticles in the 20% (w/w) Poloxamer hydrogel matrix loaded with 1% vancomycine HCl (n = 3).

Figure 64. Representative images of the inhibition effects after incubation at 37 °C overnight. P_A, P_B, 20% (w/w) Poloxamer; V_{S1}, V_{S2}, reference vancomycin HCl 30 μg; V_{1A}, V_{1B}, and V_{2A}, V_{2B}, 20% (w/w) Poloxamer loaded with vancomycin HCl (245 μg, 490 μg. respectively).

Figure 65. Representative plates showing the diameter of inhibition of System A.

Figure 66. Representative plates showinng the diameter of inhibition of System B.

Figure 67. Comparison between the API release kinetics as the mathematical best fit to the model *versus* the experimental data from an API buffer solution, to determine the D_M.

Figure 68. Comparison between the API release kinetics as the mathematical best fit to the model *versus* the experimental data from an API containing Poloxamer hydrogel, to determine the D_G.

Figure 69. Comparison between the API release kinetics as the mathematical best fit to the model *versus* the experimental data as the API from the PLGA microparticles loaded into the hydrogel to determinate the D_P.

LIST OF TABLES

CHAPTER 1:
INTRODUCTION

1.1. JOINT ANATOMY

Joints are commonly referred to as articulation points or arthroses, and they represent the location at which two or more bones are connected. Bone is a structure that is exquisitely adapted to resist stress, support the body, and provide leverage for movement. Bone is vascular, mineralized, connective tissue, and it comprises cells and extracellular matrix. It is mainly composed of organic materials, such as collagen fibres, and inorganic salts that are rich in calcium hydroxyapatite and phosphate. The connection points for bones, i.e., the joints, are projected to allow movement and force transmission between the diverse bones, with the exception of the skull and the sacral, sternal and pelvic bones; although these are anatomically considered as joints, they are not mobile. Generally, joints provide mechanical support during movement, which allows the locomotion of living vertebrate organisms[1]. The joints are classified in many ways, according to their structure and functions. The structure and tissue configuration of a joint will define its properties, which includes its mobility, strength and stability. Joints can be classified by the type of tissue present. Using this method of classification, we can split the joints of the body into fibrous, cartilaginous and synovial joints[1], as follows:

1. Fibrous joints: A fibrous joint is where the bones concerned are bound by tough, fibrous tissue; these are strength joints.

2. Cartilaginous joints: In cartilaginous joints, the bones are attached by diverse types of cartilage. These can be split into primary and secondary cartilaginous joints.

3. Synovial joints: A synovial joint is a joint that is filled with synovial fluid. These joints tend to be fully moveable (known as diarthroses), and they are the main type of joint throughout the body. They can allow a huge range of movements, which are defined by the arrangement of their surfaces and the supporting ligaments and muscles.

It is commonplace to classify synovial joints according to their movement. Indeed, joints can also be classified by whether they undergo large movements, or little movements, or no

movement at all. According to this mobility classification, the joints can be divide into[1]:

1. Synarthrosis: Joints that allow no mobility. Most synarthrosis joints are fibrous joints, such as the skull sutures.

2. Amphiarthrosis: Joints that allow minor mobility. Most amphiarthrosis joints are cartilaginous joints, such as the intervertebral discs.

3. Diarthrosis: Joints that are greatly mobile. All diarthrosis joints are synovial joints too, such as the shoulders, hips, elbows, and knees. The terms 'diarthrosis joint' and 'synovial joint' are considered equivalent.

This Introduction mainly focusses on an understanding of the joint structure, and associated diseases and surgical remedies concerning this last typology of joints, the diarthrosis/ synovial joints. For this purpose, to highlights the most important concepts regarding the overall theme of this class of joints, the hip joint will always be used as an example. This choice is mainly due to its enormous importance for human motion, and because over the last few decades the hip joint has gained the attention of the medical field for the tremendous economic impact of the surgical procedures involved, an impact that is affecting the Health Systems all around the world[2]. The hip represents the largest human joint, and it is subjected to a wide variety of stresses, and for this reason, premature failure of this joint is a common risk.

The hip region is located lateral and anterior to the gluteal region, inferior to the iliac crest, and overlying the greater trochanter of the femur. In adults, three of the bones of the *pelvis* have fused into the hip bone, which forms part of the hip region. The hip joint is anatomically referred to as the acetabulofemoral joint, and its primary function is to support the weight of the body in static, standing and dynamic (i.e., walking, running) postures. The hip joints are the most important part for maintenance of the balance of the lower part of the body, which is considered to be the *pelvis* to the lower limb. The hip joint has a commonly defined ball-and-socket joint structure.

The bones of the hip are the femur and the *pelvis*. The top end of the femur is shaped like a ball. This ball is known as the femoral head. The femoral head fits into a round socket on the side of the *pelvis*. This socket is called the *acetabulum*. The femoral head is attached to the rest of the femur by a short section of bone known as the femoral neck. A large bump juts outwards from the top of the femur, next to the femoral neck. This bump is known as the greater *trochanter*, and it can be felt along the side of the hip. Large and important muscles connect to the greater *trochanter*. One of these muscles is the *gluteus medius*, which is a key muscle for keeping the *pelvis* level while walking. This arrangement gives the hip the large amount of motion that makes this joint so important for human locomotion (Figure 1).

Articular cartilage is the material that covers the ends of the bones of any joint, and it is about 6 mm thick in the large, weight-bearing joints like the hip. Articular cartilage is white and

shiny. and it has a rubbery consistency. It is slippery, which allows the joint surfaces to slide against one another without causing any damage. Normal articular cartilage performs two functions:

1. Along with the synovial fluid, it provides virtually friction free movement within the joint;

2. In weight-bearing joints, such as the hip, it spreads the load across the joint surface in a manner that allows the underlying bones to absorb shocks and the body weight.

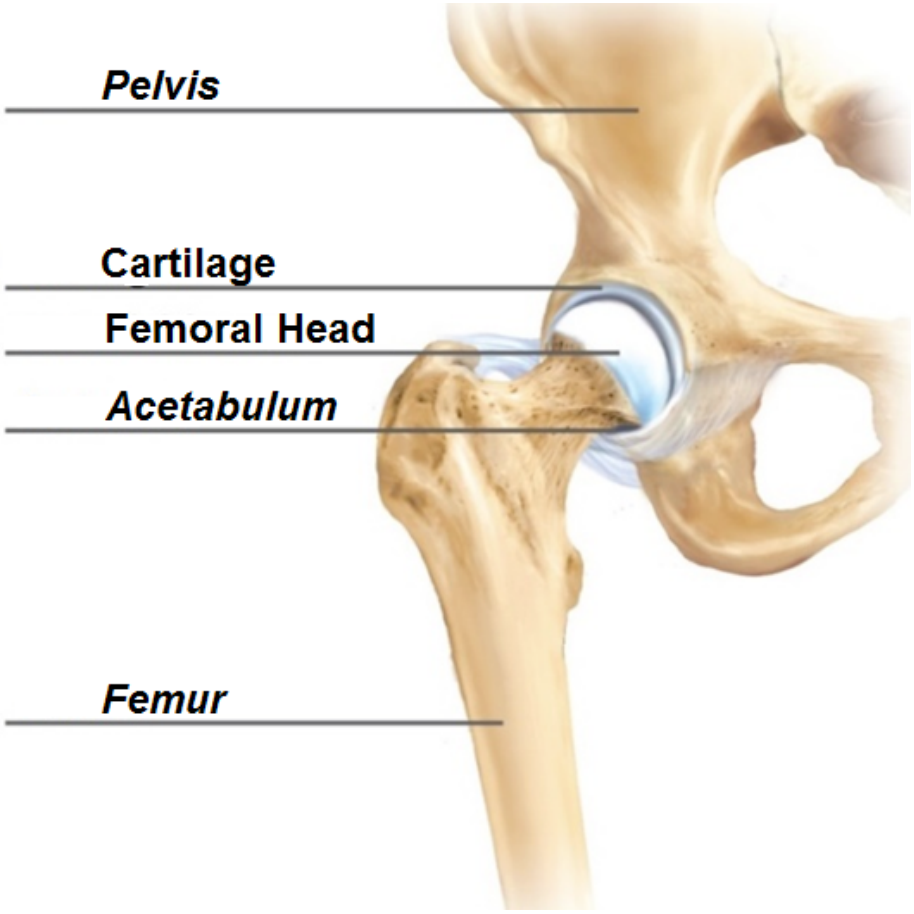

Figure 1. *Schematic representation of the hip joint.*

These functions require the cartilage to be elastic and to have tensile strength. These attributes are provided by proteoglycans and type II collagen, respectively, both of which produced by chondrocytes. There is articular cartilage essentially everywhere that two bony surfaces move against one another, or *articulate*. In the hip, the articular cartilage covers the end of the femur and the socket portion of the *acetabulum* in the *pelvis*. The cartilage is especially thick in the back part of the socket, as this is where most of the force occurs during walking and running.

Another important structure in joints are the ligaments in the hip, which are soft tissue structures that connect bone to bone and help to hold the hip in place. A joint capsule is a watertight sac that surrounds a joint. For the hip, the joint capsule is formed by a group of three strong ligaments that connect the femoral head to the *acetabulum*. These ligaments are the main source of stability for the hip. A small ligament connects the very tip of the femoral head to the *acetabulum*. This ligament is known as the *ligamentum* teres, and it does not have any role in controlling hip movement like the main hip ligaments do. It does, however, have a small artery within the ligament that brings a very small blood supply to part of the femoral head. A special type of ligament forms a unique structure inside the hip, known as the *labrum*. The *labrum* is attached almost completely around the edge of the *acetabulum*. The shape and the way the *labrum* is attached create a deeper cup for the *acetabulum* socket. This small rim of cartilage can be injured and cause pain and clicking in the hip.

As well as the ligaments, another important fascial structure is the tendons. The function of tendons is primary to attach the muscles to their respective bone. A long tendon band runs alongside the femur from the hip to the knee. This is the *iliotibial* band, and it provides a connecting point for several of the hip muscles. A tight iliotibial band can cause hip and knee problems.

To complete the description of the joint and muscle skeletal system, the hip is surrounded by thick muscles. The *gluteals* make up the muscles of the buttocks, on the back of the hip. The inner thigh is formed by the *adductor* muscles. The main action of the adductors is to pull one leg inwards towards the other leg. The muscles that flex the hip are in front of the hip joint. These include the *iliopsoas* muscle. This deep muscle begins in the low back and *pelvis*, and connects to the inside edge of the upper femur. Another large hip flexor is the *rectus femoris*. The *rectus femoris* is one of the quadriceps muscles, the largest group of muscles on the front of the thigh. Smaller muscles going from the *pelvis* to the hip help to stabilise and rotate the hip. Finally, the hamstring muscles run down the back of the thigh, starting from the bottom of the *pelvis*. As the hamstrings cross the back of the hip joint on their way to the knee, they help to extend the hip, pulling it backwards.

There are nerves and blood vessels that send impulses and a nutrient supply to the hip. All of the nerves that travel down the thigh pass by the hip. The main nerves are the femoral nerve at the front, and the sciatic nerve at the back of the hip. A smaller nerve, known as the obturator nerve, also goes to the hip.

These nerves carry the signals from the brain to the muscles that move the hip. The nerves also carry signals back to the brain about sensations, such as touch, pain and temperature. Travelling along with the nerves, there are the large blood vessels that supply the lower limb with blood. The large femoral artery begins deep within the *pelvis*. It passes across the front of the hip area and goes down towards the inner edge of the knee. The femoral artery has a

deep branch, known as the *profunda femoris* (profunda means deep). The *profunda femoris* has two vessels that branch off it and pass through the hip joint capsule. These vessels are the main blood supply for the femoral head. As mentioned earlier, the *ligamentum* teres contains a small blood vessel that provides a very small supply of blood to the top of the femoral head.

Where friction occurs between muscles, tendons and bones, there is usually a structure called a *bursa*. A *bursa* is a thin sac of tissue that contains fluid to lubricate the area and to reduce friction. A *bursa* that sometimes causes problems in the hip is sandwiched between the bump on the outer hip (the greater *trochanter*) and the muscles and tendons that cross over the bump. This *bursa* is known as the greater *trochanteric bursa*, and it can get irritated if the iliotibial band (see above) is tight. Another *bursa* sits between the *iliopsoas* muscle and where it passes in front of the hip joint. A third *bursa* lies over the ischial tuberosity, the bump of bone in the buttocks that is used to sit on[1].

It is easy to understand that a complex system built up of muscles, tendons, ligaments, nerves, blood vessels, cartilage and bones that are all meant to work together. The friction production, the forces created, and the absorption that takes place between these causes a wide spectra of stress to the hip joint. Indeed, due to its fundamental position in the human body for the creation of movement, and due to all of these stresses that can occur during the development of movement, the hip is one of the most susceptible joints to a wide variety of pathologies and disease, especially considering elderly and obese patients[3].

1.2. JOINT DEGENERATIVE PROCESSES

The joints are subjected to a wide variety of disorders, including degeneration, infection, immune-response injury, metabolic degeneration, and neoplasms. Herein, the most common form of arthritis will be discussed (Figure 2); namely osteoarthritis, or degenerative joint disorder.

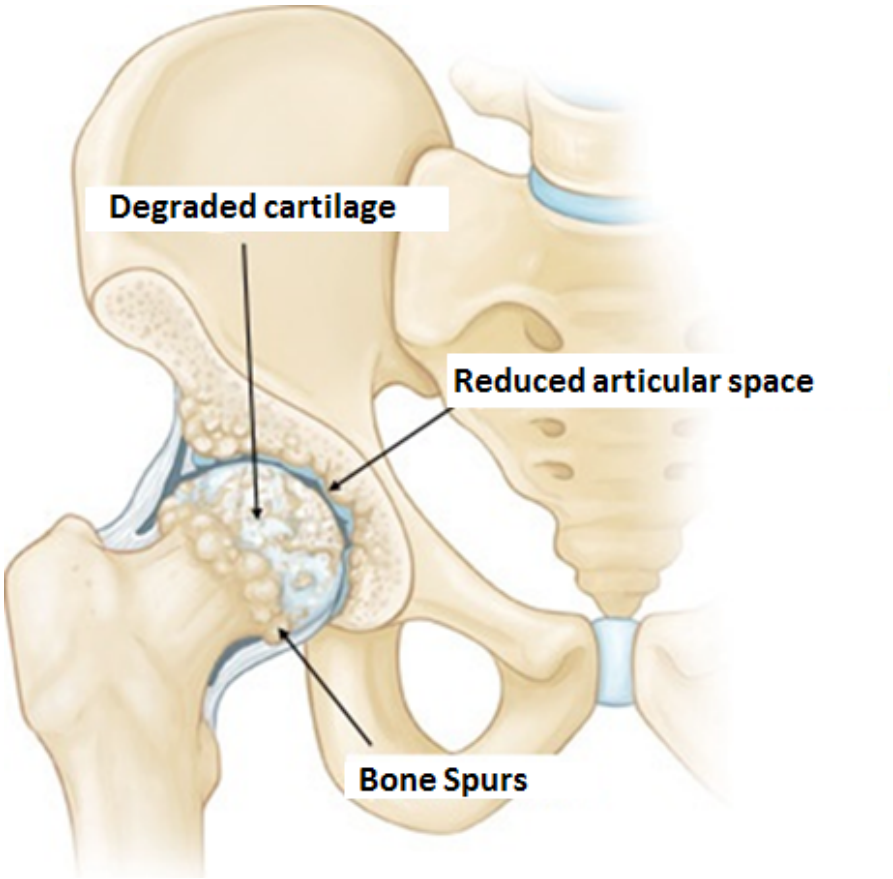

Figure 2. *Schematic representation of the hip osteoarthritic process, with the damaged cartilage and the formation of bone spurs that form in response to biomechanical signals.*

Osteoarthritis, or degenerative joint disorder, is the most common joint disorder. The US Centers for Disease Control and Prevention estimated that in 2005 more than 48 million Americans were suffering from chronic hip osteoarthrosis pain. Osteoarthritis is a frequent, if not inevitable, part of ageing, and is an important cause of physical disability in people older than 65 years of age[4].

The fundamental feature of osteoarthritis is degeneration of the articular cartilage. The associated structural changes in the underlying bone appear to be secondary effects. Although osteoarthritis implies an inflammatory disease, osteoarthritis is primarily a degenerative disorder of the articular cartilage in which the chondrocytes respond to the biomechanical and biological stresses in a way that results in the breakdown of the matrix. In most cases, osteoarthritis appears insidiously with age, and without apparent initiating cause (i.e., primary osteoarthritis). In such cases, the disease is usually *oligoarticular*, i.e., it affects only a few joints, with those of the hands, knees, hips and spine most commonly affected. In unusual circumstances (i.e., <5% of cases), osteoarthritis can strikes in youth, where there is typically some predisposing condition, such as previous trauma or developmental deformity, or an underlying systemic disease, such as obesity. In these settings, the disease is known as secondary osteoarthritis, and this can often involve one or several predisposed joints. Gender has some influence on the patterns of osteoarthritis, as the knees and hands are more commonly affected in women, while the hips are more commonly affected in men.

As can be seen in Figure 2, the changes that take place in osteoarthritis include alterations in the composition and structure of the cartilage matrix. Chondrocytes have limited capacity to proliferate, and some divide to form small colonies of cells that secrete newly synthesised matrix. Subsequently, vertical and horizontal fibrillation and cracking of the matrix can occur, as the superficial layers of the cartilage are degraded. This early stage condition is known as *chondreomalacia*. Small fractures can dislodge pieces of cartilage and subchondral bone into a joint, to form loose bodies. In response to these, the immune system produces inflammation, which in long term leads to chronic inflammation and joint pain.

There are a few more typologies of osteoarthritis, such as rheumatoid arthritis, systemic, chronic inflammatory autoimmune disease, juvenile rheumatoid arthritis, and infection arthritis, where microorganisms of any type can lodge in joints during haematogenous dissemination, to cause an infection.

Even if these cited types of arthritis show diverse pathogenesis, this essentially causes similar clinical outcomes, with inflammation and chronic pain causing limitation, or in the worst case, complete loss of motion capacity for that joint[5].

As previously indicated, considering the importance of the hip joints for human posture and movement, when late stage hip osteoarthritis occurs, there is the absolute need to find an alternative. The medical and scientific technological achievements of our days are incredible, but to date, there is no cure for osteoarthrosis. A large variety of treatments are available to manage symptoms, such as:

1. Physical activity: One of the most beneficial ways to manage osteoarthrosis is to get moving. Indeed, this is considered an important part of the treatment plan. Studies

have shown that simple activities can reduce the pain and help to maintain a healthy weight. Strengthening exercises build muscles around osteoarthrosis-affected joints, which eases the burden on these joints and reduces the pain. Aerobic exercise helps to improve vascularisation, and thus oxygenation, of the joints[6].

2. Weight management: Excess weight adds additional stress to the weight-bearing joints, such as the hips, knees, feet and back. Losing weight can help people with osteoarthrosis by reducing the pain and limiting further joint damage[6].

3. Stretching: Daily stretching of joints can improve flexibility, lessen stiffness, and reduce pain, and thus improve the elasticity of the various fibres surrounding the joints.

4. Pharmaceutical treatments: Non-steroidal anti-inflammatory drugs (NSAIDs) are widely used to relieve pain in musculoskeletal tissues, although their use can come at the cost of toxicity, with 2% to 4% annual incidence of serious gastrointestinal ulcers and complications, an incidence that is 4-fold higher than in NSAIDs non-users. NSAIDs have been applied topically for decades. This route possibly reduces gastrointestinal adverse reactions by maximising local delivery and minimising the systemic toxicity. Some experimental evidence supports this, but for large joints such as the hip, blood-borne delivery might be the predominant mechanism for actions on the deep tissues[7].

5. Assistive devices: Assistive devices can help with function and mobility when osteoarthritis occurs in an elderly patient. These include items such as scooters, canes, walkers, splints and shoe orthotics, and also helpful tools, such as jar openers, long-handled shoe horns, and steering wheel grips.

6. Surgery: Joint surgery can repair or replace severely damaged joints, especially hips and knees. When conservative treatments have not helped and the pharmacology treatments have failed, replacement surgery might be the only option, especially if the arthritis associated pain interferes with daily activities. Arthritis damage is the most common reason for the need for joint replacement, and the hip is one of the most frequent joint involved. Surgical hip replacement and repair is also known as *total hip arthroplasty* (THA) and *hip arthroplasty* respectively.

1.3. MUSCULOSKELETAL PROCEDURES: JOINT REPLACEMENT

Trauma, back pain, and as described above, osteoarthritis, are the three most common musculoskeletal conditions. The rate of musculoskeletal diseases is greater than that of circulatory diseases and respiratory diseases, which affect about one in three people, with the majority reporting relatively easily treatable conditions, such as chronic hypertension or hay fever and bronchitis[8]. Osteoarthritis on the other hand causes pain and dysfunction that impact on health-related quality of life, and it is reflected in substantial use of health-care resources, and the associated costs. When conservative treatments fail to alleviate hip and knee joint dysfunction associated with high levels of pain and caused by arthritis, joint replacement, or *joint arthroplasty*, is an elective surgical option that can provide significant pain relief and improved function. This improves the health-related quality of life, and it thus also represents a life-altering 'cure.'

Primary and secondary osteoarthritis account for the largest proportions of total joint arthroplasties (TJAs) performed. In excess of 326,136 THAs and 693,420 total knee arthroplasties (TKAs) are performed annually in the USA (Table 1). Joint arthroplasty procedures for hips and knees are the most common form, but arthroplasties have been expanding to other joint sites over the past few years. Joint arthroplasties represent one of the fastest growing procedures in the USA. As surgery for TJAs has evolved and the population has aged, the rates of TJAs have steadily increased[8].

Table 1. *Total hip arthroplasties and total knee arthroplasties performed annually in the USA* (2013)[8].

Arthroplasty procedure	Males		Females		Total number of procedures
	Number of procedures	% Total procedures	Number of procedures	% Total procedures	
All hip replacements	222,974	36.9	290,579	63.1	512,553
Total hip replacements	149,868	46.0	176,268	54.0	326,136
Revision hip replacements	22,276	46.9	25,229	53.1	47,505
All knee replacements	279,393	36.9	477,906	63.1	757,299
Total knee replacements	261,584	37.7	431,836	70.8	65,177
Revision knee replacements	19,005	29.2	46,172	70.8	65,177

Total joint arthroplasties are effective interventions, with low mortality rates and few severe adverse outcomes. In-hospital death rates are less than 1% for TJAs[9]. The risk factors for mortality following TKA include older age, primary arthroplasty, as compared to revision arthroplasty, use of cement, pre-existing cardiopulmonary disease, and simultaneous bilateral TKAs. The risk factors for mortality following THA include older age, men, patients with lower socioeconomic status, comorbid conditions, and patients with osteonecrosis[9].

Benefits towards joint pain and functional status following THA and TKA are known within the orthopaedic literature (Figure 3). The recovery usually occurs within the first few weeks after surgery, with the largest benefits seen within the first 3 to 6 months. Patients with THAs report important pain relief within a week after surgery[10]. However, a significant number of patients still report marked pain at 3 months from surgery. Functional gains are typically seen later than pain relief, with larger gains reported for THA than TKA. Patients often report dysfunction during the initial recovery phase, with functional improvement seen over the subacute phase of recovery[11].

In the future, the need for TJAs is projected to increase in frequency, which will be caused primary by the ageing of the population. In particular, by 2030, and only considering the USA, the demand for primary THA is estimated to grow to 572,000 procedures, while the demand for primary TKA is projected to grow to 3.48 million procedures[12]. Considering those numbers, THAs and TKAs are going to become extremely frequent surgical operations, and for this reason, any complications and risk associated with these surgeries will become more important.

1.4. TOTAL HIP ARTROPLASTY: HISTORY AND TYPOLOGY

Total hip arthroplasty is considered to be one of the most successful orthopaedic interventions of the last 100 years[13]. The earliest hip replacement was recorded in Germany in 1891, where Professor Themistocles Glück presented the use of ivory to replace the femoral heads of patients whose hip joints had been destroyed by tuberculosis.

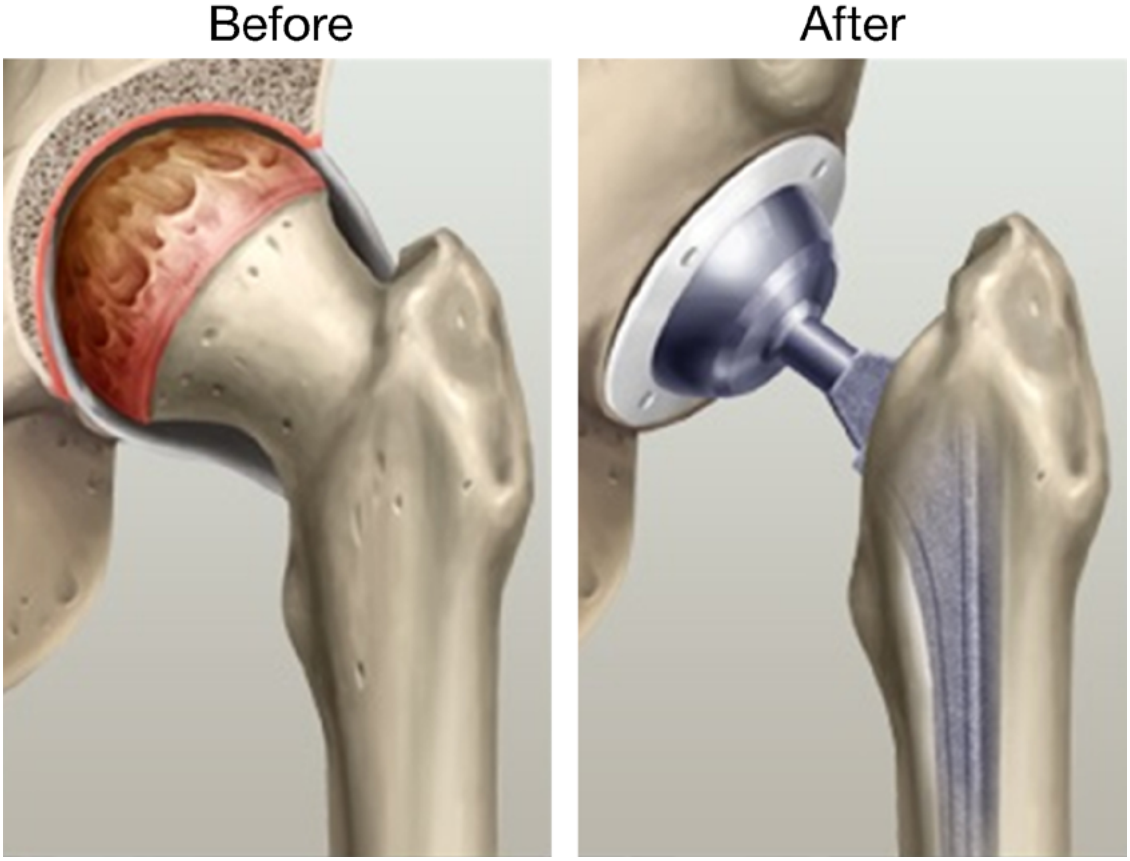

Figure 3. *Schematic representation of the joint situation before (left) and after (right) total hip arthroplasty.*

The first use of a metal-on-metal prosthesis was for an English surgeon, Dr. George McKee. In 1953, he began by using the modified Thompson stem (a cemented hemiarthroplasty used for treatment of fractures of the neck of the femur) with a new one-piece cobalt-chrome socket as the new acetabulum. However, it is the orthopaedic surgeon Sir John Charnley who has to be considered the father of modern THA. The low friction implant arthroplasty that he designed in the early 1960‘s is identical, in principle, to the prostheses used today. It consisted

of three parts: a metal femoral stem; a polyethylene acetabular component; and acrylic bone cement, which was borrowed from dentists. It could also be considered the first modern cemented hip replacement.

There are now three different implants typologies (Figure 4) that are installed according to two different techniques[13].

The implants are classified as follows (Figure 4):

1. Metal-on-polyethylene (MoP) implants;
2. Metal-on-metal (MoM) implants;
3. Ceramic-on-ceramic (CoM) implants.

While the two techniques are (Figure 5):

1. Cementless prosthesis installation;
2. Cemented prosthesis installation.

Figure 4. *The three different hip implant typologies.*

To use one or the other of the installation techniques, the implant itself has to be predisposed for that particular technique. For example, cementless implants have rough surfaces and trabecular structures that allow and promote bone growth inside the structure (i.e., osteointegration), while cemented implants have smooth surfaces that need to be fixed with cement (Figure 5).

Figure 5. *A cementable implant (A) and a cementless implant (B).*

1.4.1. METAL-ON-POLYETHYLENE IMPLANTS

Metal-on-polyethylene implants (Figure 4) are the most widely used and rigorously followed-up of all prostheses. MoP implants became famous due to the early success of the Charnley prosthesis in the 1970's, when they almost completely displaced all of the other bearing surfaces. The main concern with MoP prostheses is debris from the polyethylene part, which can create prosthetic osteolysis through the release of cytokines and proteolytic enzymes, which leads to implant failure[14]. Debris can be minimised through irradiation of polyethylene with gamma particles, which greatly improves the wear resistance of the material. However, implant failures have led to renewed interest in MoM bearings.

1.4.2. METAL-ON-METAL IMPLANTS

Metal-on-metal implants (Figure 4) are at present undergoing a revival after previously falling out of favour in the 1970's, when concerns were raised relating to the potential for the bearings to generate metal ions, which had a theoretical carcinogenic risk, as well as being associated with hypersensitivity reactions and prosthesis loosening. It is now thought that the cause of this aseptic loosening in the first-generation MoM models was due to poor design and improper implantation technique, rather than the MoM bearings themselves.

1.4.3. CERAMIC-ON-CERAMIC IMPLANTS

Ceramic-on-ceramic implants were first introduced by the French surgeon Pierre Boutin in

1970, and half of the THAs in central Europe use these ceramic heads (Figure 4), although there is much lower use in the UK and the USA. The benefits of CoC bearings are their high level of hardness and their scratch resistance, and the inert nature of the debris compared to the MoM and MoP versions[15]. These prostheses create improved lubrication, and therefore have a lower coefficient of friction and show excellent wear resistance. CoC bearings are the best choice for implants in young, active patients, due to the reduced wear. However, the cost of ceramic implants is higher that their counterparts, and for this reason these bearings are used infrequently in the Orthopaedic Units of National Health Systems.

1.4.4. HYBRID HIP PROSTHESIS

There is one more typology of implants, and this is represented by the mix of the above-mentioned techniques: the hybrid hip prosthesis. A hybrid hip prosthesis is formed from a cemented femoral stem and acetabular cup fixed in place with cementless techniques. This is a good choice for young, active patients also, as it prevents pelvic bone loss while providing solid fixing and good usage.

1.4.5. CEMENTLESS/ CEMENTED TECHNIQUES

Cementing hip arthroplasties were first performed by Glück in 1891, using methacrylate bone cement to improve prosthetic fixing, but it was Charnley in the late 1950‘s that made this technique famous, who used cement taken from dentists. However, the cementing often failed, and so attention shifted to the development of cementless techniques.

Cementless techniques allow easier planning of hip revision surgery, particularly in younger patients, with greater preservation of bone tissue. Better short-to-medium-term clinical outcomes have been obtained for cemented over cementless techniques, with no radiological differences seen, although long-term comparisons are difficult to make due to the lack of large randomized controlled trials.

1.4.6. IMPLANT CHARACTERISTICS

The components of a hip implants are constant across every typology of the implants described, and they need to have the same characteristics[16], as follows:

1. They need to be biocompatible to be integrated within the human body with no immune responses;

2. They need to be resistant to corrosion and mechanical stress;

3. The need to have low friction between the various articular surfaces.

The components that comprise hip a plants are illustrated in Figure 6.

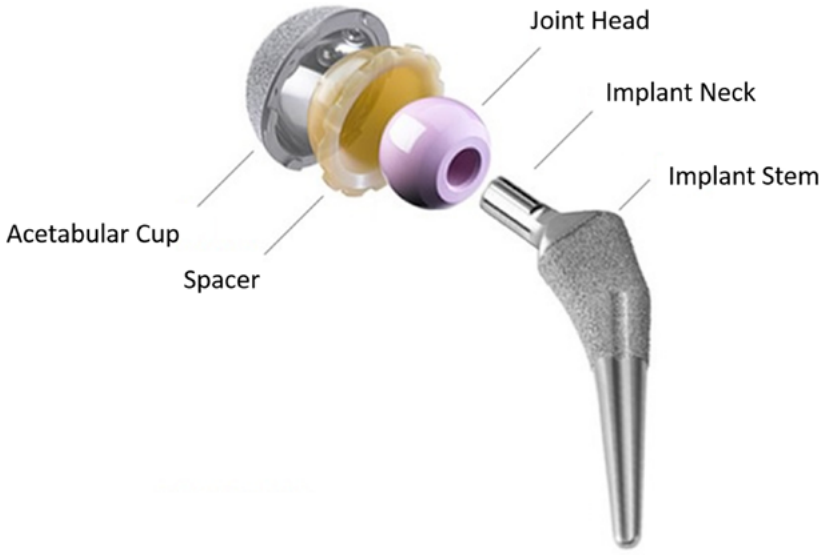

Figure 6. *The components of a hip implant.*

1.5. TOTAL HIP ARTHROPLASTY: SURGICAL PROCEDURES

Total hip arthroplasty is a relatively simple surgical procedure. Indeed, THA can be performed traditionally or by using what is considered as a minimally invasive technique. The main difference between these two procedures is the size of the incision. During standard THA, the patient is given general anaesthesia or spinal anaesthetic, and might be given help to prevent pain as an alternative.

The surgeon makes a cut along the side of the hip and moves the muscles connected to the top of the thighbone, to expose the hip joint. The ball portion of the joint is removed by cutting the thighbone with a saw Figure 7, 1). Then an artificial joint is attached to the thighbone. The surgeon then prepares the surface of the hipbone while removing any damaged cartilage, and attaches the replacement socket part to the hipbone (Figure 7, 2). The new ball part of the thighbone is then inserted into the socket part of the hip (Figure 7, 3, 4). Finally the surgeon reattaches the muscles, and closes the incision.

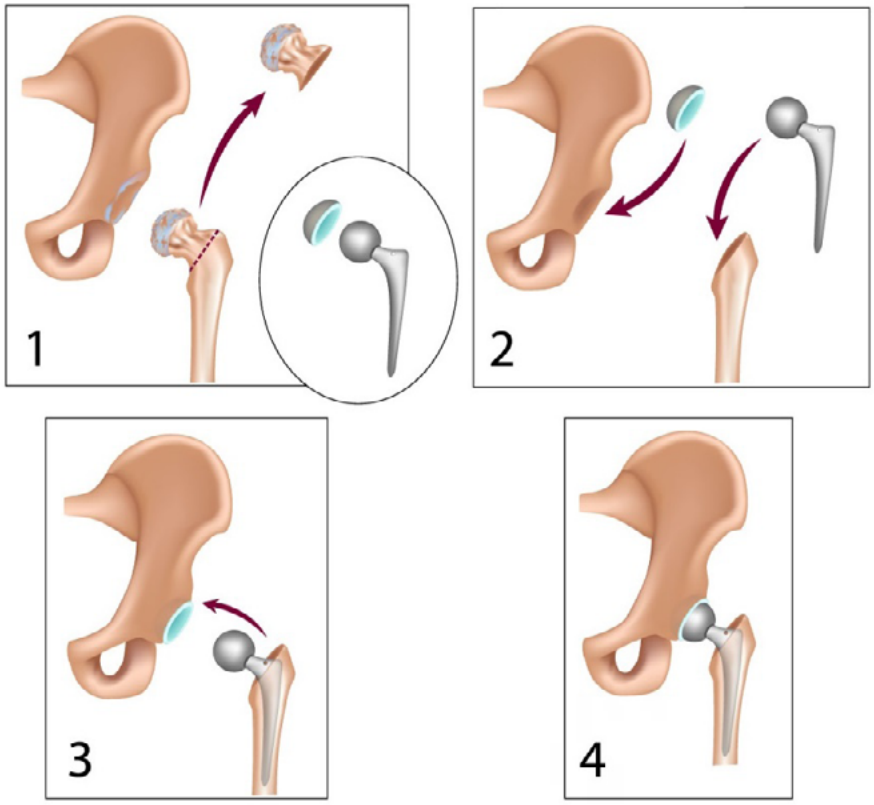

Figure 7. *Schematic representation of total hip arthroplasty.*

While most surgery for THA today is performed using the standard technique, with an 8 cm to 10 cm cut along the side of the hip, in recent years, some surgeons have been using a minimally invasive technique. In this minimally invasive approach, the surgeons make one or two cuts from 2 cm to 5 cm long. The same procedure can be performed through these small cuts as with the standard surgery for THA[17].

1.6. RISKS OF JOINT REPLACEMENT

As previously indicated, TJAs represent safe operations; however, as a major surgical procedure, patients who undergo arthroplasty are at risk of certain complications. Many of these complications can be avoided or successfully treated if they arise.

Most common risks are correlated to the arthroplasty procedures, and these include:

1. Blood clots: Blood clots in large veins of the leg and pelvis, or deep venous thrombosis, can occur after joint replacement. If a blood clot develops, it is possible for the clot to travel to the lungs and thus cause a pulmonary embolism, which is potentially fatal. This risk is present in every deep surgical procedure.

2. Stiffness and scarring: After surgery, the body's natural response is to make scar tissue. This is true both on the surface of your skin and deep inside the joint. If you develop scar tissue, the joint may become stiff and difficult. This risk is also present in every deep surgical procedure.

3. Implant loosening/ failure: Implants can wear out, and they can loosen, or the attachment of the arthroplasty prosthesis might fail. New materials have helped implants to last longer and to be integrated into the body better. This is more of a problem in younger patients, who live longer with the implant, and who typically place more demands on the artificial prosthesis. If the joint wears out, revision surgery can be performed. However, this issue is the first that strictly correlates with the implant itself, and it represents the most frequent problem associated with joint replacement[18].

4. Hip dislocation in THA: Dislocation of a hip replacement occurs when the ball is dislodged from the socket. This can occur for many reasons, but it often occurs after a fall.

5. Orthopaedic infections and prosthesis joint infections (PJIs): PJIs are the most devastating problem correlated with arthroplasty procedures. These infections are both challenging to diagnose and hard to manage, and thus they are associated with significant cost. Treatments against infections have become even more complicate, mainly because bacterial pathogens are becoming increasingly resistant to currently available antimicrobial chemotherapy drugs. Early diagnosis relies on laboratory, radiological, and microbiological findings. Consultation with both orthopaedic surgeons and infectious disease specialists is suggested for optimal management of these difficult infections. Surgical re-intervention, called revision, is often necessary to obtain the necessary cultures, to debride the infected area, and to remove the

prosthetic device. Antimicrobial therapies should be initiated after cultures are obtained, and prolonged courses of antibiotic therapy are often warranted[19].

1.7. THE RISKS OF PROSTHESIS JOINT INFECTION

The incidence of orthopaedic PJI has increased over the past decade, despite the large use of intravenous antibiotic prophylaxis and of aseptic surgical techniques[20]. Arthroplasty infections occur in 2% of primary arthroplasties and 3% to 5% of revisions[21]. As the demand for joint replacements increases with the aging of the population, the number of infections is projected to rise from 17,000 to 266,000 per year by 2030, with the number of arthroplasties due to exceed 3.8 million surgical procedures[13].

The treatment of this kind of infection is exceedingly difficult. Bacteria colonies, and especially *Staphylococcus aureus*, form a particular sort of shield, or biofilm, on implanted metallic/ plastic materials. The biofilm is as extracellular anionic polysaccharide covering that blocks the penetration of immune cells and antibiotics, which protects and promotes bacterial survival[22]. The forming of a biofilm represents a basic survival mechanism by which a bacterial colony resists external and internal environmental factors, such as antimicrobial agents and the host immune system[23]. These microorganisms can thus live clustered together in a highly hydrated extracellular matrix that is attached to the prosthetic surface. Depletion of metabolic substances or waste product accumulation in biofilms causes microbes to enter a slow or non-growing state[24]. Biofilm microorganisms, therefore, can be significantly more resistant to growth-dependent antimicrobials than their planktonic, free-living counterparts [25].

Within biofilms, microorganisms grow in organised and complex communities with structural and functional heterogeneities, which resemble multicellular organisms in which water channels serve as a rudimentary circulatory system. The release of cell-to-cell signalling molecules allows microorganisms in a biofilm to respond in concert by changing their gene expression in terms of biofilm differentiation. It is of fundamental importance to note that a mature biofilm can be formed within 6 h after of implantation of a prosthesis. After the mature biofilm is formed, the microorganism colonies are virtually invulnerable to typical oral antimicrobial therapies[26].

When biofilm-correlated infection becomes chronic, surgical removal of the entire prosthesis is necessary. The re-operation, or revision, can easily cause other complex-to-treat issues, such as re-infection, extended disability, and in general, worse clinical outcomes. In arthroplasty infections, the main bacteria involved is a staphylococcal species (Table 2) as well as virulent antibiotic-resistant strains, such as methicillin-resistant *S. aureus* (MRSA), which further complicates the eradication treatment[23].

Prosthesis joint infections can be divided in three subgroups:

1. Early infections: these occur within 3 months of the surgery;

2. Delayed infections: these occur from 3 to 12 months after the surgery;

3. Late infections: these occur after 12 months from the surgical operation.

Table 2. *The most common microorganisms involved in prosthetic joint infections.*

Microorganism	Frequency (%)
Staphylococcus aureus	47
Staphylococcus epidermidis	23
Gram-negative *bacillus*	10
Polymicrobic infections	20

It is commonly believed that the early and delayed infections can be correlated to the surgical procedure itself, while the late infections are most commonly due to a haematogenous spread[27]. For these specific kinds of infections, the common use of antibiotic treatments produces enormous economical expenditure for public health systems, both as *os* (oral administration) and *iv* (intravenous). These are also often not particularly effective. The diagnosis can also be challenging, as the symptoms are variable and the diagnostic tests are non-specific.

The pathogenesis of implant-associated infections involves interactions between the implant and the host (Figure 8).

Exogenous bodies, such as implants, remain devoid of any microcirculation, which is critical for host defences and the delivery of antibiotics. It the late 1800's, a definition of the microbial colonisation of newly introduced implants in an organism was proposed. The proposed concept was the "race for the surface" (Figure 9), whereby the host and bacterial cells compete in determining the ultimate fate of the implant[28]. Accordingly, when host cells colonise the implant surface first, the probability of attachment of bacterial cells is very low, and *vice versa*. This concept has stimulated technological and biomaterial progress while emphasizing the role of implant biocompatibility and tissue-integration.

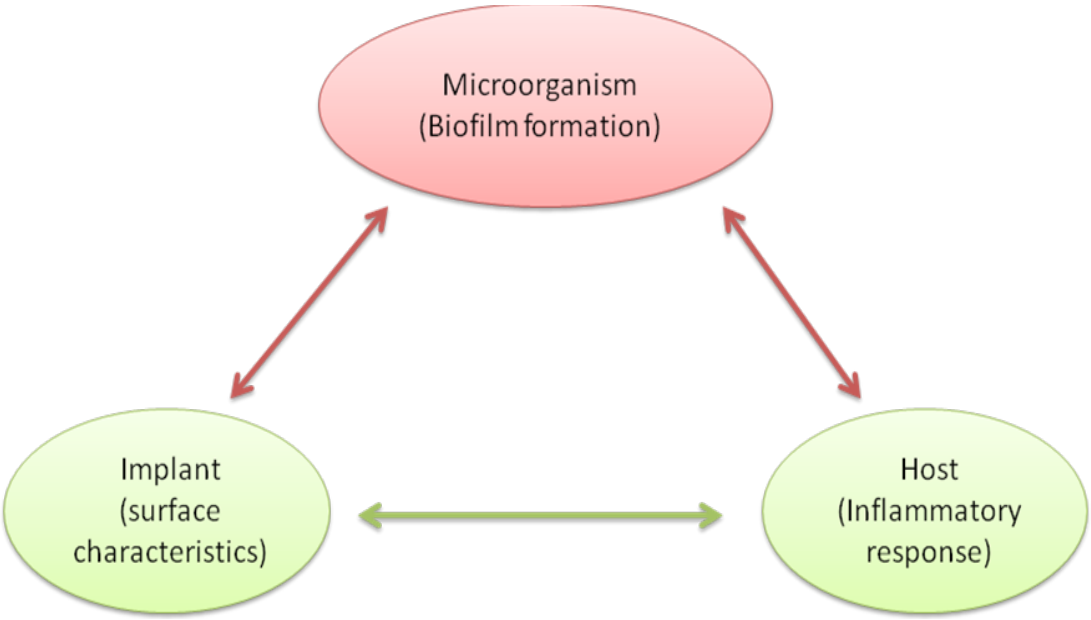

Figure 8. *Interactions between microorganisms, the implant, and the host in the pathogenesis of implant-associated infections.*

Currently, the gold standard technique in the USA to treat chronic arthroplasty infection is a two-stage revision procedure, which is divided into:

1. Surgical removal of all prosthetic components and bone cement, debridement of necrotic tissue, placing of antibiotic-impregnated material at the site of infection, administration of a 6-week course of intravenous antibiotics (during which time the patient is unable to bear weight on the affected limb).

2. Revision arthroplasty after the infection has cleared. In severe infections and refractory cases, arthrodesis, resection arthroplasty, and amputation can be necessary[29].

The treatment of arthroplasty infections involves extensive medical and surgical care and prolonged disability, and rehabilitation needed for the significantly worse outcomes[20]. In addition, these infections represent an enormous economic burden, due to the extra medical costs and resource use, as well as indirect costs through lost wages and productivity[20]. These medical costs alone can average €133,574, compared with €27,880 for an uncomplicated arthroplasty, which corresponds to an annual national healthcare burden of €7.97 billion by 2015 in the USA; similar numbers and levels can also be observed for European countries[2].

Based on the high cost of treatment for orthopaedic infections, it is important to point out the relevance of implementing measures to prevent and control PJIs.

1.8. BIOFILM FORMATION

Bacterial cells constitute the most successful living organism, and hence form of life, on Earth, in terms of their total numbers, their phylogenetic diversity, and the extent of the habitats that they have colonised. Bacteria exist in two main forms: free-floating planktonic, and as biofilms. Microbiologists have always focused on free-floating microorganisms grown in suspensions in a liquid growth medium. However, it is now generally known that the majority of microbial cells on Earth are living in spatially distinct communities, referred to as biofilms, Indeed, it has been estimated that 99% of all bacteria exist in biofilms, with only 1% living in the planktonic state, and that 65% of microbial infections are associated with biofilms[30].

Biofilms constitute microbial multicellular environments, and they are defined as organised communities of bacteria that collaborate with each other and are attached to an inert, as a prosthesis, or living surface. The entire bacterial community is contained in a self-produced polymeric matrix that is made in a great part of exopolysaccharides[31]. This matrix contains polysaccharides, proteins and DNA originating from the bacterial cells, and the bacterial colony can co-exist with further living species. Structural examination of biofilms has shown that their component micro-colonies are divided by ramifying the water channels that carry the bulk fluid into the community by convective flow[32]. This allows the bacterial cells to interact with each other and to establish metabolic cooperation. Biofilms can be formed by populations developed from a single species, or from a community made up of multiple bacterial species. The evolution and life advantages of forming biofilms include protection from the environment, nutrient availability, metabolic cooperation, and the acquisition of new genetic traits[32]. The association of bacteria in biofilms can thus be seen as a survival strategy, with the bacteria benefiting by acquiring nutrients and protection from antibacterial drugs. In cases of adverse conditions, such as desiccation, osmotic shock, or exposure to toxic compounds, or even to UV radiation, the microbial community as a whole can provide its own protection. Moreover, biofilms are also sites where genetic material is shared because of the proximity of the cells, and thus this is a way that the bacteria can easily acquire resistant mechanisms against antibacterial drugs[33].

The strategy of bacteria biofilm creation starts with their ability to adhere to all natural and synthetic surfaces, as included in prostheses. Bacterial cell membranes contain various types of adhesins for a wide range of synthetic material surfaces. Environmental and surface characteristics of a biomaterial, such as surface roughness, hydrophobicity, and electrostatic charge, have only conditional roles[34]. A reservoir of receptors for bacterial adhesive ligands that mediate the adhesion of free-floating bacteria to the surface of a biomaterial can offer a

conditional protein film that covers an implant immediately after its placement into the host[35].

Conceptually, the process of bacterial adhesion can be divided into two basic phases: reversible and irreversible (Figure 9)[36]. The reversible form is mechanically and biologically less stable than the irreversible.

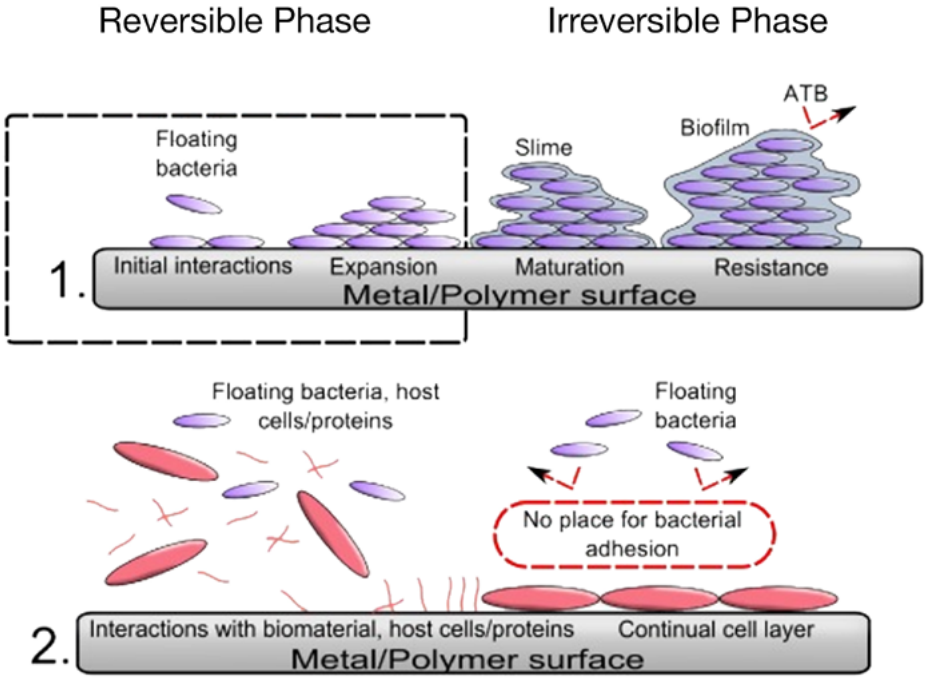

Figure 9. *Representation of the reversible/ irreversible formation phase (1) and the "race for the surface" of the bacterial biofilm (2) on a prosthesis surface*

The explanation here lies in part on the origin of non-specific interactions between implant surface characteristics and bacterial surface adhesins. The second phase is mediated by molecular and cellular interactions that are closely associated to expression of biofilm-specific gene clusters in reversibly attached bacteria. An adhesion phase is followed by gene expression for secretion of the protective 'slime'. This process makes the bacteria extremely resistant to both the host immune system and antibiotic diffusion. The transition between reversible and irreversible phases of biofilm formation coupled with phenotypical change is the last window of opportunity for clinically reasonable preventive measures.

Biofilms can act as physical diffusion barriers to exclude antibiotics from reaching their targets. Antibiotic drugs have been shown to penetrate these structures to reach the targets,

but their concentration within the biofilm did not reach the minimum inhibitory concentration (MIC) in some parts, due to the physical and/or chemical properties of the matrix, which resulted in an apparent increase in resistance. Indeed, recent mathematical modelling has predicted that while limited antibiotic diffusion can lead to the death of the outer layer of bacteria, it also stimulates subpopulations of bacteria buried deeper within the biofilm to enact adaptive changes, thereby countering the insult[37]. Decreased penetration and diffusion of antimicrobials through the biofilm matrix has been shown to influence biofilm survival in some cases. For example, at sub-MIC concentrations of β-lactam antibiotics, increased alginate synthesis in *Pseudomonas aeruginosa* biofilms was induced, and also an enhancement of the biofilm matrix of some slime-producing coagulase-negative staphylococci[33].

Free living bacteria are generally more susceptible to antibiotic treatments and to host defence mechanisms than those in a biofilm. Indeed, the MIC and the minimal bactericidal concentration of antibiotics to biofilm-growing bacteria can be up to 100–1000-fold higher than for planktonic bacteria, and they can be 150–3000-fold more resistant to disinfectants. Despite many efforts in research, very little is known about the molecular mechanisms of antibiotic resistance in biofilms[33]. Low nutrient concentrations and oxygen limitation inside biofilms might result in altered metabolic activity and lead to slow growth of the bacteria within the biofilm.

Inspection of environmental as well as *in-vitro* biofilms has revealed that oxygen levels can be high at the biofilm surface, but low in the centre of the biofilm, where anaerobic conditions might be present, which would result in slow or no growth. This is one of the explanations put forward for reduced susceptibility of biofilms to antibiotics[38]. Indeed, antibiotics are generally more effective in killing rapidly growing cells. For example, penicillin and ampicillin have an absolute requirement for cell growth to kill bacteria, with the mortality rate being proportional to the growth rate. Additionally, even though more advanced β-lactams, such as the cephalosporins, aminoglycosides and fluoroquinolones, can kill non-growing cells, they are distinctly more effective in killing rapidly dividing cells. On this basis, slow growth appears to contribute to biofilm resistance to the killing of the bacteria[33].In addition, slow growth is a major factor in increased resistance of stationary planktonic cells to being killed. Related to this, the existence of microenvironments that antagonise the actions of antibiotics (e.g., pH variations) and the degrading mechanisms that are active in some parts of biofilms might also have roles[33].

1.9. PROTHESIC JOINT INFECTIONS: CLINICAL MANIFESTATIONS AND DIAGNOSIS

As indicated above, the most frequent issue with joint replacements is the failure of the implantation that as known as 'implant loosening'. Such failure of the arthroplasty surgical procedure appears to occur mainly in two different manners:

1. Aseptic loosening: when the procedure failed without the presence of bacterial colonisation, and thus without infection;

2. Septic loosening: when there is bacterial infection in the surgical site.

The ability to distinguish between aseptic and septic failure of a prosthesis is a critical point for a better understanding of the treatments that have to be followed to restore the best patient condition. This is especially in the case of PJI, which in the majority of cases necessitates surgical strategies that aim to eradicate the infecting bacteria[39].

There are a few infection signs notable for clinical manifestations that can occur during one of the three infection periods after arthroplasties. As previously indicated, infections that occur within 1 to 3 months after implantation are classified as 'early', infections that occur from 3 to 12 months after implantation are classified as 'delayed', whereas those that occur 1 year after prosthesis implantation are classified as 'late'. The early and delayed types of infection are believed to be acquired most often during prosthesis implantation. Early and delayed infections will often show local signs of cellulitis, erythema, swelling, pain, drainage, and delayed wound healing, which might or might not be accompanied by systemic symptoms, such as fever and chills[40]. Late infection can occur many years after prosthesis implantation, and it typically presents with non-specific symptoms, such as chronic pain, without systemic symptoms, as well as the prosthesis loosening. These scenarios can be challenging to distinguish from aseptic loosening by patient history and physical examination.

Although any painful prosthesis can represent a PJI, the absence of an obvious mechanical reason for a painful prosthesis in the first few years following implantation should raise the suspicion of PJI. Late infections that occur >1 or 2 years after prosthesis implantation are due to haematogenous seeding of the prosthesis, or less likely, to late manifestation of an infection that was acquired during prosthesis insertion. Late infections are often characterised by acute septic arthritis syndrome, with sudden onset of pain concomitant with recent infection occurring elsewhere in the body (e.g., skin and soft tissue, respiratory tract, urinary tract infections) [41].

Nowadays, orthopaedic surgeons use a wide spectrum of diagnostic tests to rapidly and clearly diagnose PJI. In this setting, the Musculoskeletal Infection Society recently published a

definition of PJI[42] The intention here was to have a 'gold standard' definition for PJI that can be universally adopted by all physicians, surveillance authorities (including centres for disease control, medical and surgical journals, and the medicolegal community), and all involved in management of PJI.

Based on the Musculoskeletal Infection Society criteria taken into consideration, PJI can be diagnosed when:

1. There is a sinus tract communicating with the prosthesis; or

2. A pathogen is isolated by culture from at least two separate tissue or fluid samples obtained from the affected prosthetic joint; or

3. Four of the following six criteria are satisfied:

(I) Elevated serum erythrocyte sedimentation rate (ESR) and serum C-reactive protein (CRP) concentration;

(II) Elevated synovial leukocyte count;

(III) Elevated synovial neutrophil percentage (PMN%);

(IV) Presence of purulence in the affected joint;

(V) Isolation of a microorganism in one culture of peri-prosthetic tissue or fluid; or

(VI) Greater than five neutrophils per high-power field in five high-power fields observed from histologic analysis of peri-prosthetic tissue at 400x magnification.

However, PJI can be present even if fewer of these criteria are met, although not usually less than four.

The definition is based on the observed clinical data outcomes obtained from the following tests:

1. Local measures of synovial inflammation, synovial fluid white blood cell (WBC) count, and synovial tissue histology[43, 44];

2. Systemic measures of inflammation markers. The most important values to measure are serum CRP levels, ESR, and interleukin (IL)-6[45];

3. Radiographic tests, [46] as radiographs, bone scans, magnetic resonance imaging, computed tomography, positron emission tomography;

4. Bacterial isolation techniques, such as Gram staining for bacterial growth, cultures[47].

Moreover, there is clear evidence that there is a primitive, specific, innate immune response to

pathogens[48]. The recognition of pathogens by the innate immune system triggers a cascade of protective pathways in the host. Thus, not all of the patient immune systems react in the same way, and for this reason, not all of these the markers can be detected in each patient, even if there is PJI[49].

1.10. STANDARD TREATMENT STRATEGIES

As previously described, making a precise diagnosis of PJI is often a challenge in itself, and due to this, large efforts have been made to choose the optimal method to treat an infected joint. Currently, treatment for PJI can be divided in the surgical and non-surgical methods mostly depending on the health status of the patient. However, surgeons tend to use both of these strategies to minimise the re-infection risk. The different strategies available for the orthopaedic surgeon to manage PJI are as follows:

The surgical procedures can be divided into:

1. Irrigation and debridement (I&D);
2. One-stage revision (OSR);
3. Two-stage revision (TSR).

The non-surgical procedures can be divided into:

1. Oral antibiotic therapy (OAT);
2. Systemic antibiotic therapy (SAT);
3. Multiway antibiotic therapy (MAT).

In particular, the surgical procedures and then the non-surgical procedures are now explained in more detail.

1.10.1. IRRIGATION AND DEBRIDEMENT

Over the past few decades, I&D has been considered as the treatment of choice for PJI[50]. This strategy consists of a surgical procedure where the infected implant is cleaned and the infected area in the joint is treated with an irrigation of antibiotic and chemical biocide solutions. By undertaking I&D, the bacterial load in the joint can be diminished, and the patient morbidity minimised. More recently, it has been suggested that depending on timing of infection, symptoms, pathogenicity of the infecting organism, and immune status of the infected patient, I&D might not be the procedure of choice for all PJIs[51].

1.10.2. ONE-STAGE REVISION

Considering that the TSR strategy is the treatment of choice for PJI in the USA, many European hospitals have favoured the use of a single stage procedure, as the OSR. This has been

supported by indications of decreased morbidity, lower costs, and comparable outcomes. This choice is mostly due to the increasing importance of the burden on the health systems, and for this reason, OSR is undergoing renewed interest all over the world. This procedure consist in the complete removal of the infected implant and the installation of a new one, whereby the entire process takes place as a single surgical procedure[51].

1.10.3. TWO-STAGE REVISION

This represents the gold standard for PJI surgical treatment, and in North America, TSR is the treatment of choice for PJI of the hip and knee[52]. The major reason for considering TSR as the gold standard in PJI treatment is the superior success rates of this approach when compared to the other treatment strategies. Thus infection eradication using TSR is relatively high, as it can range from 85% to 100% for both the hip and knee joints. As the name suggests, the surgical TSR procedure is divided into two operation stages that are separated by a certain time period[51]. The first stage involves total resection of the foreign materials, debridement of the surrounding infected tissues, and placement of an antibiotic impregnated cement spacer. The second stage involves removal of the spacer, removal of any necrotic tissue, and placement of a new prosthetic implant, with a 4 week to 8 week course of IV antibiotics between these two stages[53]. TSR benefits are that the spacer allows increased joint stability, prevents soft tissue contraction, and facilitates the re-implantation procedures[54]. Moreover, the *in-situ* installed antibiotic cement allows high antibacterial activity locally at the site of PJI, and this also minimises potential systemic toxic effects caused by highly concentrated IV therapy[55].

1.10.4. NON-SURGICAL ANTIBIOTIC THERAPIES

While antibiotic therapies could be used during or following I&D, OSR and TSR, chronic antibiotic suppression alone can be reserved for those patients who are immune compromised or who have comorbidities that are too significant to undergo the required complicated and delicate surgical procedures. This is because the higher risk of (further) morbidity and mortality for these patients if they undergo surgery would be greater than from their PJI alone. However, there is a lack of literature that considers the treatment of PJI with chronic antibiotic suppression alone, and thus with no surgical intervention. Indeed, evidence from standardised clinical trials is lacking for surgeons to appropriately select patients who would do better with chronic antibiotic suppression rather than undergoing surgical procedures. However, in these high risk patients, antibiotic suppression can be a viable option[51]. Moreover, in the non-surgical procedures, the route of antibiotic administration as OAT, SAT or MAT will depend on infection rate, susceptibility of bacterial strains, pharmacodynamics characteristics of the selected antibiotic agent, and patient health status[56].

1.11. PROSTHESIS JOINT INFECTIONS: PREVENTION

There are numerous strategies that rely on decreased bacterial load and the creation of a bacteria-free environment around an implant during the perioperative period[38]. Here, there are two different general strategies: systemic antibiotic prevention therapies; and local antibiotic prophylaxis. Further to these, educational programmes aimed at educating orthopaedic surgeons in the perioperative strategies of PJI prevention are now improving the positive outcomes of this dangerous issue.

For the present PhD project, the attention was focussed here on the development of a local strategy, mainly due to the better results that can be obtained compared to the systemic strategies[33]. Herein, the state of the art of local systems for PJI prevention are reported (Figure 10). To act locally, there are a few possibilities. The design of a suitable local strategy could be applied to the prosthesis itself, and so coatings or surface modifications of a prosthesis need to be implemented[57].

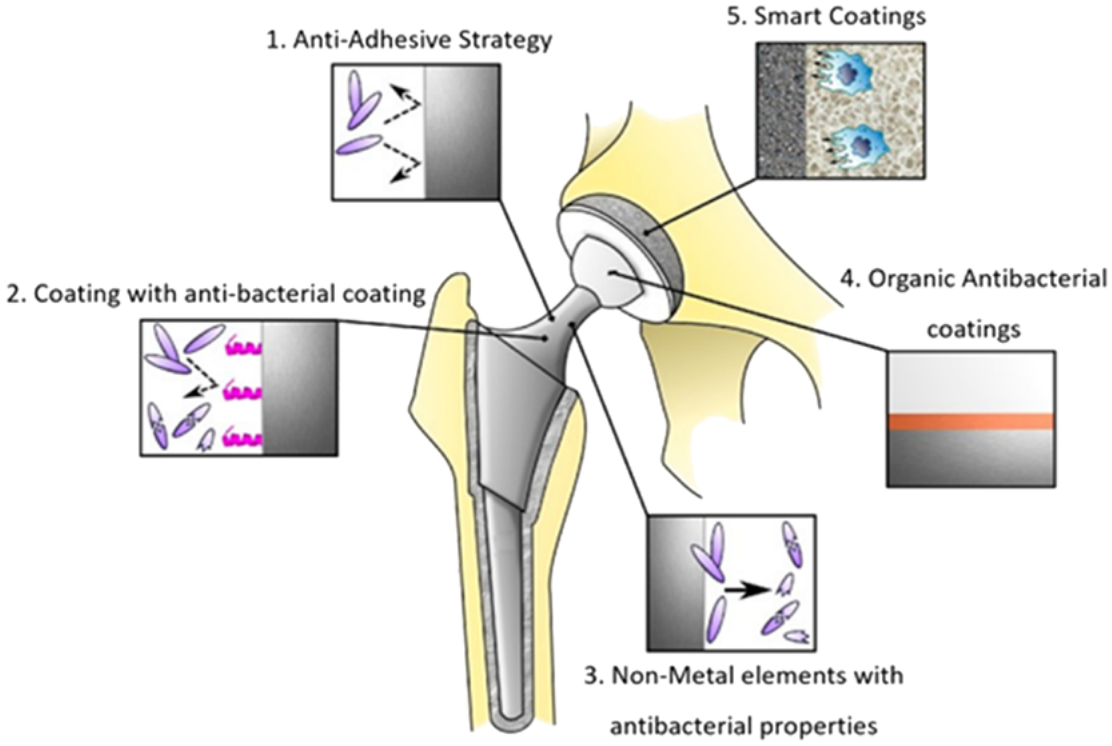

Figure 10. *Schematic representation of the local strategies in PJI prevention and eradication.*

On the other hand, for the prostheses that need to be cemented into the bone, antibiotic-loaded cement can be used. The cement used in this strategy is not, however, of a material that has been considered for use as a drug-delivery system, and thus their use in the majority of cases would be inadequate. In particular, these cements are usually formed of a polymethyl meta-acrylate polymer that was not designed for controlled release of a loaded drug, such as to supply an efficient drug profile over time[58].

Alternatively, changes could be made to the surface of the implant either by chemically or physically altering the surface layer of the existing biomaterial, for example by oxidation or mechanical modifications like roughening/ polishing/ texturing the implant. Such anti-infective surfaces can be classified as 'contact killing' and antimicrobial agent eluting. Another method implies coating the existing surface with a new layer of material/ biomaterial with a different composition and properties, such as a hydroxyapatite coating, antibiotics bound covalently to the implants, or the fixing of other antimicrobial compounds[59]. In terms of durability, we can distinguish between degradable and non-degradable biomaterial coatings.

1.11.1. AN ANTI-ADHESIVE STRATEGY

Implant surfaces can be treated in a manner so as to prevent the critical step of bacterial biofilm formation. Modification with hydrophilic, highly hydrated, and non-charged materials might be a suitable possibility. These modifications have been shown to prevent many bacterial species *in vitro* from implant adhesion, by limiting the contact between the bacterium and the potential surface placement sites[36]. However, host cells attachment can also be negatively affected by some surface treatments. Such strategies cannot be used in the setting of implants that requiring bone integrations, such as in cementless arthroplasty implants, because of potential inhibition of this process. Attention in recent years has been focused on hydrophobic and superhydrophobic surface treatment technologies and their antibacterial repellent effects[60].

Treating protein surfaces and/or protein-bacteria interactions might be a good strategy for inhibition of bacterial adhesion to implants[61]. Proteins such as albumin, fibronectin, fibrinogen, laminin, denatured collagens, and some plasma/ tissue lipids are the first host substances that interact with the surface structure of the biomaterial[62]. Reduction of the formation of the conditional lipid-protein layer can be achieved by changing the surface physicochemical characteristics, and/or the surface micro-morphology-

1.11.2. AN ANTI-BACTERIAL COATING

1.11.2.1. Metal elements with antibacterial properties

The antibacterial activities of the majority of metal coatings correlate with the ionic or nano forms, rather than with the bulk material. Despite extensive research, routine coating of implants with such a thin layer of metal is still not a standard approach. The main issues preventing wider use of such technologies are the cytotoxicity and the resultant decreased biocompatibility of the implant. Finally here, the risk of bacterial resistance to metallic coatings remains a concern, as a phenomenon that is common to all antibacterial strategies[63].

Silver is the prevalent metal used in biomedical applications as an anti-infective. Dissolved silver cations are biochemically active agents that interfere with the functions of the bacterial cell membrane. In addition, silver contributes to the formation of reactive oxygen species and other mechanisms that potentially influence prokaryotic cells. However, there have been issues about the toxicity of silver ions. Research efforts have focused on the development of silver coating technologies that reduce, or even eliminate, this toxicity, while maintaining constructive antibacterial effects[64].

Vanadium, aluminium, cobalt-chrome and titanium alloys are the most commonly used materials in TJA implants. Several technologies have been proposed to expand the antibacterial properties of these implants. The anti-infective potential of titanium dioxide layers has also been widely investigated, both alone and in combination with other substances[65, 66].

1.11.2.2. Non-metal elements with antibacterial properties

Hydrogen, chlorine, iodine and oxygen are commonly used in biomedicine for their anti-infective properties. They have not been indicated for antibacterial coating technologies in orthopaedic implants mainly due to their general softness and brittleness, and thus they are not adequate for orthopaedic applications. Selenium bound covalently onto the surface of titanium or titanium alloy implants prevented *S. aureus* and *Staphylococcus epidermidis* attachment without affecting osteoblast viability. Selenium also catalyses the formation of superoxide radicals, and subsequently inhibits bacterial adhesion and growth[67].

1.11.2.3. Organic antibacterial coatings

Studies have investigated the efficacy of surfaces coated with covalently linked antibiotics.

Such implants are limited to infections caused by bacteria that are sensitive to the specific antibiotic that has been coupled. In addition, strong forces, such as covalent binding, are not sensitive enough to react to weak external stimuli, to overcome these issues. Combinations of antibiotics with other compounds have also been proposed either alone or in association with a particular mechanism of controlled release[68, 69].

A new approach in the prevention of orthopaedic infection involves coating implants with antimicrobial peptides, cytokines, or other molecules that are critical for host responses to bacteria invasion. Like antibiotics, antimicrobial peptides work through the damage of the cell wall and the inhibition of key bacterial protein synthesis. Additionally, they have an influence on inflammation, tissue healing, and apoptotic events. Notably, resistance to antimicrobial peptides has been reported less frequently than to antibiotics[70].

Chitosan is a polycationic polymer that is derived from chitin and that shows antibacterial and antifungal activities. The exact mechanism(s) of action of chitosan remain unknown. Studies have suggested that macrophages are more effective when working on a chitosan surface. Derivatives of chitosan have recently been studied in relation to antibacterial uses in biomedicine. One such compound, quaternised chitosan, has shown strong antibacterial activities against both Gram-positive and Gram-negative bacteria. There is evidence that chitosan derivatives can be strongly attached to titanium alloys, and that they have a protective effect against some bacterial species, either alone or in combination with other antimicrobial substances, like antibiotics or antimicrobial peptides[71].

1.11.2.4. Smart coatings

New smart coatings with anti-infective properties that can maintain perioperative tissue homeostasis have been reported recently. In this setting, a functional polymer brush coating has been proposed. This is composed of an anti-adhesive molecule that repels bacteria, an antimicrobial peptide that kills bacterial upon contact, and a substance that contains arginine-glycine-aspartate, which facilitates tissue integration[72]. This strategy of multicomponent coatings that simultaneously provide more than one effect, as producing anti-bacterial and pro-integrational responses, would probably be one of the main strategies that will develop in the near future for implant coatings for the prevention of orthopaedic infection.

1.12. THE AIMS OF THE STUDY

As described in the introductory sections above, PJI represents a serious issue with a tremendous economic load for the worldwide national health systems. Moreover, and of much greater importance from our point of view, there are the dramatic complications for the patient, who has to undergo a long-term series of surgical and non-surgical procedures to have the chance of eradicating a bone infection that might otherwise lead to immobility or, in the worst case scenario, death. In the last decade, the local antibacterial strategies have increased in importance in PJI treatments for optimal infection eradication. In PJI, most bacterial strains involved can form biofilms on orthopaedic devices, thus promoting refractory infections with the commonly used therapies. These biofilm show phenotypic resistance to antibiotics. In addition, the standard medical protocols for both prevention and treatment of infection, such as the conventional systemic delivery of antibiotics, suffers from the drawbacks of systemic toxicity[56] and low biofilm penetration[33].

Considering the systemic strategies and their weakness, a more efficient way of antibiotics delivery is essential in PJI prevention and treatment. This has given rise to a variety of local delivery devices, such as antibiotic bone cements. The main advantage of the *in-situ* release of antibiotics is that it allows therapeutic doses to be delivered at or near the locations involved, which maximises the antibacterial efficiency while minimising the systemic side effects[73].

In this setting, a controlled local delivery system will be of benefit. Indeed, controlled release systems are powerful therapeutic tools for the eradication of bacterial contamination. However, they have a number of shortcomings. First, high local antibiotic concentrations are only achieved over the short term[74], mainly because cements or other commonly used orthopaedic local release systems were never designed to provide controlled release. Thus, to design a local controlled release system that can provide long-term antibiotic elution, we aimed here to create a local delivery system that comprises two different components for antibiotic release. These were designed to provide different kinetics, to cover in this way a long time period. The basis for this local biphasic drug delivery system is illustrated in Figure 11, and it comprises:

1. The first phase delivery system that releases the antibiotic during the operation, as the fast-release component;

2. The second phase delivery system as the internal part of the biphasic system for antibiotic release over a prolonged period after the operation, as the slow-release component. This will thus provide *in-situ* inhibition of potential bacterial colonisation after the surgical procedure is complete, with the release of antibiotic concentrations just over the MIC for each microorganism.

In this context, during the first year of this study, a biodegradable matrix system was created that could be applied intra-operatively on the implant itself, as the fast-release drug carrier of the local system. As the secondary approach, we added a system of microparticles to the matrix, which contained the same antibiotic as the primary matrix system. Microparticles can be created using a mixture of biodegradable polymers that will be degraded, with the consequent slow release of the antibiotic. The antibiotic release rate from the matrix is thus rapid release over the first stage, to provide 6 hours of inhibition of biofilm formation[26]. This is followed by the extended release provided by the microparticles. Indeed, these microparticles have to guarantee the maintenance of the therapeutic dose over several days following the operation.

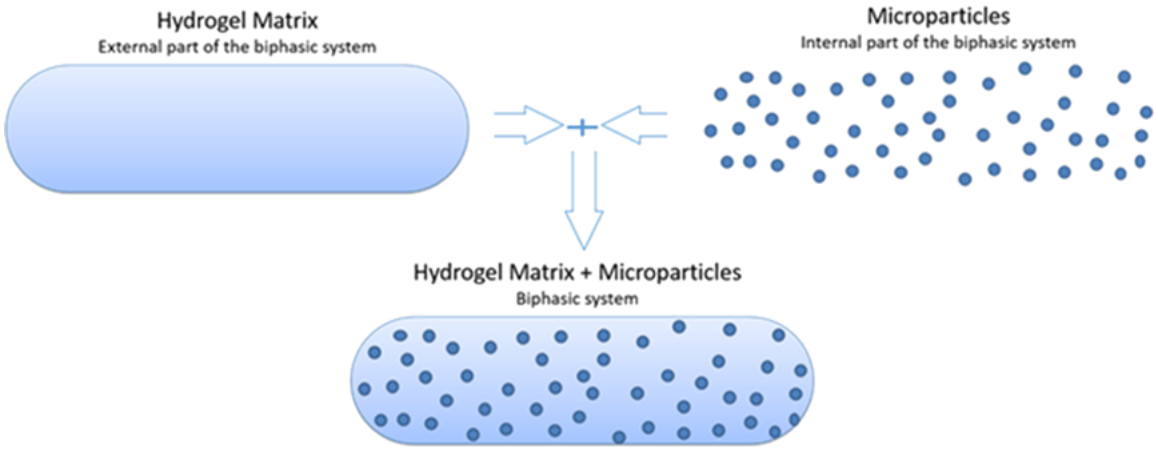

Figure 11. *Design of the hydrogel matrix and microparticles of the local biphasic drug delivery system.*

CHAPTER 2:
MATERIALS AND METHODS

2.1. MATERIALS

The raw materials used in the formulation of the antibacterial system were:

2.1.1. DICHLOROMETHANE, ETHYL ACETATE AND CHITOSAN

Purchased from Sigma Aldrich, Saint Louis, Missouri, USA.

2.1.2. VANCOMYCIN HYDROCLORIDE POWDER

Kindly donated by Lek Pharmaceuticals, Ljubljana, Slovenia.

The selected antibiotic was vancomycin (Figure 12), which belongs to the glycopeptide group, and represents a common first-choice antibiotic against infections of Gram-positive strains that are resistant to other chemotherapy drugs. Vancomycin hydrochloride was selected as the model drug for two main reasons: its high water solubility, and its strong activity against the two main bacterial strains involved in the PJI: MRSA, which is an important nosocomial and community-acquired pathogen that has developed resistance to various antibiotics (e.g., β-lactams, quinolones, aminoglycosides), and *S. epidermidis*.

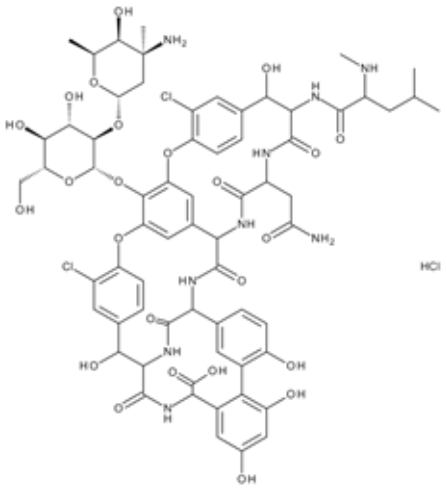

Figure 12. *Chemical structure of vancomycin hydrochloride.*

Vancomycin hydrochloride acts as a chemotherapy agent through its binding the D-Ala-D-Ala portion of N-acetylmuramic acid and N-acetylglucosamine through multiple H-bonds (Figure 13). This means that the N-acetyl precursor in bacterial cell wall synthesis cannot continue through the following steps, thus making the bacterial cell not compatible with life[75].

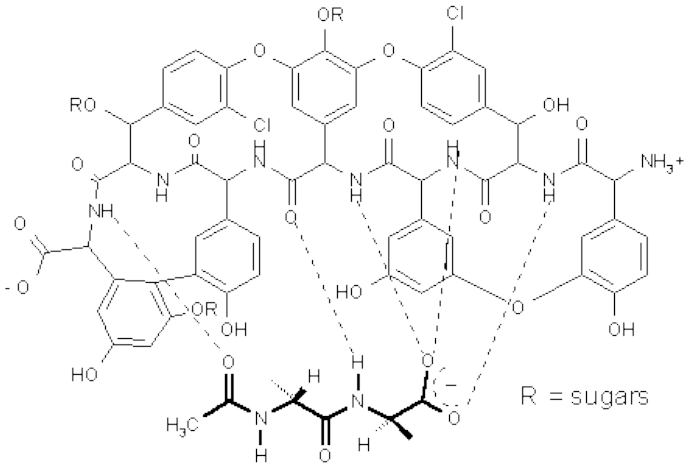

Figure 13. *Vancomycin H-bonding with the D-Ala-D-Ala portion of N-acetylmuramic acid and N-acetylglucosamine, to prevent correct cell wall formation.*

2.1.3. POLOXAMER P407

Purchased as flakes from Sigma Aldrich, Saint Louis, Missouri, USA.

Poloxamer is an amphiphilic non-ionic thermosensitive and thermoreversible copolymer. It is organised as a linear triblock of polyethylene oxides and polypropylene oxides, as shown in Figure 14. Poloxamer belongs to a large polymer class that are defined by various molecular weights, shapes and compositions. To make it easier to distinguish each Poloxamer, and to describe their properties (Table 3), an *ad-hoc* nomenclature was created.

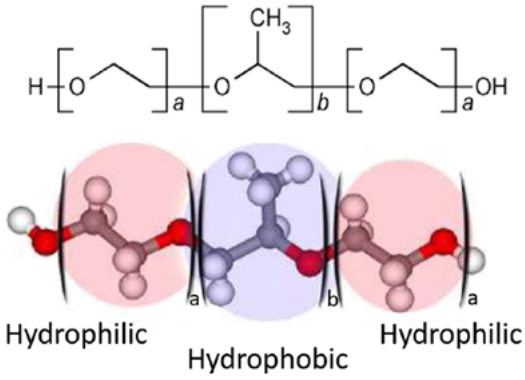

Figure 14. *Chemical structure and physicochemical properties of the Poloxamer triblock.*

Table 3. *Physicochemical properties of the different Poloxamers.*

Poloxamer	Monomer number*		Physical state
	a	b	
124	12	20	Liquid
188	80	27	Solid
237	64	37	Solid
338	141	44	Solid
407	101	56	Solid

*, for a, b, see Figure 14

In the Poloxamer nomenclature, the first two digits multiplied by 100 represented the approximate molecular weight of the hydrophobic polypropylene oxide portion, while the last digit multiplied by 10 represented the percentage in weight of the hydrophilic polyethylene oxide portion (Figure 15).

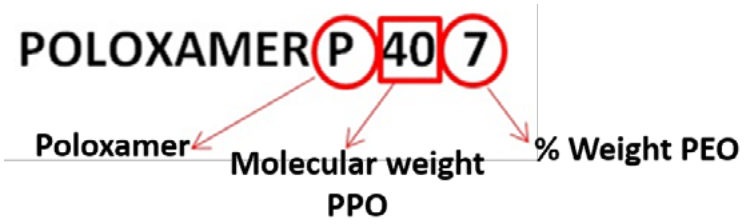

Figure 15. *The Poloxamer nomenclature used in this study.*

Poloxamer 407 has been approved by the US Food and Drug Administration as a food additive, pharmaceutical excipient, drug delivery carrier, and a component of injectable formulations[76]. In particular, as a pharmaceutical excipient, Poloxamer has been defined as a functional excipient, which is in contrast with the usual definition of an excipient as an inert material. This particular definition arises because Poloxamer can improve the unfavourable properties of class II and class IV drugs according to the Biopharmaceutical Classification System, as an active pharmaceutical ingredient (API)[77].

2.1.4. POLYLACTIC-CO-GLYCOLIC ACID 50:50

Purchased as a powder from Sigma Aldrich, Saint Louis, Missouri, USA.

Polylactic-co-glycolic acid (PLGA) is a biodegradable and biocompatible copolymer of polylactic acid and polyglycolic acid (Figure 16). Polylactic acid has a methyl group in the α position, which makes its physico-chemical nature more hydrophobic. Its two enantiomeric forms are poly-D-lactic acid and poly-L-lactic acid. Usually PLGA is intended as the poly-

D,L-lactic-co-glycolic acid form in which these two polylactic acid enantiomers are present at equally levels (i.e., 50:50 ratio). The polyglycolic acid represents the more hydrophilic part of the copolymer, and indeed its level determines the different solubility and biodegradability rates of the entire polymer[78]. PLGA has also been approved by the US Food and Drug Administration as a food additive, pharmaceutical excipient, and drug delivery carrier. In the eukaryotic tissue environment, PLGA degradation is carried out via physiological metabolic pathways; moreover, its degradation time is dependent on pH, crystallinity of the raw material grade, and the enzyme activity. In the human body, it has been shown that the degradation process can last from a few days to a few months, considering all of these variables. The degradation rate is also ratio controlled: increasing the polyglycolic acid to polylactic acid molar ratio increases the biodegradation rate, with a maximum value when the polylactic acid/polyglycolic acid ratio is 50:50[78].

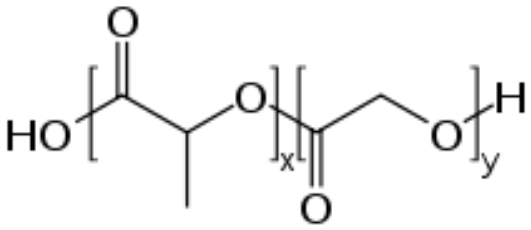

Figure 16. *Chemical structure of poly-lactic-co-glycolic acid (x indicates the number of lactic acid units, and y the number of glycolic acid units).*

To exploit these physiological biodegradability properties, PLGA 50:50 was used in this study as a controlled drug delivery carrier to provide 'days of controlled release' of the selected API. At the same time, it provided a well-tolerated drug delivery system with a copolymer that has been extensively studied in the pharmaceutical formulation field over the recent decades.

2.1.5. DOUBLE-SYRINGE MIXING DEVICE

The double-mixing tube injection device was purchased from Medmix, Risch, Switzerland. It comprises a double syringe with a valve and a mixing device, which allows the pre-filled storage of two components. This integrated system provides a simple mixing method with minimal risk of contamination (Figure 17). The dispenser for the controlled application of the high viscosity biomaterial was also purchased from Medmix (Figure 18).

Figure 17. *The double-syringe mixing device.*

Figure 18. *The dispenser for the application of the high viscosity biomaterials.*

2.2. METHODS

2.2.1. PREPARATION OF POLOXAMER SOLUTION AND VANCOMYCIN-HCL-LOADED POLOXAMER SOLUTION

These represented the external part of the proposed biphasic antibacterial system. To obtain this external part, Poloxamer was added to distilled water to provide a thermosensitive gelling solution. After several minutes at a certain temperature, this solution becomes a gel, as a Poloxamer hydrogel matrix, which itself represent the external part of the proposed antibacterial system. From now on, the Poloxamer solution will be referring to as the liquid (sol) phasic state, while the Poloxamer hydrogel will be referring to as the 'soft solid' (gel) phasic state of the system. Several Poloxamer solutions were prepared in distilled water at different concentrations, using a magnetic stirrer (Vetrotecnica, Verona, Italy), with stirring at 250 rpm while under a cooling system (Thermo Fisher Scientific, Waltham, Massachusetts, USA) to maintaining the solutions at 4 °C. Due to the low temperature used here, this method is referred to as the 'cold method' for the preparation of the Poloxamer solution. After adding the Poloxamer flakes to the water, the suspension was left stirring for 12 h. After this time, the solution was completely clear and transparent, as shown in Figure 19.

For the experiments with vancomycin HCl loaded in the external part of the proposed antibacterial system, the preparation of the Poloxamer solution was slightly different. In this case, an aqueous solution of vancomycine HCl was initially prepared using distilled water as the solvent. Afterwards, the Poloxamer polymer flakes were added to this solution, under stirring and according to the cold method described above.

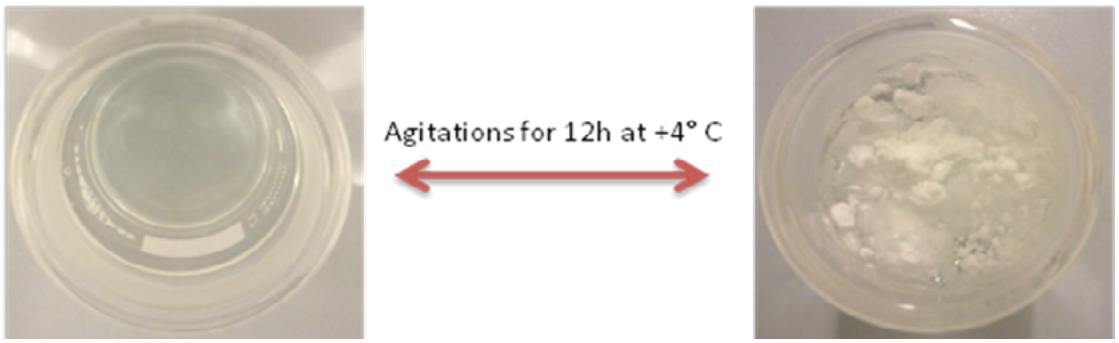

Figure 19. *Cold method for the preparation of the Poloxamer solutions.*

2.2.2. PREPARATION OF VANCOMYCIN-HCL-LOADED PLGA MICROPARTICLES

This represented the internal part of the proposed biphasic antibacterial system. To create this internal part, the vancomycin-HCl-loaded microparticles, different size classes of the microparticles were created using different technologies.

There are innumerable methods for preparing microparticles for use in various applications. Here, the two most common techniques were used, starting from a double emulsion (Figure 20) that is commonly used as a production technique in the pharmaceutical formulation field. Both of these methods have been extensively studied and successfully applied at the pharmaceutical industrial scale as well:

1. Spray drying
2. Solvent evaporation

The selection of the starting double emulsion formulation was mandatory because of the physico-chemical characteristics of the API. To encapsulate a hydrophilic API, such as vancomycin HCl, the double emulsion method is needed (Figure 20). The starting double emulsion is prepared as follows: during the first step of the preparation, the primary A_1/O emulsion is formed, in which the API is solubilized in a 1% (w/v) chitosan aqueous solution (A_1), while the PLGA (50:50) polymer is solubilised in dichloromethane or ethyl acetate (O).

The primary emulsion is created by adding the above chitosan aqueous solution (A_1) to the previously described polymeric PLGA 50:50 solution (O). Then the primary emulsion is added to the secondary 0.25% to 0.5% (w/v) chitosan aqueous solution (A_2) under vigorous stirring (Vetrotecnica, Verona, Italy) at 1,000 rpm. The addition of chitosan to the aqueous phases was important, to ensure the interface stability between the different phases of the double emulsion over long time periods, and especially during the spry drying/ solvent evaporation processes.

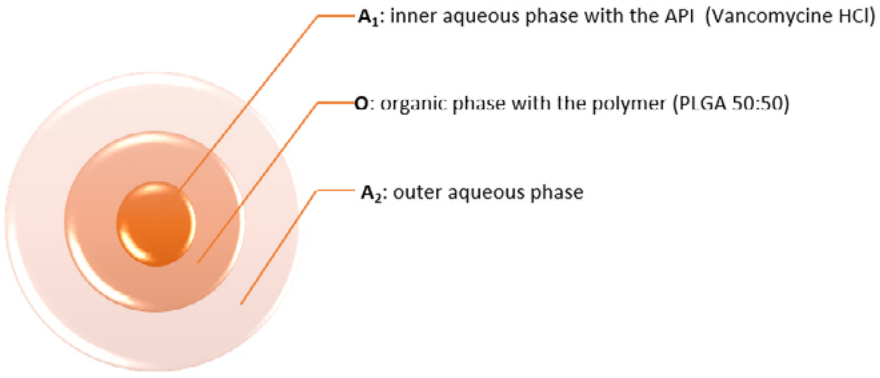

Figure 20. *Schematic representation of the starting double $A_1/O/A_2$ emulsion formulation.*

For both of these technologies of spray drying and solvent evaporation, which are explained in further detail below, the same starting double emulsion preparation methodology was used.

2.2.2.1. Spray drying

The starting double emulsion formulation was then processed through spray drying (Büchi, Flawil, Switzerland) (Figure 21). The spray-drying technique is commonly used in the pharmaceutical formulation field to encapsulate various APIs, to obtain microparticles that for drug delivery carriers.

The mini spray dryer operates according to a co-current air and product stream. This means that the sprayed product and hot air have the same flow direction (Figure 22). The mini spray dryer has an integrated two-fluid nozzle, whereby compressed air is used to disperse the double emulsion (or whatever the fluid body is) into fine droplets that are subsequently dried in the cylinder (Figure 23). The nozzle consists of a nozzle tip with a 0.7-mm diameter hole, and the nozzle cap of 1.4-mm diameter. This geometry results in the mixing of the fluid body and the gas. The nozzle cap has an inserted ruby stone with a precise opening and sharp edges to guarantee precise and reproducible spray cones.

Figure 21. *The Büchi 190 mini spray dryer.*

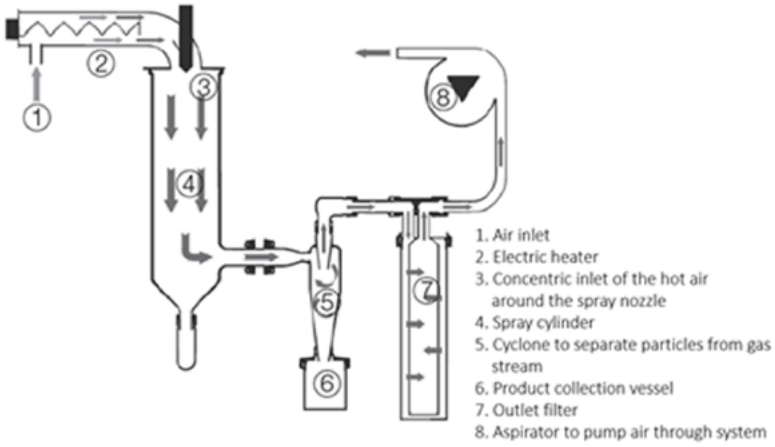

Figure 22. *Schematic representation of the drying airflow of the spray dryer (Operation Manual Mini Spray Dryer B-290).*

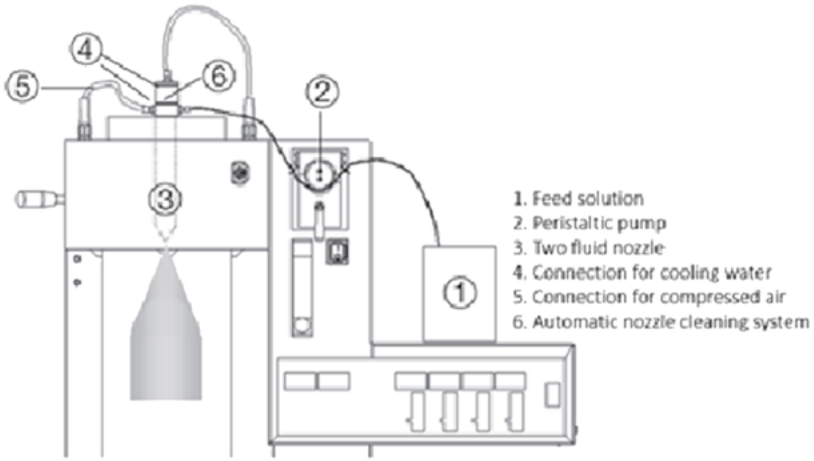

Figure 23. *Schematic representation of the spraying process in the spray dryer (Operation Manual Mini Spray Dryer B-290).*

To optimize the process and evaluate its different API loading, five different batches were produced (i.e., A1-A5), with different operation conditions used for each batch, as given in Table 4.

Table 4. *The spray-dryer parameters used*

Parameter	Batch number				
	A1	A2	A3	A4	A5
Flux (L/h)	0.25	0.25	0.25	0.25	0.25
Entering air temperature (°C)	135	135	135	144	145
Outgoing air temperature (°C)	85	85	85	93	95
Nozzle diameter (mm)	0.7	0.7	0.7	0.7	0.7

2.2.2.2. Solvent evaporation

The technique of microencapsulation by solvent evaporation is widely used in the pharmaceutical industries. Water-insoluble polymers are used as the encapsulation matrix in this technique. The biodegradable polymer PLGA is frequently used as an encapsulation material, so the vast literature available provided support for this methodology[79].

To compare the particle size distributions of the microparticles produced with the different techniques, a batch (A6) was prepared using the solvent evaporation technique (Figure 24).

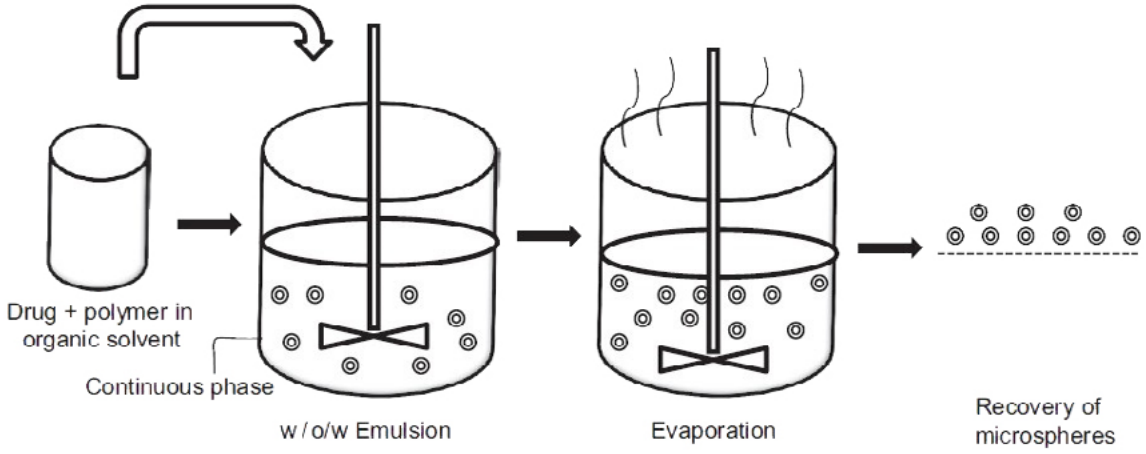

Figure 24. *Schematic representation of the solvent evaporation microencapsulation methodology (www.cysonline.org)*

The previously described double-emulsion formulation was left under constant stirring at 600 rpm (Opto-Lab, Modena, Italy), at room temperature for 24 h in a 500-mL beaker. The product that was suspended in the aqueous solution was then centrifuged at 4,500 rpm (Thermo Fisher Scientific, Waltham, USA), and lyophilized (SciQuip, Newtown, UK).

2.2.3. PARTICLE SIZE ANALYSIS

To understand in detail how the release behaviour of the different microparticles obtained was affected by the dimension, morphology and shape, particle size analysis was performed. A microscope imaging analysis technique for determination of the microparticle size distribution was applied to batches A1-A6. The microparticle morphology and size distribution were determined under a microscope (Olympus BH-2) equipped with a video camera (CCD Camera ICD-42E, Tokyo, Japan) and a computer-controlled image analysis system (Optomax V, Cambridge, UK). The microparticles were dispersed on a microscope slide. The microscope field was scanned by the video camera. The images of the scanned fields were digitised and analysed using the software, to determine the microparticle mean diameter and particle size

distribution. In all of the measurements, at least 1,500 particles were examined.

The zeta potential of the particles was determined in 10 mM NaCl (pH 6.7) at 25 °C, using photon correlation spectroscopy (Zeta-sizer 3000; Malvern Instruments, Malvern, UK).

For the scanning electron microscopy analysis, the samples were sputter-coated with Au/Pd using a vacuum evaporator (Edwards, Crawley, UK) and analysed using a scanning electron microscope (Philips XL-30, Eindhoven, The Netherlands) at a 25-kV accelerating voltage.

2.2.4. RHEOLOGICAL EXPERIMENTS

Rheology is the science of the flow and deformation of matter, liquids or 'soft' solids under the effect of an applied force. Deformation is defined as the change in the shape and the size of a body due to applied forces, and it could be divided according to:

1. Irreversible deformation: Viscous flow deformation, where the matter does not revert to the original state when the force is removed;

2. Reversible deformation: Elastic flow deformation, where the matter reverts to the original form after the stress is removed.

Rheology today is fundamental in the understanding of the basic nature of a given material, to determine the effects of different parameters on the properties of the system constituted by the material itself. Rheological analysis is commonly used in the following industries:

1. Chemical

2. Pharmaceutical

3. Food

4. Cosmetics

5. Oil-drilling

In the pharmaceutical industry, rheology is mostly used in relation to injectable and polymer systems. Here, the Poloxamer solution represented the external part of the proposed antibacterial system, as described in this thesis, and it turns in a hydrogel matrix starting from a liquid polymer solution in a temperature-depending manner. Rheology was applied here to determine the most suitable concentration of polymer to be used to obtain an appropriate sol-gel transition time, and to determine the thermo-reversibility capacity of this external part of the antibacterial system. Moreover, the idea was also to determine whether the presence of vancomycine HCl and/or microparticles have important roles on this properties.

The rheological evaluation was performed using a rotational rheometer (Discovery HR-1

Rheostress RS150; TA Instruments, New Castle, USA) (Figure 25), where the plates had a parallel geometry (Figure 26). Tests of temperature, time, and stress sweep were performed, with two parameters considered:

1. Elastic modulus (G'): a direct indicator of the solid behaviour of the material;
2. Viscous modulus (G"): a direct indicator of the liquid behaviour of the material.

Every test was conducted in the linear zone of the viscoelasticity of the polymer, and of the microparticles within the polymer.

Figure 25. *A Rheostress RS150 rheometer.*

Figure 26. *Parallel geometry of the rheometer plates.*

Various Polaxamer concentrations were tested, to evaluate the G' G" trends (as the elastic and viscous moduli, respectively) as a function of the progressive increase in temperature, and of time and stress. Briefly, 2 mL Poloxamer solution at each concentration was loaded onto the rheometer plate. After individuation of the most suitable concentration of Poloxamer for the polymer solution, the rheological test was performed on the most appropriate batch of microparticles as a dispersion inside the Poloxamer solution. For this purpose, batch A5 of the microparticles was added to the Poloxamer solution, with simple mixing with a spatula, to determine whether the rheological characteristic of the derived Poloxamer hydrogel matrix changed after addition of the microparticles.

In more detail, the rheological protocol comprised the following:

1. An oscillation sweep at temperature (T) 15 °C, frequency (f) 1 Hz, share (τ) 0.4 Pa, for 120 s;

2. A temperature sweep from 15 °C to 37 °C, with a temperature gradient of 1 °C/min, at f 1 Hz, τ 0.4 Pa;

3. An oscillation sweep at T 37 °C, f 1 Hz, τ 5 Pa, for 300 s;

4. A stress sweep from 0.4 to 1,000 Pa at T 37 °C, f 1 Hz.

2.2.5. AUTOCLAVE STERILISATION

A sterilisation process for the Poloxamer solution was performed to define whether the mechanical behaviour of the derived Poloxamer hydrogel matrix significantly changed during the sterilisation process. A cycle of 120 °C for 65 min was used in an autoclave (Vacuklav 30 B+; Melag, Berlin, Germany), as shown in Figure 27.

Figure 27. *A Vacuklav 30 B+ autoclave.*

2.2.6. IN-VITRO DISSOLUTION EXPERIMENTS

To obtain the release of the vancomycin HCl from the Poloxamer hydrogel matrices from different batches of microparticles, and to understand the effects of the Poloxamer hydrogel matrix systems on the release of the vancomycin from those microparticles, *in-vitro* dissolution experiments were performed. Here, the selected content of the Poloxamer polymer in the hydrogel matrix was kept constant at 20% (w/w).

The Poloxamer hydrogel matrices with vancomycin HCl, or the Poloxamer hydrogel matrices with the addition of microparticles, were loaded onto the extraction cell following the technical dissolution specifications listed in the assay for transdermal patches in the Official Pharmacopoeia of the Republic of Italy (Farmacopea Ufficiale della Repubblica Italiana, XII edition 2008, page 355), Analysis Methods section (Figure 28). A mixed cellulose ester membrane (HAWP type) and 0.45-µm mesh were used (Millipore, Billerica, USA).

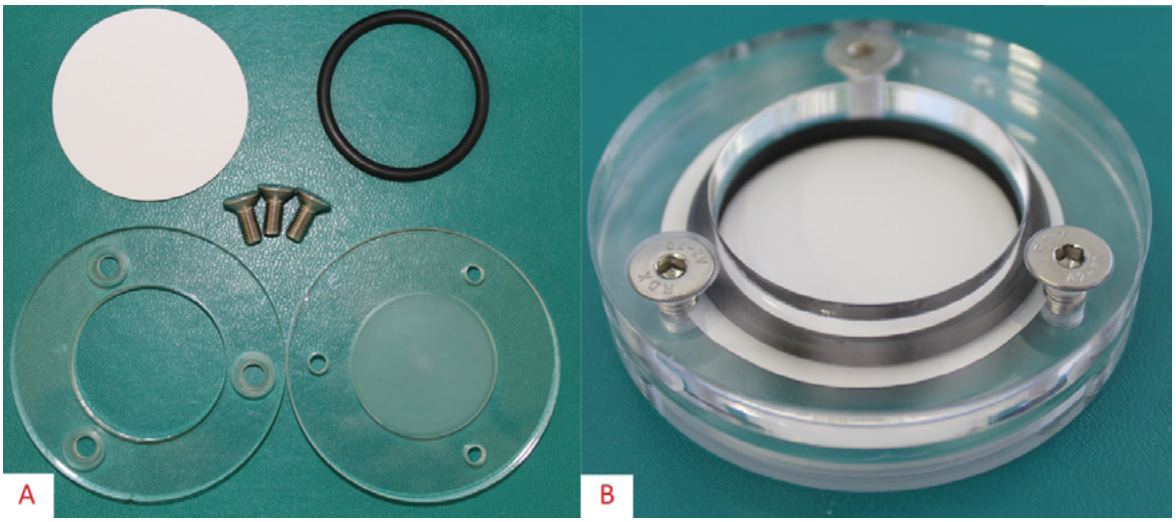

Figure 28. *The extraction cell used for the dissolutions experiments (A) and the extraction cell with the antibacterial system loaded under the membrane (B).*

A dissolution apparatus (Hanson Research, Chatsworth, USA) was used, with it maintained at 37 ±0.1 °C under a stirring rate of 100 rpm. The dissolution medium was 500-mL buffer at pH 7.4. The dissolution medium was continuously pumped into an *in-situ* flow cell in a UV spectrophotometer (Zeiss, Oberkochen, Germany), and the absorbance was recorded at the maximum wavelength for the drug (282 nm) (Figure 29). The polymer did not interfere with the UV analysis.

The dissolution test continued for 24 h for the Poloxamer hydrogel matrix loaded with vancomycin HCl, while it lasted for 7 days when the microparticles were added to the

Poloxamer hydrogel matrix. The absorbance at each time point were collected using the proprietary software (Zeiss Spectra, Zeiss, Oberkochen, Germany), and are expressed as means ±sd values (n = 3, SD <4%).

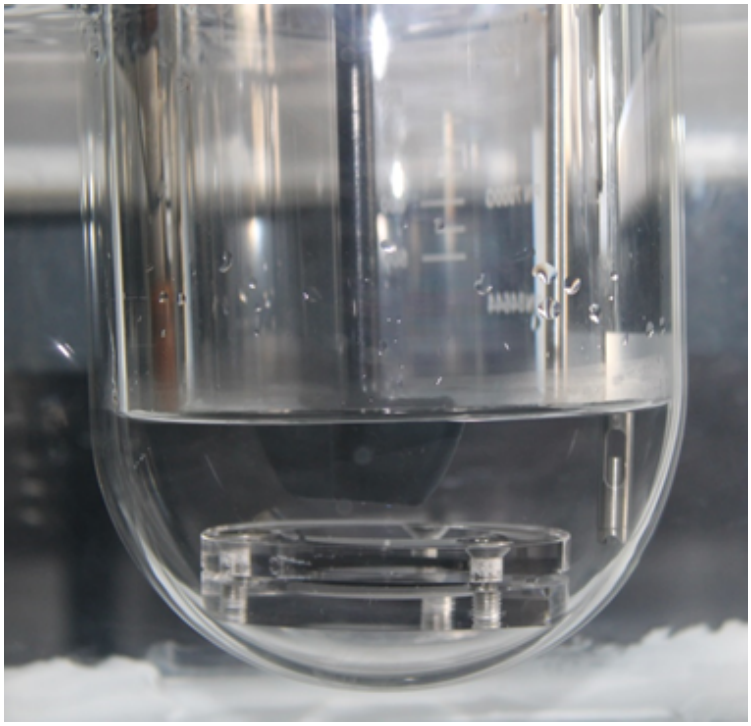

Figure 29. *The vessel with the buffer solution, extraction cell, and the in-situ UV cell.*

2.2.7. MICROBIOLOGICAL EXPERIMENTS

To evaluate the antibacterial performance of the biphasic system studied here, microbiological assays were performed separately on the two phases of the double-phase system. The following samples were tested:

1. Poloxamer matrix hydrogel loaded with different concentrations of Vancomycin HCl;

2. Microparticles loaded with vancomycin HCl as a dispersion in the Poloxamer matrix hydrogel.

For this purpose, a diffusion test on modified agar culture plates was used. Mueller-Hinton Broth growth medium (Difco, New Jersey, USA) was prepared and sterilised as the bacterial growth medium. In the middle of the solidified growth medium, a hole of 150 mm^3 was made, to create a space in which the sample was settled. In this test, MRSA and *S. epidermidis* R (Resistant) were used, as these represent the main bacterial species in orthopaedic infections. A few (2-3) drops of the solution containing about 1.5 $x10^8$ colony-forming units (CFU)/

mL was spread over the solidified growth medium. The zone of inhibition is expressed as the diameter of the inhibition, and it was evaluated as the predictive value for the inhibition efficiency of the antibacterial system against bacterial growth.

For the Poloxamer solution loaded with vancomycin HCl, the 150 mm^3 hole was filled with 138 μL of two systems of Poloxamer 20% (w/w):

1. V1A, V1B: containing 245 μg vancomycin HCl;
2. V2A, V2B: containing 490 μg vancomycine HCl.

Afterwards, the inoculated plates were incubated overnight in a controlled temperature air oven at 37 °C.

For the test of the microparticles loaded with vancomycin HCl as a dispersion in Poloxamer 20% (w/w), the *modus operandi* was slightly different. The dispersion of the microparticles in the Poloxamer solution was loaded onto a trabecular Ti_6Al_4V disc, which was used as a prosthesis-like sample, and which had been infected previously with the same CFU as above.

After this procedure, the disc was introduced into the hole inside the solid growth medium, and this was then incubated overnight in an oven at 37 °C, to check the inhibition capacity (Figure 30).

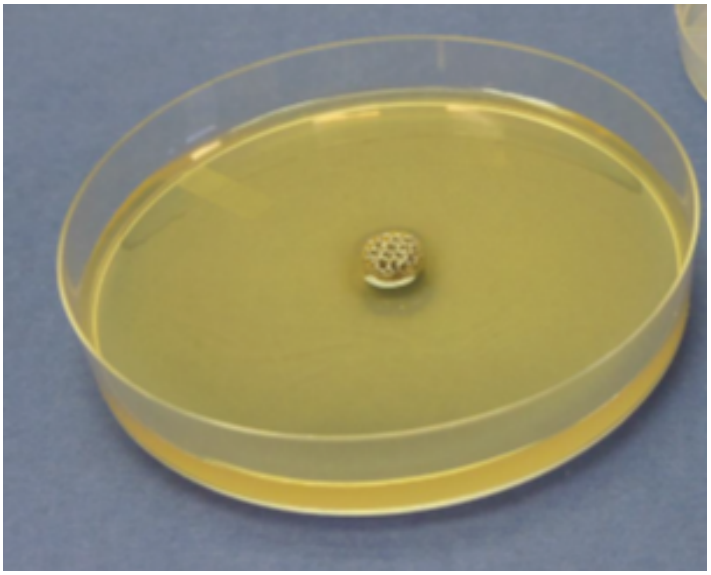

Figure 30. *Growth medium plate with the Ti_6Al_4V disc settled in the central hole.*

2.2.8. MATHEMATICAL MODEL

Once the biphasic antibacterial system had been prepared, physically characterised and microbiologically tested, the release properties of the system were investigated from a

mathematic point of view. The intention was to create a suitable mathematical model that could describe how changing the principal values of the system, such as the diameter of the microparticles and the Poloxamer concentration, changed the release capacity of the biphasic system. This is a fundamental step in the creation of an antibacterial system that is to be technologically transferred into an industry, and thus has to be scaled up.

2.2.9. PRESENTED MODEL

To study the release properties of this biphasic antibacterial system, a mathematical model was set up that referred to the physical framework illustrated in Figure 31. The physical framework is simply the mathematically expressed representation of the experiment conducted using the extraction cell described in the section 2.2.6 above. The biphasic gel, of thickness L_G and volume V_G, constitutes the donor environment, and it is separated by a membrane of thickness L_M from the receiver environment, of volume V_R and thickness L_R.

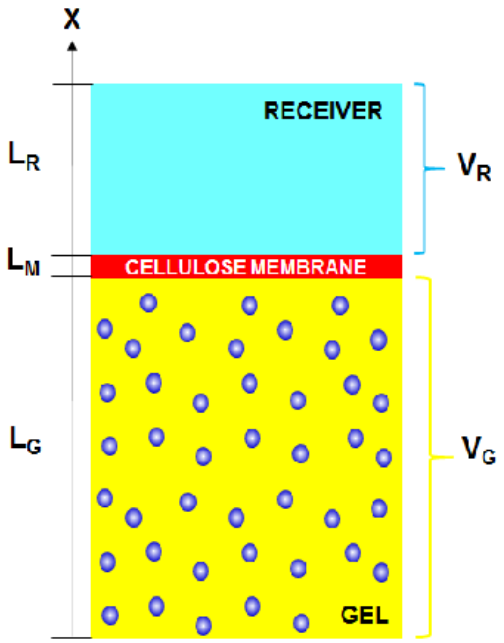

Figure 31. *Representation of the biphasic hydrogel system used to study the mathematical model.*

Theoretically, the release process is a complex three-dimensional problem, which implies drug release from the PLGA particles, drug diffusion through the gel network, and finally, drug diffusion through the membrane, for drug accumulation in the receiver environment. However, this problem can be considerably simplified if it is assumed that:

1. The PLGA particles do not move inside the gel matrix;

2. The PLGA particles are uniformly distributed inside the gel;

3. The particles are characterised by the same radius (R_p);

4. The particle diameter is small in comparison to the donor environment thickness (L_G), such that at fixed distance X from the donor environment bottom, the particle surfaces experience the same external concentrations.

2.2.10. WORKING EQUATIONS

Relying on these hypotheses, the three-dimensional problem reduces to a much simpler one-dimensional problem according to the drug radial (r) diffusion inside the particles, and the drug axial (X) diffusion in the gel phase and in the membrane. In other words, it can be assume that the drug diffuses radially from the inner part of the particles towards the particle surface, to move into the gel phase. Here, purely axial diffusion takes place towards the membrane and the receiver environment. Accordingly, the governing equations of the model are:

Diffusion in the membrane:

$$\frac{\partial C_M}{\partial t} = \frac{\partial}{\partial X}\left[D_M \frac{\partial C_M}{\partial X} \right] \quad (1);$$

Diffusion in the gel phase:

$$\frac{\partial C_G}{\partial t}(1-\varphi) = (1-1.5\varphi)\frac{\partial}{\partial X}\left[D_G \frac{\partial C_G}{\partial X} \right] - D_P \left.\frac{\partial C_P}{\partial r}\right|_{R_P} \frac{3}{R_P}\varphi \quad (2);$$

Diffusion inside particles:

$$\frac{\partial C_p}{\partial t} = \frac{1}{r^2}\frac{\partial}{\partial r}\left[r^2 D_p \frac{\partial C_p}{\partial r} \right] \quad (3);$$

where t is time, C_M, C_G and C_p are the local drug concentrations in the membrane, in the gel, and in the particles, respectively, D_M, D_G and D_p are the drug diffusion coefficients in the membrane, in the gel, and in the particles, respectively, X and r are the axial and radial coordinates, respectively, and φ is the particle volume fraction in the gel (i.e., [1-φ] represents the gel volume fraction in the donor environment, as shown in Figure 32). Inspection of Equations (1)-(3) reveals that the drug transport occurs according to a purely diffusive mechanism, as described by Fick's law. It is also worth noting that Equation (2) refers to the drug transport in the gel phase, and this is the reason why the gel volume fraction (1-φ) appears in the left-hand term. In addition, the second right-hand term, which refers to the drug diffusion in the gel phase, arises because due to the presence of the PLGA particles, only the fraction φ_s (= 1-1.5*φ) of the donor environment cross-section is available for drug

diffusion. Finally, the third right-hand term of Equation (2) represents the drug flux entering in the gel phase, and coming from all of the particles situated at the axial position *X*.

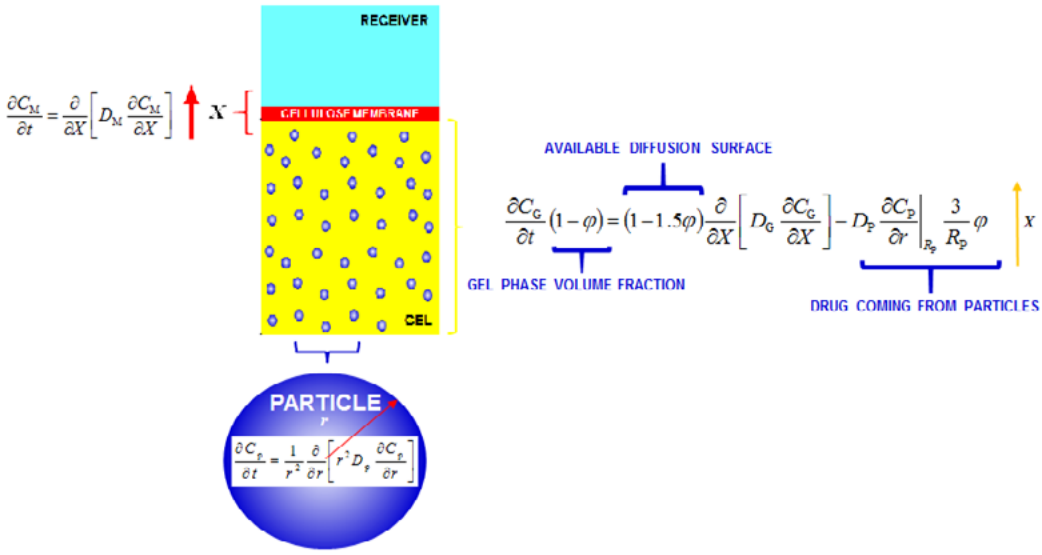

Figure 32. *Schematic representation of the working equations used for the mathematical modelling.*

2.2.11. BOUNDARY CONDITIONS

Equations (1)-(3) have to be numerically solved (spatial and temporal discretisation according to the control volume method, coupled with the Gauss–Seidel solution scheme), according to the following boundary conditions, which can also be seen in Figure 33:

$$D_{\mathrm{G}} \left.\frac{\partial C_{\mathrm{M}}}{\partial X}\right|_{X=0} = 0 \qquad (4);$$

$$\left.\frac{C_{\mathrm{p}}}{C_{\mathrm{G}}}\right|_{r=R_{\mathrm{p}}} = k_{\mathrm{P\,G}} \qquad (5);$$

$$D_{\mathrm{G}} \left.\frac{\partial C_{\mathrm{G}}}{\partial X}\right|_{X=L_{\mathrm{G}}} = D_{\mathrm{M}} \left.\frac{\partial C_{\mathrm{M}}}{\partial X}\right|_{X=L_{\mathrm{G}}} \qquad \left.\frac{C_{\mathrm{G}}}{C_{\mathrm{M}}}\right|_{X=L_{\mathrm{G}}} = k_{\mathrm{G\,M}} \qquad (6);$$

$$\left.\frac{C_{\mathrm{M}}}{C_{\mathrm{R}}}\right|_{X=L_{\mathrm{G}}+L_{\mathrm{M}}} = k_{\mathrm{M\,R}} \qquad (7);$$

$$M_0 = V_{\mathrm{R}} C_{\mathrm{R}} + \int_0^{L_G} C_G S(1-\varphi)\mathrm{d}X + \int_0^{L_G} \frac{3\varphi}{R_{\mathrm{p}}^3} S\mathrm{d}X \left(\int_0^{R_{\mathrm{p}}} C_{\mathrm{p}} r^2 \mathrm{d}r \right) + \int_{L_{\mathrm{G}}}^{L_{\mathrm{G}}+L_M} C_M S\mathrm{d}X \qquad (8).$$

where *S* is the donor and receiver environment cross-sectional areas.

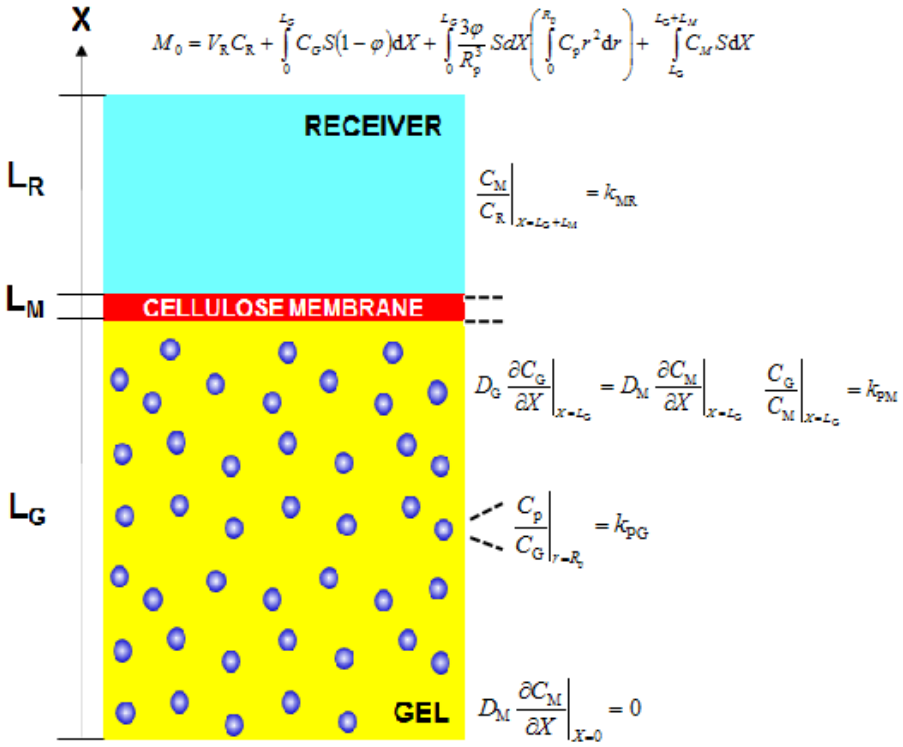

Figure 33. *Schematic representation of the boundary conditions used for the mathematical modelling.*

Equation (4) defines the existence of an impermeable wall at the bottom of the donor phase, while Equation (5) expresses the drug partitioning condition at the particles/ gel phase interface (k_{PG} is the partition coefficient). Equation (6) establishes that the drug flux leaving the gel phase is equal to that entering the membrane, while k_{GM} is the partition coefficient at the gel/ membrane interface. Equation (7) is the partitioning condition at the membrane/ receiver environment interface (K_{MR} is the partition coefficient), while Equation (8) is the global mass balance that ensures that at any time the initial drug dose (M_0) must be equal to the sum of the drug mass present in the receiver environment, in the gel phase, inside the particles, and in the membrane.

The typical initial conditions imply the presence of the drug in the particles (uniform distribution) at a known concentration C_{p0}, and the absence of drug in the gel, in the membrane, and in the receiver environment.

2.2.12. DEPOSITION TEST

To test the biphasic system and its potential application using an existing injectable device in a real environment, such as a surgical room, at 21 °C, a deposition assay was performed. The preparation of the injectable device was divided into two steps, according to the following.

2.2.12.1. Mixing operation

The microparticles and the Poloxamer solution were prefilled. The transfer of the hydrogel into the microparticles powder chamber was achieved by turning the selector ring of the valve clockwise from the 'closed' to the 'transfer' position, and pushing the plunger of the liquid chamber. The mixing operation was carried out by moving the mixing device back and forth while simultaneously rotating it. After mixing the biomaterial, the plunger was removed from the Poloxamer solution chamber, and attached to the shaft of the mixing device. The residual air was removed by slowly pushing the plunger forward. The mixed material was then ready to be dispensed.

2.2.12.2. Dispensing the mixed biomaterial

To dispense the mixed biomaterial, the selector ring of the valve was turned clockwise to the 'inject' position. After attaching the plunger to the shaft of the mixing device, the mixed biomaterial was dispensed and applied with minimal waste directly to the prosthesis (Figure 34).

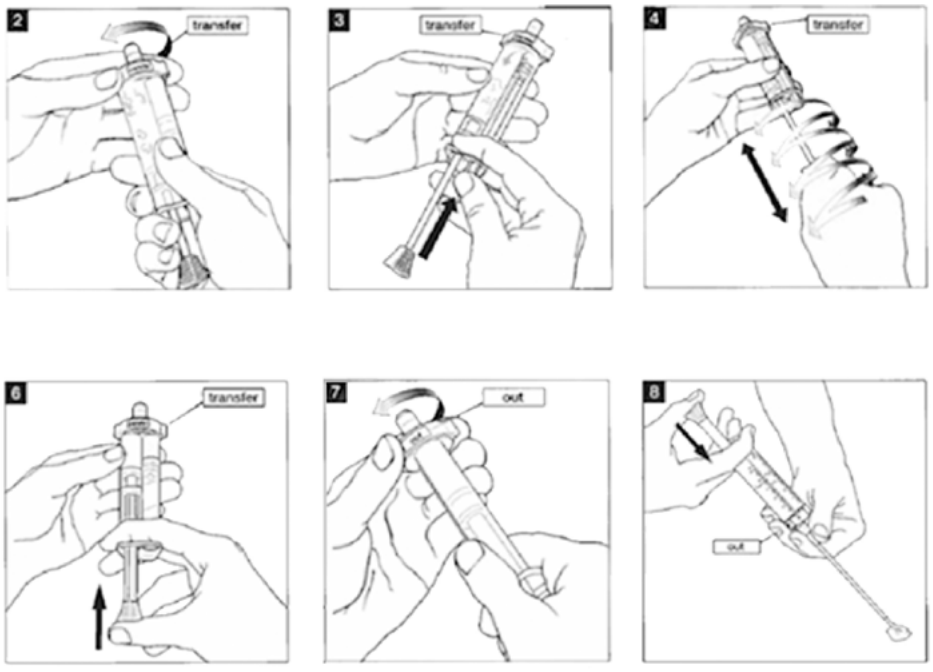

Figure 34. *Preparation scheme for the injectable device.*

Once the biphasic system was prepared and ready to use, it was spread on the prosthesis surface, as illustrated in Figure 35. The time needed to complete the gel setting process, the applicability, and the permanence of the biphasic system on the prosthesis surface were then evaluated.

Figure 35. *Illustration of the spreading procedure on the prosthesis surface.*

CHAPTER 3:
RESULTS AND DISCUSSION

3.1. POLOXAMER SOLUTION AND VANCOMYCIN-HCL-LOADED POLOXAMER SOLUTION

These represented the external part of the proposed biphasic antibacterial system. Concentrations from 10% to 25% (w/w) of Poloxamer polymer were tested to determine the best compromise to form the hydrogel matrix, between viscosity and physical stability at the temperature of interest (37 °C). According to the rheological experiments that are detailed in the relevant section below (section 3.4.), at 37° C, the 20% (w/w) Poloxamer was the most suitable for the aims of this project.

Vancomycin HCl concentration of 1%, 2%, 4%, 5%, 6%, 12% and 24% (w/w) of the 20% (w/v) Poloxamer were tested here. The 20% (w/v) Poloxamer solutions at the vancomycin HCl concentrations of 5%, 6%, 12% and 24% all precipitated immediately, while with 4% vancomycin HCl the hydrogel matrix formations was inhibited. Thus no further tests were performed on these systems (Figure 36). The cause of this vancomycin precipitation was the simultaneous presence of the two different materials dissolved in high concentrations, which resulted in an unstable system.

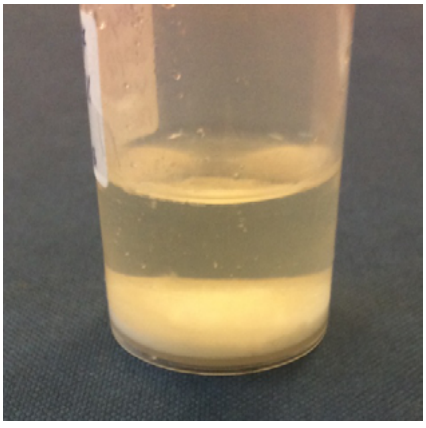

Figure 36. *Example of precipitation of vancomycin HCl in the Poloxamer hydrogel matrix.*

The main cause of the inhibition of the gel-formation process that took place for these above-mentioned concentrations of vancomycin HCl can be ascribed to the physical mechanisms involved in hydrogel matrix formation starting from the Poloxamer solution. The gel formation process from the Poloxamer solution to the hydrogel matrix is based on the transition of the Poloxamer free-chain organisation as a solution into the Poloxamer micelle structural organisation as the hydrogel (the sol-gel transition; Figure 37).

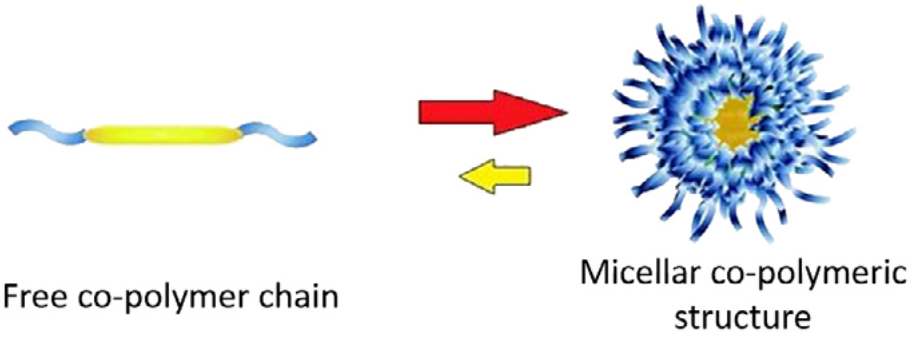

Figure 37. *Schematic representation of the chain-to-micelle transition process (sol-gel) of the Poloxamer.*

This sol-gel transition process in aqueous solution is thermodynamically governed by the concentration of Poloxamer and the temperature. Looking deeply into the concentration in terms of its thermodynamic values in aqueous solution, and plotting the temperature as a constant, it can be seen that the amphiphilic co-polymeric chains of Poloxamer can spontaneously aggregate into micelles beyond a certain concentration known as the 'critical micellar concentration'[80]. This initially not reached for the sol-gel transition, due to the low overall presence of micelles. Moreover, the sol-gel transition occurs when the critical gel concentration is reached, whereby the critical gel concentration represents the polymer concentration at which the micelle numbers are enough to provide the supramolecular organisation that is physically characterised as stable gel formation[81].

Poloxamer in solution represents a thermo-reversible gel-forming system, and therefore temperature has a fundamental role according to a thermodynamical value when, this time, the Poloxamer concentration remains constant. Under the critical micellar temperature, the polyethylene oxides and polypropylene oxides blocks are hydrated, where the polyethylene oxides are relatively water soluble. An increase in the temperature causes the polypropylene oxides cores to dehydrate, and hence to increase their hydrophobic characteristics[82]. In other words, with an increase in temperature of a Poloxamer aqueous solution, the polypropylene oxide block tends to dehydrate and form a core with an outer shell of hydrated polyethylene

oxide chains. These aggregate into spherical micelles when the critical micellar temperature is reached, which starts the gel-formation process. When the volumetric micelle fraction is >0.53, the micelles have less motion inside the solution, which takes on a more ordered structure. The entire system then becomes a crystal-like network, which is known as colloidal gel, and which represents the end of the gel-formation process (Figure 38)[81].

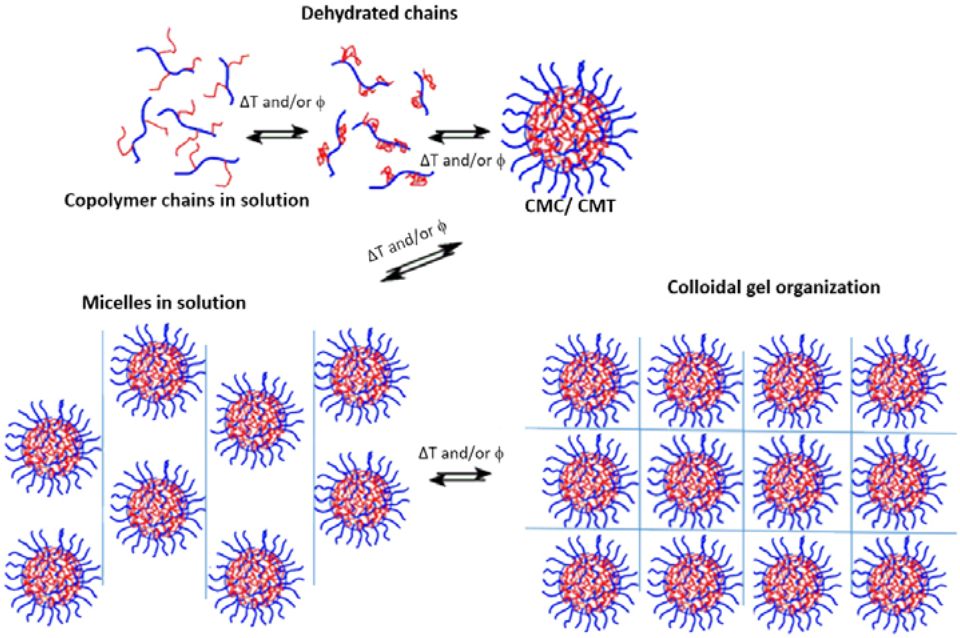

Figure 38. *Concentration and time dependent gel-formation process of Poloxamer in solution.*

When the system undergoes a further increasing in temperature, to greatly exceeding the critical micellar temperature, the hydrogel matrix disassembles, thus converting it again into free co-polymeric chains in solution.

When a solute is present, different kinetics of the gel-formation process can occur. This process in known as 'salting-in' when associated with increased critical micellar concentration and critical micellar temperature, or 'salting-out' when decreased critical micellar concentration and critical micellar temperature are involved[76]. In our studies, when vancomycin exceeded 4% (w/w) in nthe 20% (w/w) Poloxamer solution, the gel-formation process was inhibited. This was probably due to high molecular weight of vancomycin, which can destabilise the micelle organisation in colloidal gel networks.

3.2. VANCOMYCIN-HCL-LOADED PLGA MICROPARTICLES

This represented the internal part of the proposed biphasic antibacterial system. The PLGA microparticles loaded with vancomycin HCl that were obtained from the spray drying and solvent evaporation were produced according to six different formulations listed in Tables 5 and 6.

Table 5. *Qualitative-quantitative compositions of the six different formulations used for production of the batches (A1-A6).*

Batch number	**Code**	**Form**	**Composition** (g/100 mL)	**Solvent volume** (mL)	**Dry product weight** (mg)
A1*	A_1	Vancomycin HCl (inner)	2.5	8	200
		Chitosan (inner)	1	8	80
	O (EtOAc)	PLGA 50:50	1	40	400
	A_2	Chitosan (outer)	0.5	160	800
A2*	A_1	Vancomycin·HCl (inner)	2.5	30	750
		Chitosan (inner)	1	30	300
	O (DCM)	PLGA 50:50	1.5	150	2250
	A_2	Chitosan (outer)	0.5	600	3000
A3*	A_1	Vancomycin HCl (inner)	2.5	30	750
		Chitosan (inner)	1	30	300
	O (DCM)	PLGA 50:50	1.5	150	2250
	A_2	Chitosan (outer)	0.25	600	1500
A4*	A_1	Vancomycin HCl (inner)	5	16	800
		Chitosan (inner)	1	16	160
	O (EtOAc)	PLGA 50:50	1	80	800
	A_2	Chitosan (outer)	0.5	320	1600
A5*	A_1	Vancomycin HCl (inner)	5	16	800
		Chitosan (inner)	1	16	160
	O (EtOAc)	PLGA 50:50	1	80	800
	A_2	Vancomycin HCl (outer)	2	320	6400
		Chitosan (outer)	0.5	320	1600
A6**	A_1	Vancomycin HCl (inner)	5	16	800
		Chitosan (inner)	1	16	160
	O (DCM)	PLGA 50:50	1	80	800
	A_2	Chitosan (outer)	0.5	320	1600

*, Produced by *spray drying*

**, Produced by *solvent evaporation*

DCM, dichloromethane; EtOAc, ethyl acetate

Table 6. *Characteristics of the batches obtained by spray drying and solvent evaporation.*

Characteristic	**Batch**					
	A1*	**A2***	**A3***	**A4***	**A5***	**A6****
Product yield (%)[a]	27.0	22.7	28.1	28.3	51.2	16.4
Theoretical vancomycin HCl content (%)[b]	13.5	11.9	15.6	23.8	73.8	23.8
Experimental vancomycin HCl content (%)[c]	9.2	7.4	10.8	16.8	69.8	13.3
Encapsulation yield (%)[d]	68.1	62.2	69.2	70.6	94.6	55.9
Mean diameter (μm)	2.78 ±1.75	3.28 ±1.90	3.03 ±1.95	2.45 ±1.84	3.12 ±2.05	47.3 ±3.24
Z potential (mV)	31.7 ±0.6	26.6 ±0.8	30.9 ±1.3	34.3 ±1.8	44.2 ±0.5	23.5 ±0.4

*, Produced by *spray drying*

**, Produced by *solvent evaporation*

[a], (Final product weight/ Starting weight of all the components) × 100

[b], (Starting vancomycin HCl weight/ Starting weight of all the components) × 100

[c], HPLC-MS analysis performed by l'Università di Camerino (Macerata, Italy)

[d], (Experimental vancomycin content/ Theoretical vancomycin content) × 100

3.3. PARTICLE SIZE ANALYSIS

Optical imaging (as scanning electron microscopy) was used to obtain the dimensional distribution of the microparticles obtained by spray drying (Figure 39A, batches A1-A5) and by solvent evaporation (Figure 39B, batch A6). From both of these analyses, it can be seen that all of the microparticles were spherical in shape, with a smooth surface, and a mean diameter distribution of between 1.5 µm and 3 µm. From these data it appears that batch A6 (obtained by solvent evaporation) had 10-fold greater diameter that the batches obtained by the spray drying technique (batches A1-A5), and a more uniform spherical surface (Figure 40).

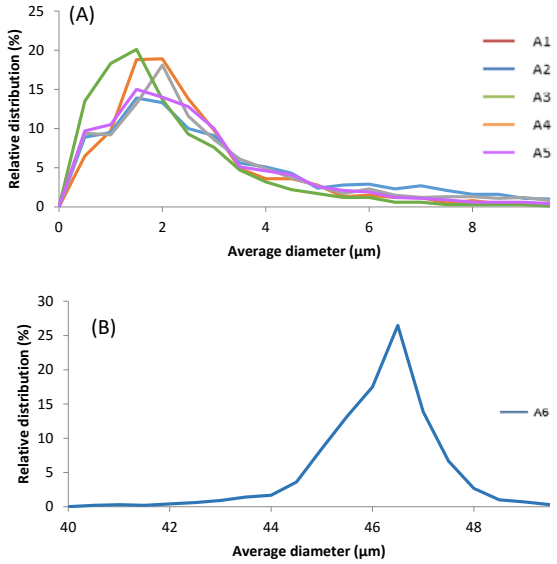

Figure 39. *Dimensional distribution of the microparticles obtained by spray drying, as batches A1-A5 (A) and by solvent evaporation, as batch A6 (B).*

From the scanning electron microscopy images shown in Figure 40, there were visible differences in the particle sizes and shapes between the two batches of microparticles analysed. In particular, in the batch obtained with the solvent evaporation (Figure 40B)there was the greater mean particle size, while better uniformity of the spherical shape can be noted for the spray-dried microparticle batches (Figure 40A).

These differences were correlated to the different solvent evaporation rates. In the solvent evaporation method, the efflux of the evaporation is slower, so that the formation of the

microparticles is more uniform in dimension, shape and surface. Conversely, the operating conditions of the spray-drying technique, and in particular for the dimension of the nozzle and the pressure, resulted in the reduced mean particle diameter.

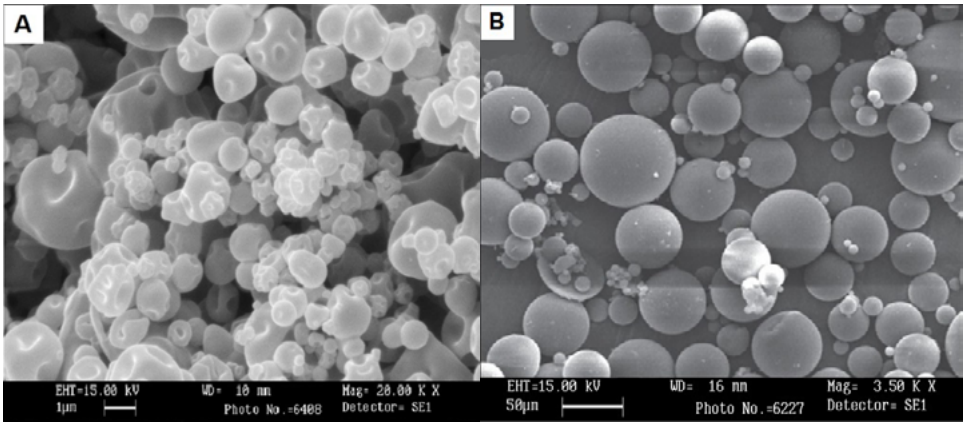

Figure 40. *Representative scanning electron microscopy images of the microparticles obtained by spray drying (A) and by solvent evaporation (B).*

3.4. RHEOLOGICAL ANALYSIS

The rheological tests were performed to select the most suitable concentration of Poloxamer in solution for the formation of a hydrogel matrix with the appropriate rheological characteristics at 37 °C. A wide range of polymer concentrations in solution was used, and G' G" modulus changes were seen. A temperature sweep test was conducted, where both frequency and applied stress were kept constant, at 1 Hz and 0.3 Pa, respectively, while the temperature was varied from 5 °C to 37 °C (Figure 41).

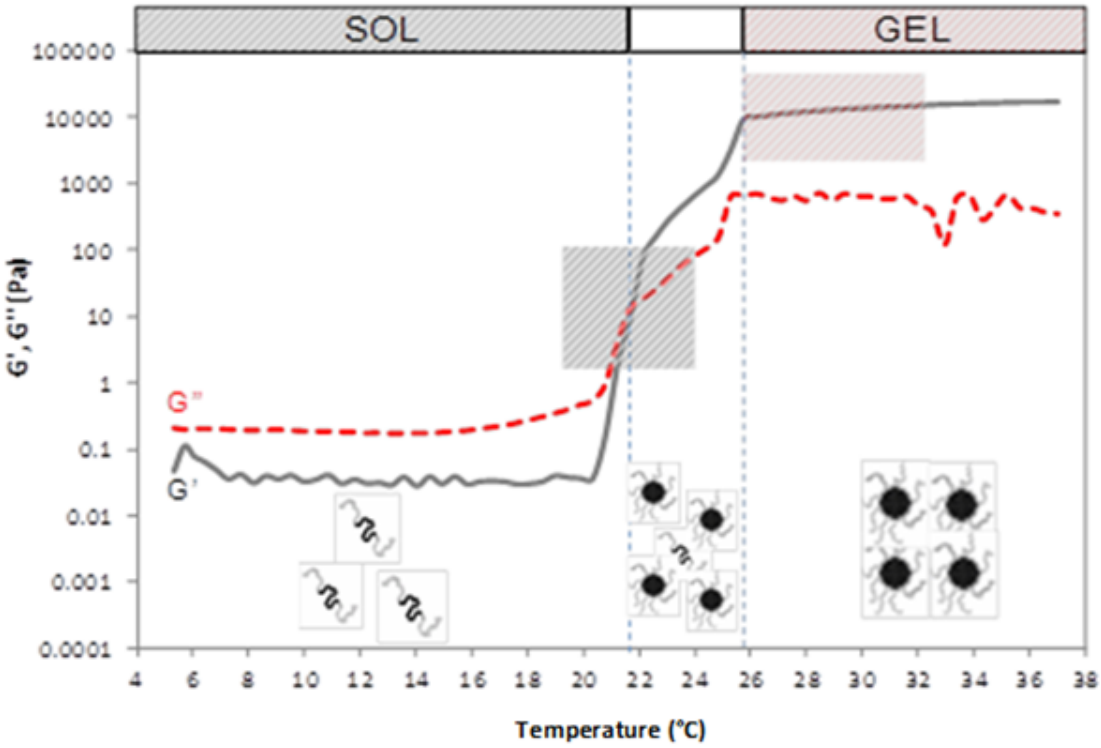

Figure 41. *Temperature sweep test of the Poloxamer 20% (w/w) solutions with the starting and finishing gelling processes highlighted (n = 3).*

As can be seen in Figure 41, at low temperatures the Poloxamer solution was in its liquid state, where the amphiphilic soluble chains would be surrounded by a hydration layer. The G" modulus was higher than that of G'. At 20.65 °C, the G' modulus underwent an increase of circa 4 orders of magnitude. The crossover point between these two moduli identifies the start of the gel-formation process, as the critical micellar temperature. At this point, the progressive de-solvation of the chains of propylene oxide occurs, due to the breaking of the H-bonds

between the copolymer and the solvent, with the gradual formation of the three-dimensional network. This was completely formed at 26 °C, indicating the end of the gel-formation process.

This test was performed for each concentration between 10% and 25% Poloxamer. For each concentration, two temperatures were chosen. The crossover (G' G") temperature is defined as the starting gel-formation temperature, and the gel-formation end temperature corresponds to the plateau of the graph (Figure 41).

The two points for each concentration of Poloxamer polymer obtained from the G' G" modulus of each solution were plotted as a function of the Poloxamer concentration. The grey and red curves shown in Figure 42 represent the trends of the starting sol-gel transition and the variation in the temperature of the end gelation, respectively.

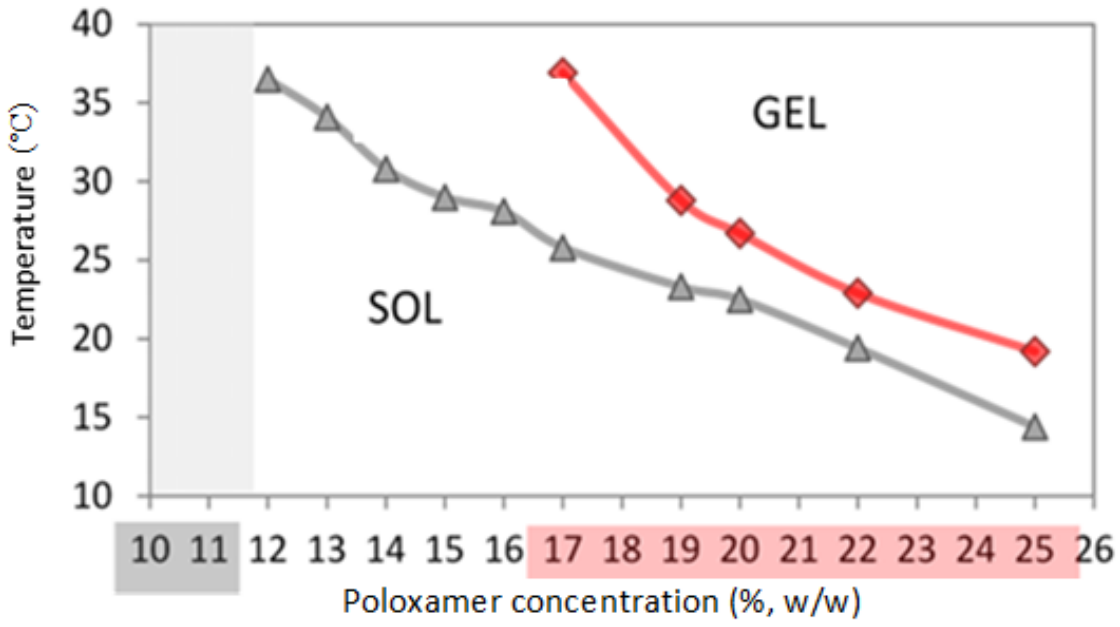

Figure 42. *Variation of the sol–gel temperature as a function of the concentration of the Poloxamer polymer (n = 3).*

Formulations with 10 to 11% (w/w) Poloxamer polymer did not form hydrogels at any experimental temperature. Formulations with 12% to 16% (w/w) Poloxamer polymer showed an initial transitional phase, but they did not reach complete formation of the hydrogel matrix in the tested range of temperatures.

These data show that concentrations of 17% to 21% (w/w) Poloxamer polymer promoted the transition from solution to gel even at room temperature, and these reached a complete hydrogel state at 37 °C. Concentrations from 22% to 25% (w/w) Poloxamer polymer were semisolid at room temperature. For the considered range of temperature, it can be said that the starting sol-gel transition and the end gel-formation temperatures decreased with increasing Poloxamer polymer concentration (Figure 43).

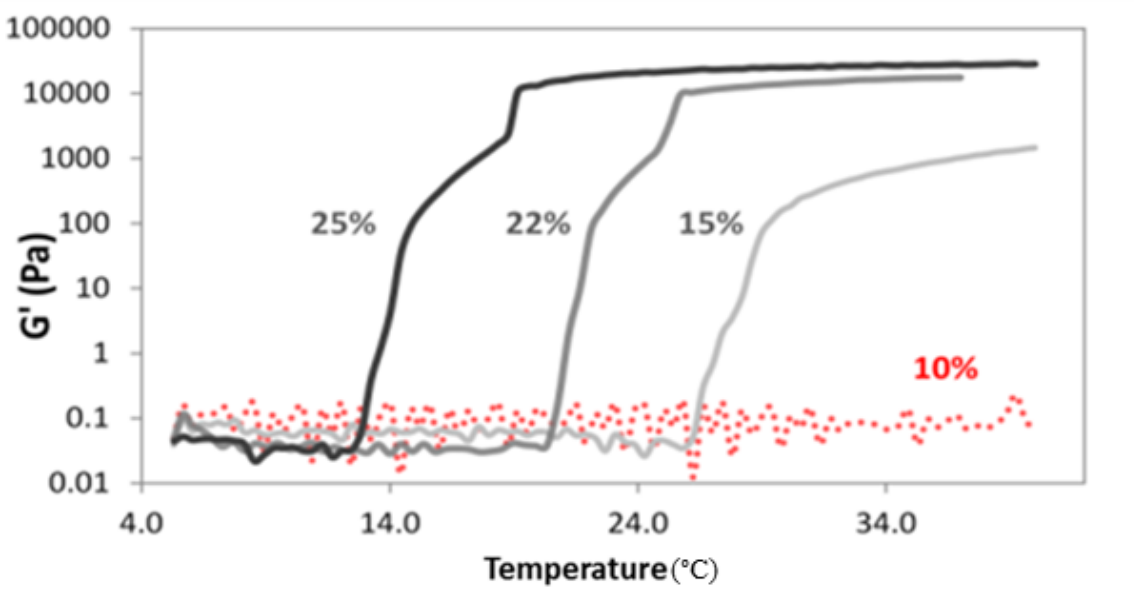

Figure 43. *Trends of G' according to the various Poloxamer concentrations (n = 3).*

Figure 43 shows the G' trends for the various Poloxamer polymer concentrations according to temperature. At the end of this analysis, and considering the results obtained, the 20% (w/w) Poloxamer polymer solution was selected as the most suitable for the purposes of this study. This provides the lowest Poloxamer concentration at which a fast sol-gel transition is obtained over a temperature range that is compatible with the temperature of a surgical operation room; i.e., 20 °C to 22 °C[9]. Therefore, only the 20% (w/w) Poloxamer was further tested from the rheological point of view, to obtain all of the mechanical characteristics of the hydrogel formed.

To evaluate the effects of the dilution after the injection of the polymer in the biological fluids, it was also important to describe the kinetics of the gel formation as a function of time. Thus, a time sweep assay was performed, keeping the frequency constant (1 Hz) and the applied stress constant (0.3 Pa), to evaluate the G' G" trends as a function of time with a heating rate of 1 °C/min (Figure 44).

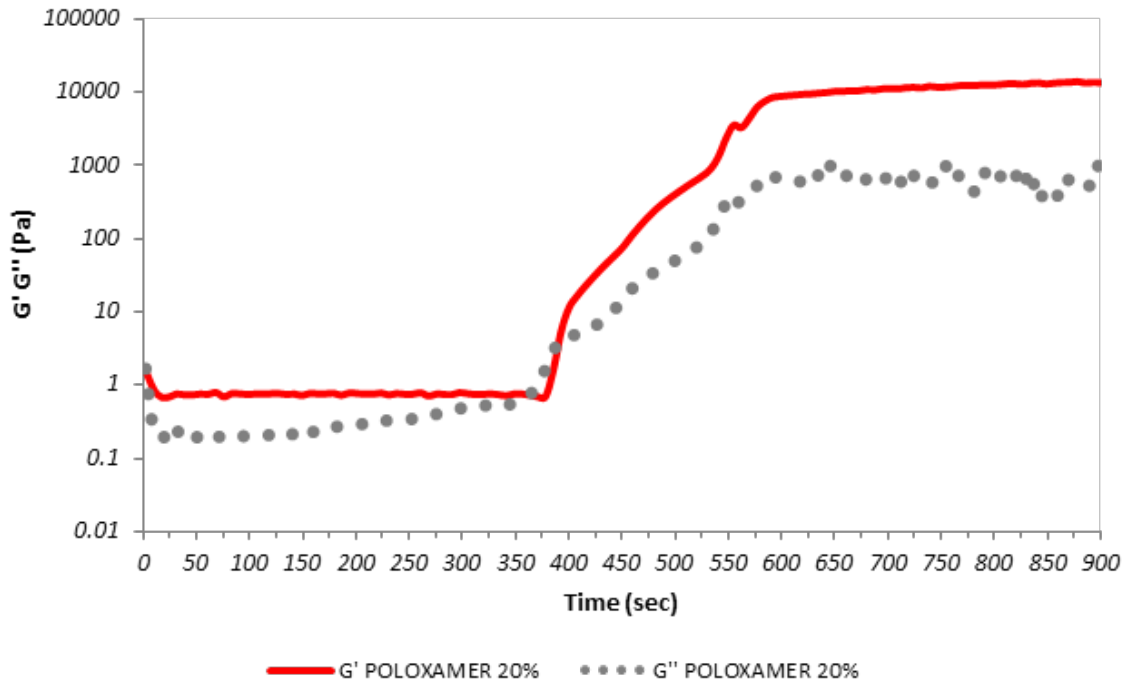

Figure 44. *Time sweep function performed for the 20% (w/w) Poloxamer hydrogel matrix (n = 3).*

A reduced gel-formation time of between 5 min and 10 min would correspond to a lower risk of dilution from the biological fluids at the site of application. Considering that the heating rate during the rheological experiments was 1 °C/min, the average time of the start of gelation was 400 s for the 20% (w/w) Poloxamer hydrogel matrix. Considering that the in-vivo heating rate will be much faster, we could assume that *in vivo* the same process will need much less time to occur, due to the immediate temperature changes from room temperature to 37 °C, so there would be no risk of dilution effects by the biological fluids.

The force of the gel was tested with a stress sweep assay. Figure 45 shows the G' and G" modulus trends as functions of the applied pressure (0.03-1000 Pa). This was performed at 37 °C, with a frequency of 1 Hz. The hydrogel formed at 37 °C (G' > G") appears stable across all of the range analysed. Collapse of the gel network was only seen when applying high stress, of 1000 Pa. Thus by rheological interpretation, this can be consider to be a strong gel.

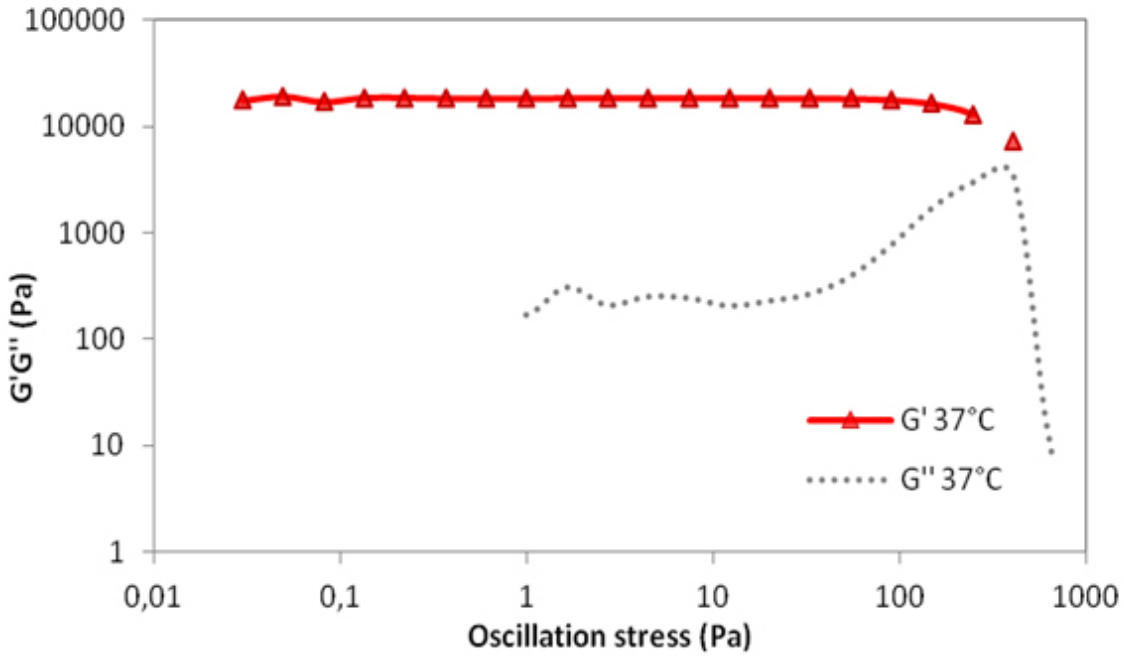

Figure 45. *Stress sweep test of the 20% (w/w) Poloxamer hydrogel matrix (n = 3).*

To evaluate the behaviour of the hydrogel matrix system when in contact with the biological fluids, the rheological experiments were also performed using 0.9 % NaCl and 0.9 % NaCl with NaHCO3 instead of distilled water to create the 20% (w/w) Poloxamer solution (Figure 46). For example, as can be seen in Figure 31, the starting gel-formation temperature point, as the critical micellar temperature, decreased from 21 °C for the aqueous Poloxamer solution to 17 °C for the 0.9% NaCl Poloxamer solution. This was due to the increased micelle stability promoted by increased de-solvation of the polypropylene oxide blocks, as a 'salting-out' effect.

From the outcome of this rheological assay, the simultaneous presence of physiological fluids with the hydrogel matrix network did not have any negative effects on the rheological performance of the Poloxamer hydrogel matrix.

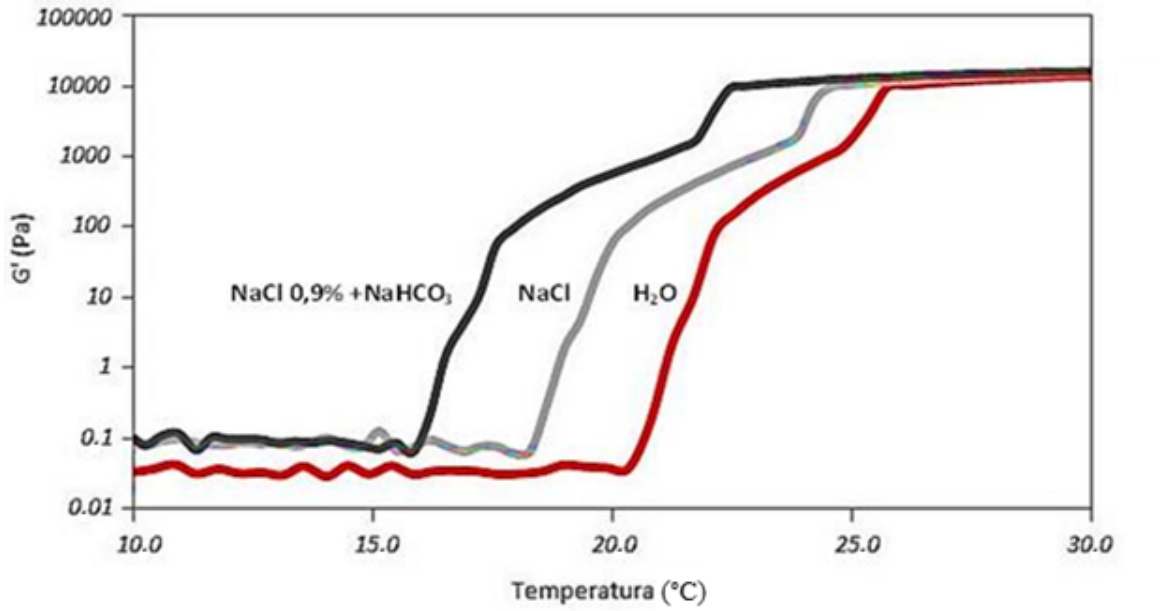

Figure 46. *Profiles for the G' modulus of the 20% (w/w) Poloxamer water solution (red), 0,9% NaCl solution (grey), and 0,9% NaCl with NaHCO3 solution (black), according to temperature (n = 3).*

Considering the aim of the hydrogel matrix system, the sterilisation process has to be evaluated as a mandatory step in the technological transfer to the industry, where this antibacterial system is meant to become a commercial product. In this setting, a rheological assay was performed to determinate the effects on the mechanical behaviour of 20% (w/w) Poloxamer solution and on the resulting hydrogel matrix of a sterilisation cycle in an autoclave. The 20% (w/w) Poloxamer solution was autoclaved at 120 °C for 65 min, as recommended by the industry. Afterwards the sample was left at room temperature for 1 min and then cooled to 15 °C. Once the sample was uniformly cooled, it was rheologically tested through the temperature sweep protocol. The results are shown in Figure 47, where there was an average increase in the starting gel-formation temperature (i.e., the critical micellar temperature) for the autoclaved sample, from 20.1 °C to 23 °C. Thus it can be concluded that the gel-formation temperature does not change dramatically after the sterilization process, and remains in the range of a surgical room.

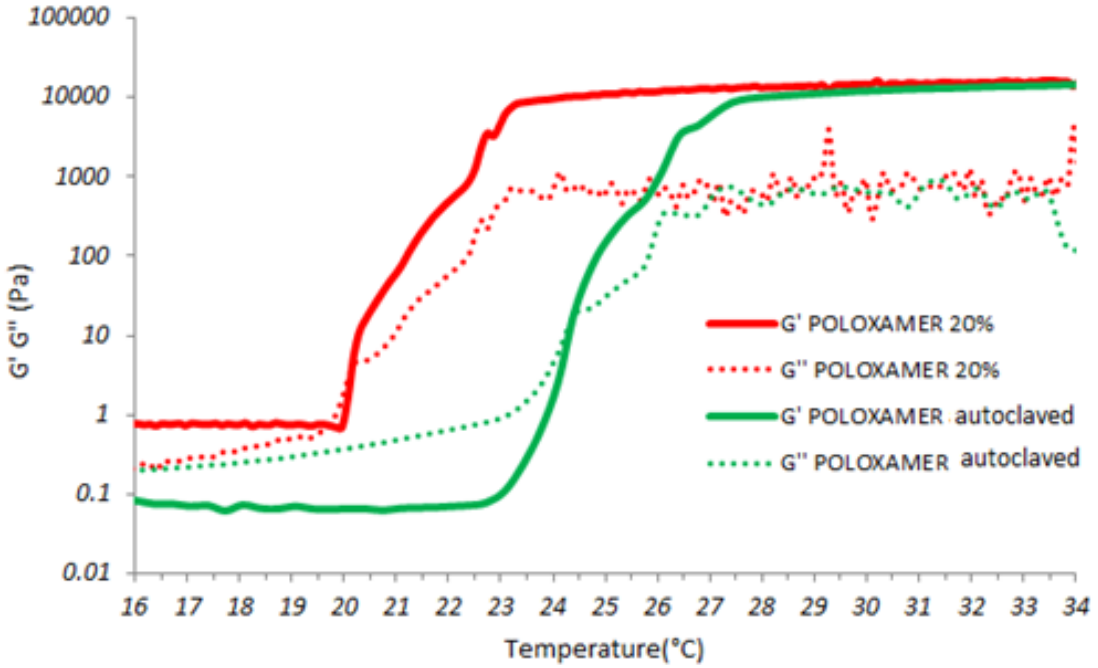

Figure 47. *Temperature sweep for the G' and G' modulus profiles of 20% (w/w) Poloxamer solution (red) and the autoclaved 20% (w/w) Poloxamer solution (green) (n = 3).*

More rheological experiments were needed to determine the vancomycin HCl contribution to the mechanical behaviour of the 20% (w/w) Poloxamer solution, and thus on the gel-formation kinetics. Vancomycin at 1% and 2% (w/w) loaded into the 20% (w/w) Poloxamer solutions were tested and compared to the pure 20% (w/w) Poloxamer reference solution. From the temperature and time sweep protocol results (Figures 48-51) it can be seen that the temperature and time of gel-formation for both the 1% (Figures 48, 49) and 2% (Figures 50, 51) vancomycin-loaded systems were 21.75 °C and 475 s, and 21.77 °C and 478 s, respectively. These data can be compared to the reference 20% (w/w) Poloxamer solution of 20.65 °C and 400 s. These data thus indicate an acceptable compromise to obtain a fast gel-forming hydrogel system at the surgical room temperature[83].

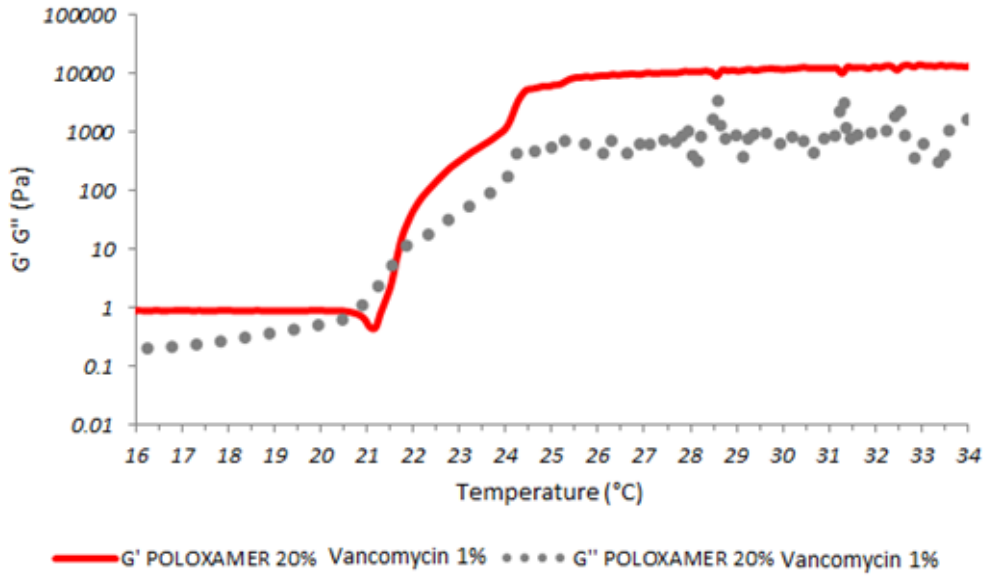

Figure 48. *The G' and G" profiles for 20% (w/w) Poloxamer loaded with 1% (w/w) vancomycin according to temperature for the temperature-sweep protocol (n = 3).*

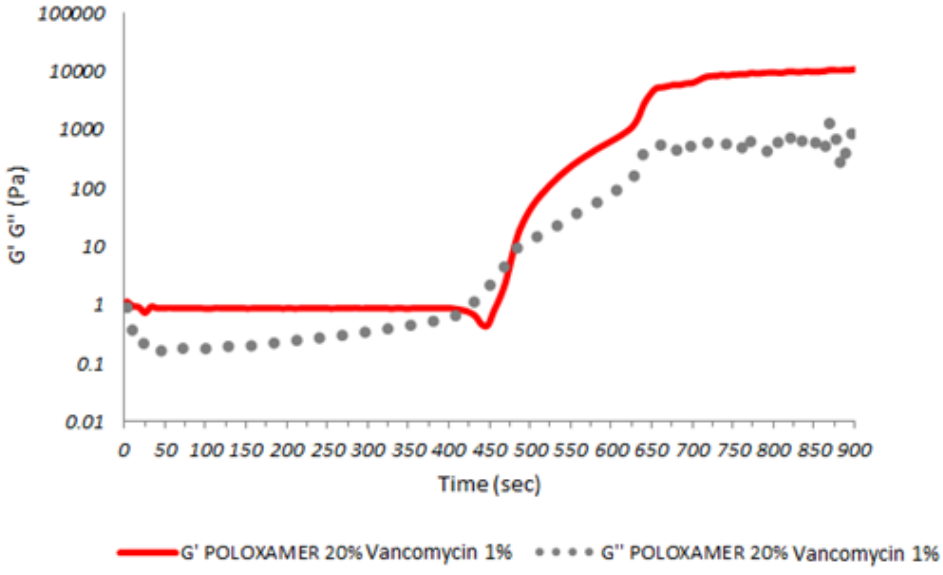

Figure 49. *The G' and G" profiles for 20% (w/w) Poloxamer loaded with 1% (w/v) vancomycin according to time for the time-sweep protocol (n = 3).*

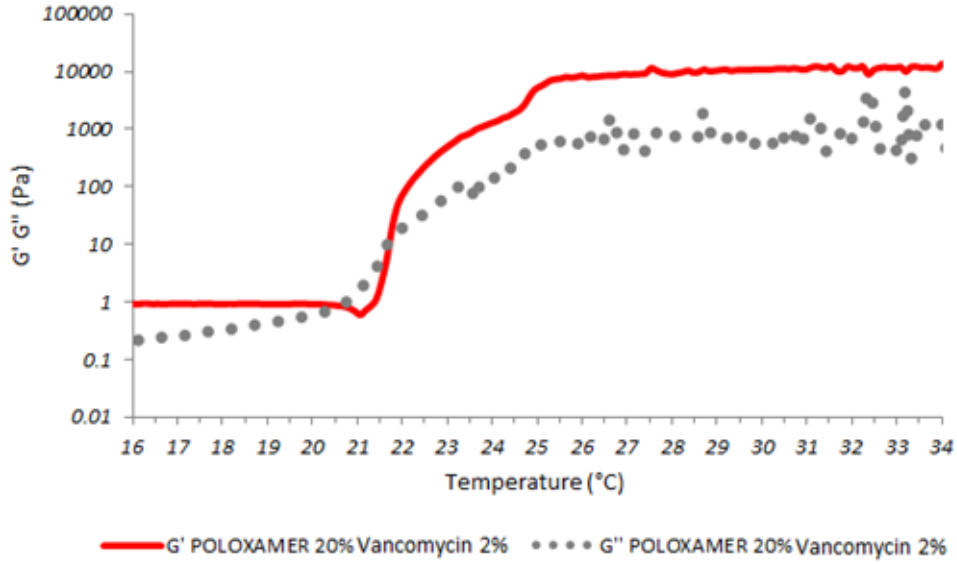

Figure 50. *The G' and G" profiles for 20% (w/w) Poloxamer loaded with 2% (w/v) vancomycin plotted according to temperature for the temperature-sweep protocol (n = 3).*

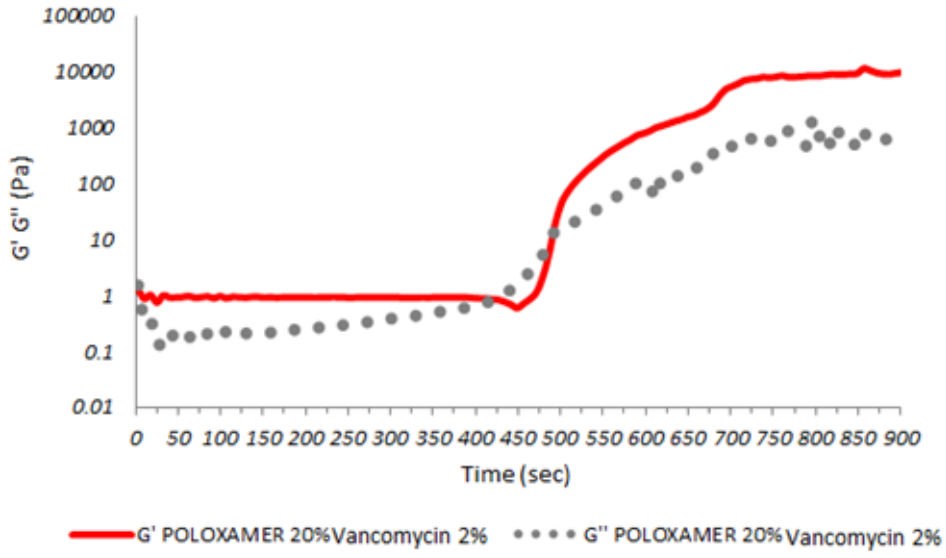

Figure 51. *The G' and G" profiles for 20% (w/w) Poloxamer loaded with 2% (w/v) vancomycin according to time for the time-sweep protocol (n = 3).*

From the stress sweep protocols that were carried out for 1% and 2% vancomycin shown in

Figures 52 and 53, respectively, the hydrogel products that were finally obtained did not lose their strong gel behaviour, compared to the reference samples.

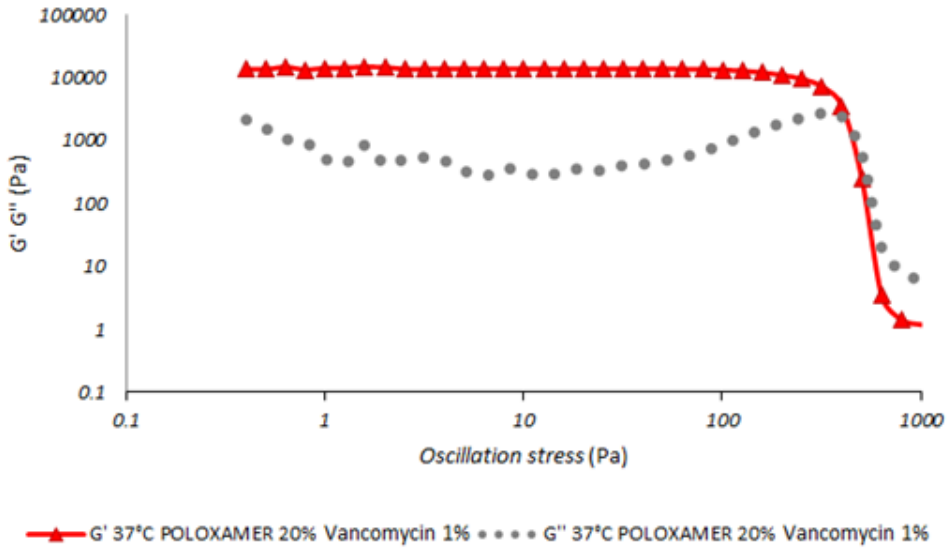

Figure 52. *Stress sweep protocol at 37 °C for 20% (w/w) Poloxamer with 1% vancomycin (n = 3).*

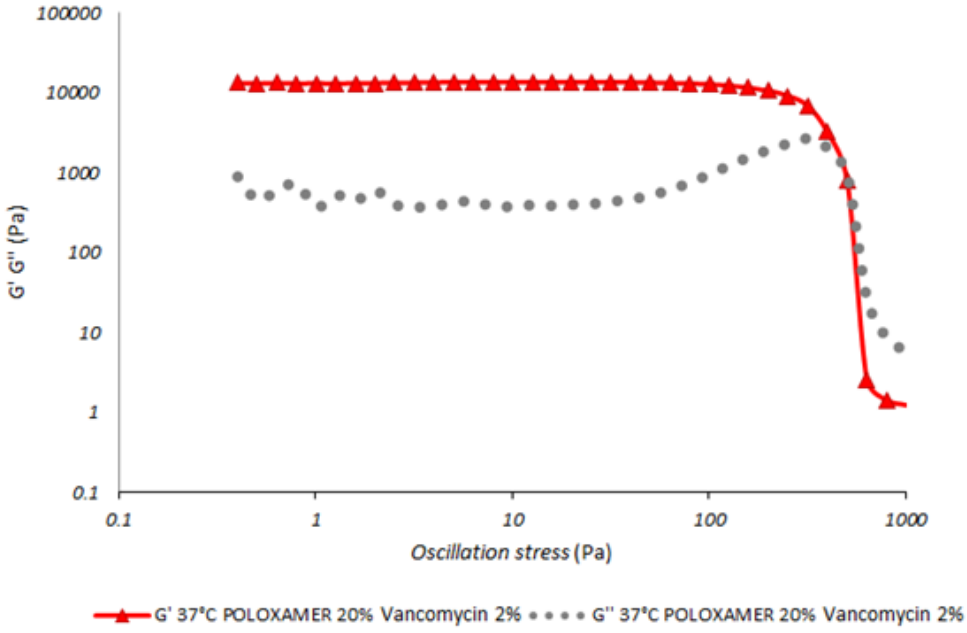

Figure 53. *Stress sweep protocol at 37 °C for 20% (w/w) Poloxamer with 2% vancomycin (n = 3).*

The overall effects of vancomycin in the hydrogel matrix is summarised in Figures 54 and

55, where an average increase in the gel-formation temperature for vancomycin-containing formulations compared to the reference sample can be seen. However, there are no significant differences between the gel-formation temperatures and times for the 1% and 2% vancomycin-loaded formulations. The increased vancomycin concentration inside the formulation did not affect the kinetics of the gel-formation process.

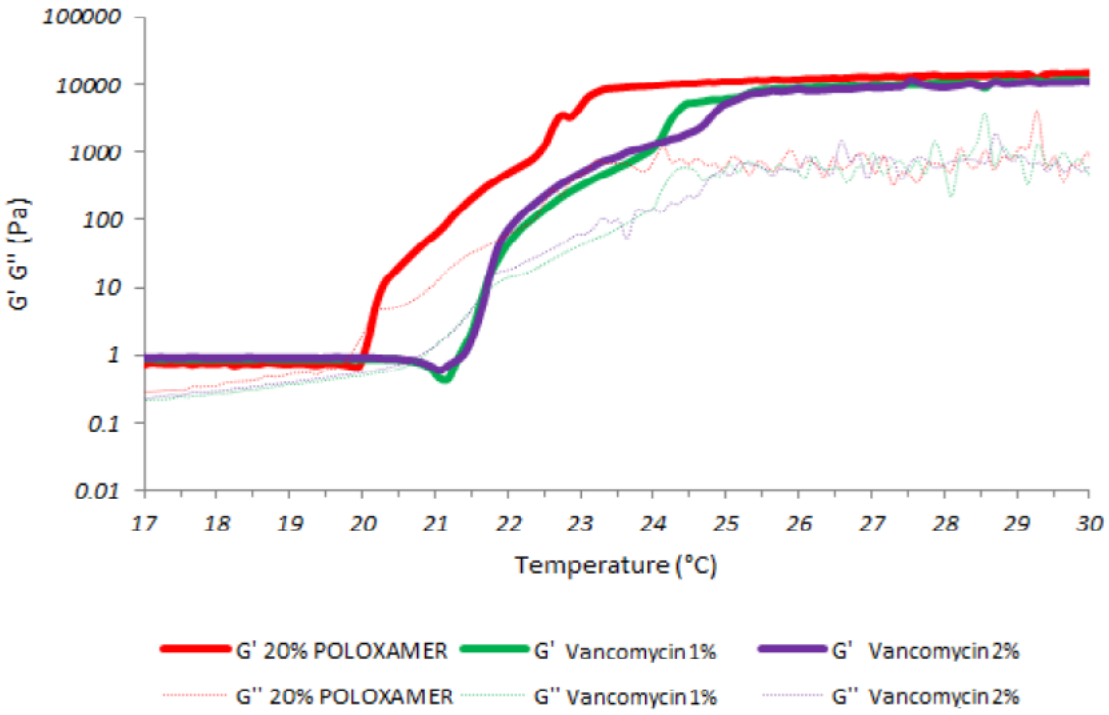

Figure 54. *G' and G" profiles of the different vancomycin formulations according to temperature (n = 3).*

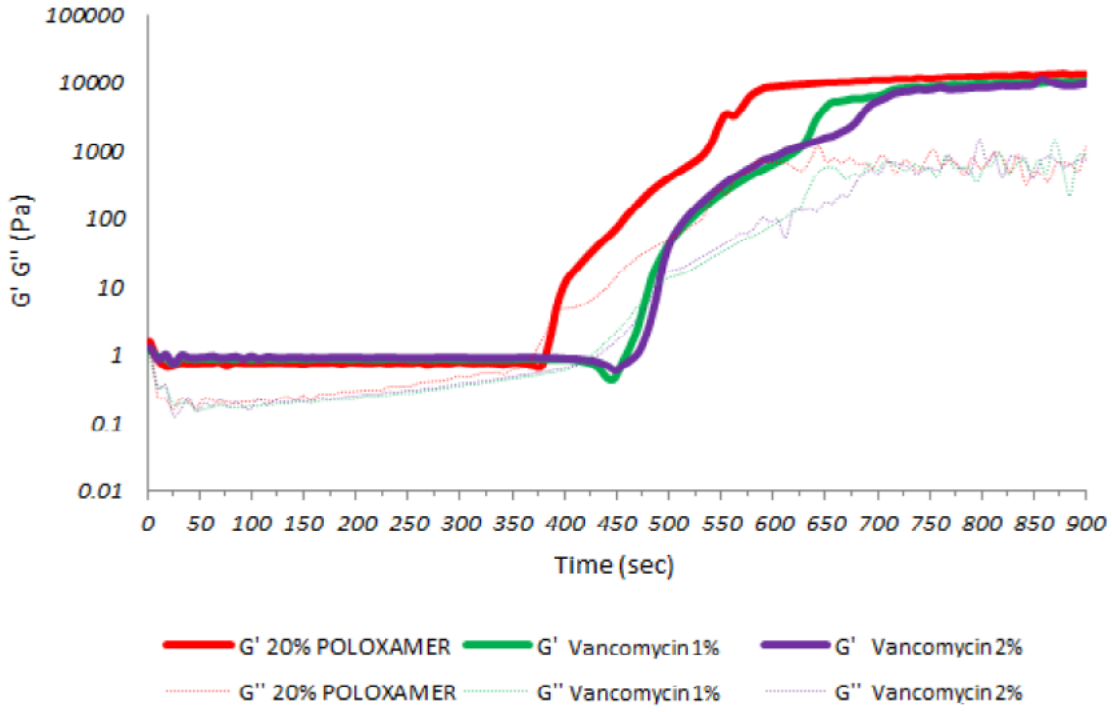

Figure 55. *G' and G" profiles of the different vancomycin formulations according to time (n = 3).*

The last part of the rheological experiments dealt with the evaluation of the effects of a 1% dispersion of microparticles into the 20% (w/w) Poloxamer hydrogel matrix. The reason for the selection of this microparticle quantity (i.e., 1%) is mainly that it allows an optimisation of the ration between the vancomycin loading into the microparticles and the concentration of microparticles loaded in the hydrogel.

As can be seen from Figures 56 and 57, with the addition of a 1% dispersion of microparticles, the temperature and time of gel-formation were slightly greater compared to the reference 20% (w/w) Poloxamer solution without microparticles, as 20.8 °C and 442 s, and 20.65 °C and 400 s, respectively. This increase is lower than that obtained with the various vancomycin concentrations, where temperature and time of gel formation for the 1% and 2% vancomycin-loaded systems were 21.75 °C and 475 s, and 21.77 °C and 478 s, respectively.

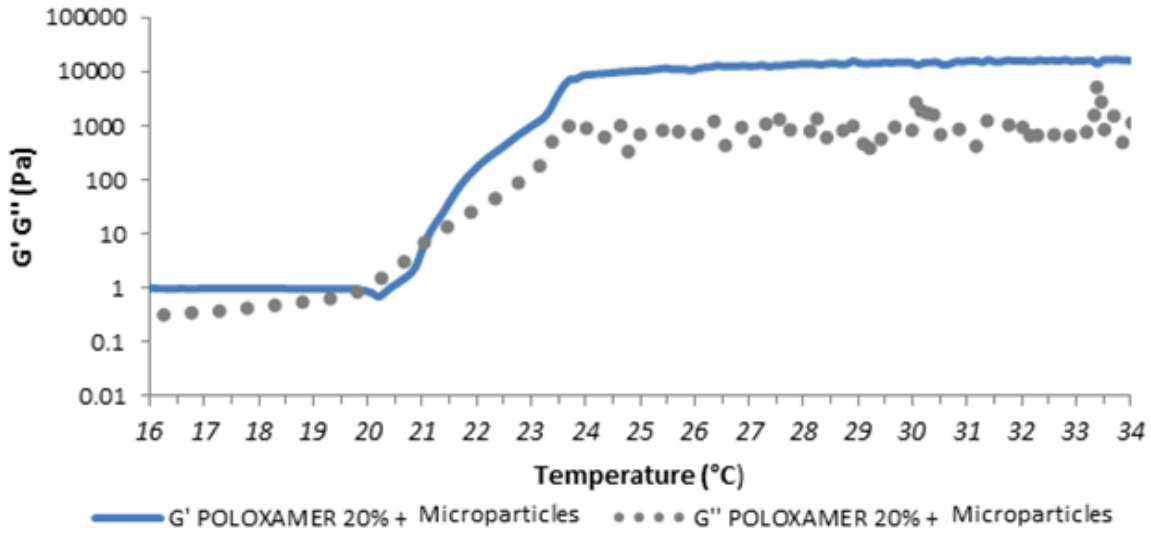

Figure 56. *G' and G" as functions of the 20% (w/w) Poloxamer hydrogel matrix with microparticles of PLGA according to temperature during temperature sweep experiments (n = 3).*

These relatively small increases in the gel-formation temperature and the time might be due to the mean diameter of the microparticles (2.25 μm) with their derived mass, which will absorb energy in terms of calories, and thus might interfere with the three-dimensional organisation of the 20% (w/w) Poloxamer hydrogel matrix network. In other words, more energy will be needed, and thus more time, to complete the formation of the mature hydrogel. On the other hand, the various vancomycin-loaded systems produced greater changes in the temperature and time of gel formation compared to the microparticle dispersion system. This might be due to the mean hydrodynamic diameter of the micelles, which is between 20 and 80 nm. The microparticles were too big to have any important interference in their organisation, while on the contrary, vancomycin has a dimeric molecular dimension, that might lead to greater interference effects on the micelle organisation[84].

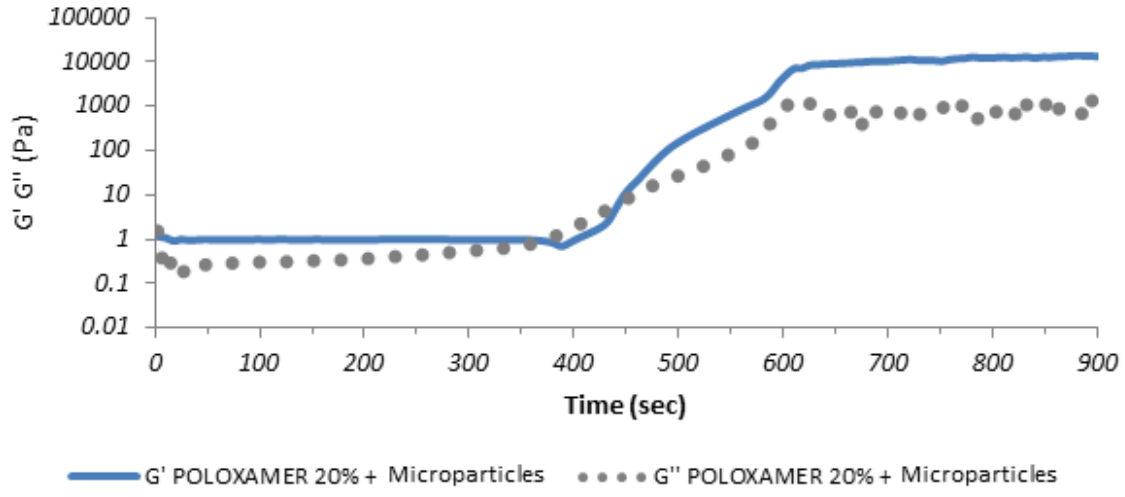

Figure 57. *G' and G" as functions of 20% (w/w) Poloxamer hydrogel matrix with the 1% dispersion of microparticles according to time during temperature sweep experiments (n = 3).*

It is interesting to note that from the stress sweep assay shown in Figure 58, the Poloxamer hydrogel matrix system with the addition of 1% microparticles as a dispersion does not lose its properties as a 'strong gel'.

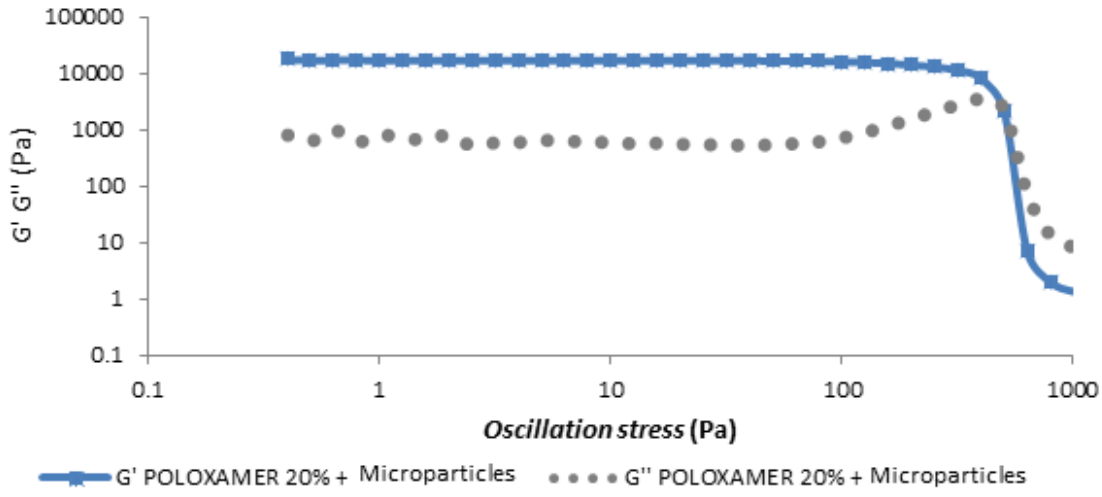

Figure 58. *Stress sweep protocol at 37 °C for 20% (w/w) Poloxamer hydrogel matrix with the PLGA microparticles (n = 3).*

3.5. IN-VITRO DISSOLUTION ANALYSIS

The *in-vitro* evaluation of the 20% (w/w) Poloxamer hydrogel matrix according to its vancomycin release capacity was performed with the vancomycin HCl loading of 1% and 2% (w/w). These data define the concentration (μg/mL) as a function of time (hours), as shown in Figure 59, while in Figure 60 shows the percentages of the release as a function of time.

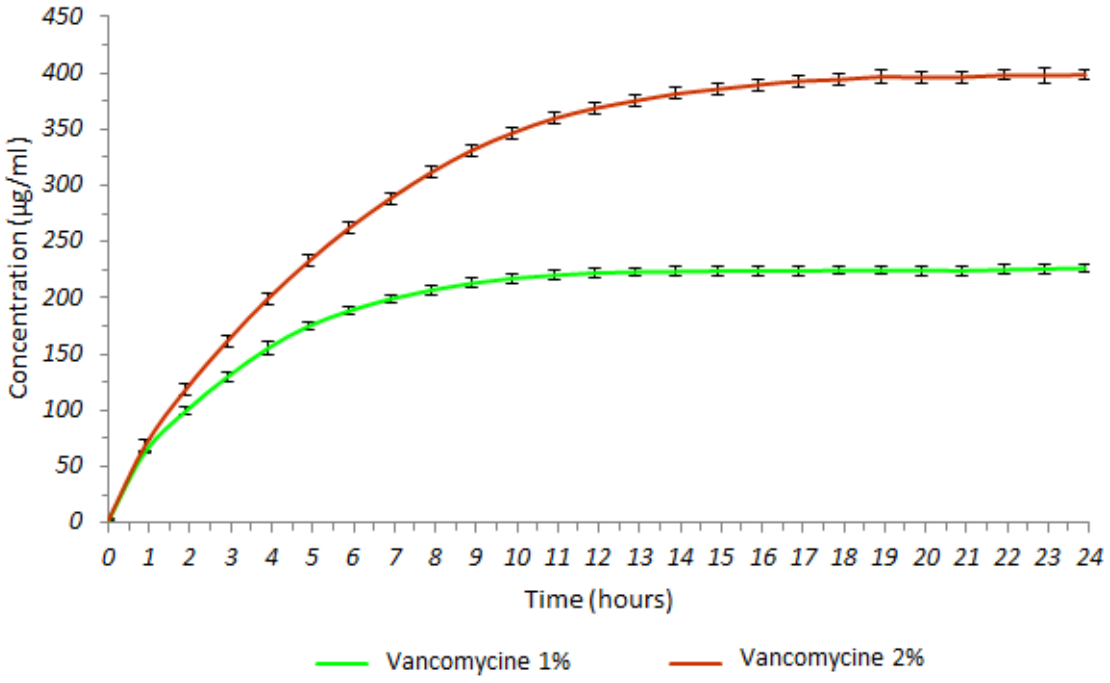

Figure 59. *Release profile (over 24 h) of vancomycin HCl from the 20% (w/w) Poloxamer hydrogel matrix (n = 3, SD <4%).*

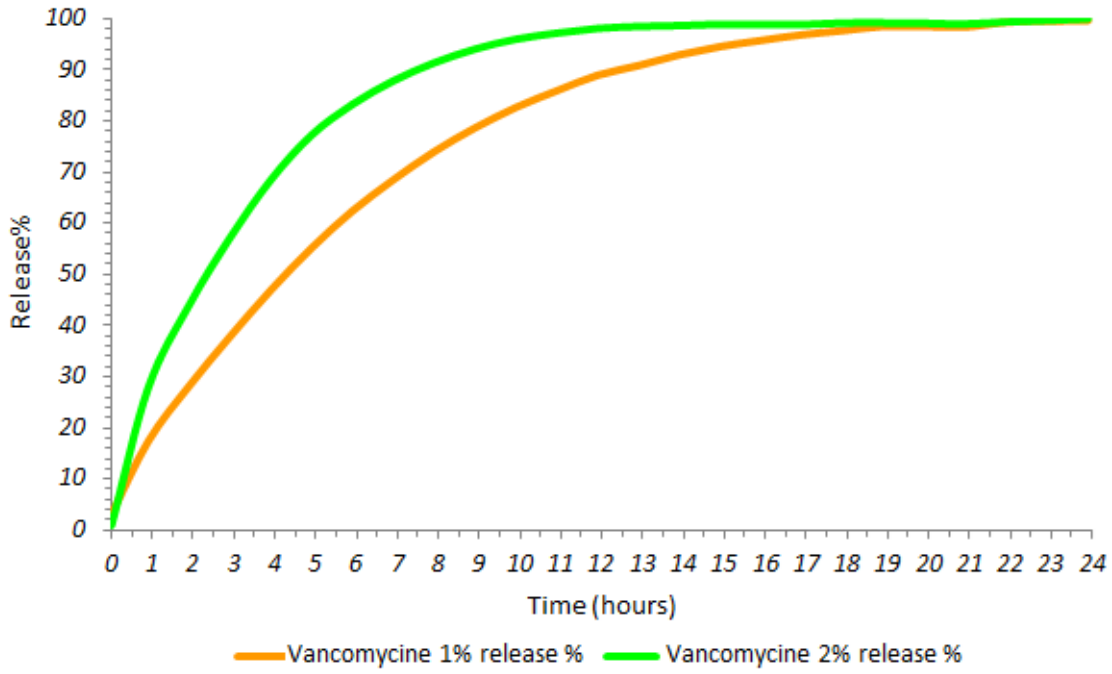

Figure 60. *In-vitro release profiles (over 24 h) of vancomycin from the 20% (w/w) Poloxamer hydrogel matrix (n = 3, SD <4%).*
This demonstrates complete release of the vancomycin HCl within the first 24 h.

From the data illustrated in Figure 59, it can be seen that the 1% and 2% (w/w) vancomicyn HCl loading into the 20% (w/w) Poloxamer hydrogel matrix released 100 μg/mL and 226 μg/mL, respectively, of the API after the first 24 h. During the first hour, these systems released 18 μg/mL and 67 μg/mL, respectively, which are values that are in the range of the MIC of *S. aureus,* one of the most common bacterial strains involved in orthopaedic infections[85] (Table 7).

Furthermore, dissolution tests were carried out for the microparticles batches (i.e., A1-A6), and the vancomycin HCl concentrations were recorded to determine the release behaviour from the PLGA 50:50 microparticles. These results are shown in Figure 61. From these outcomes, it can be seen that the microparticle system offers a controlled release carrier for the vancomycin HCl. In particular, for batches A1-A4, which were produced by spray drying, there was a controlled and prolonged release profile for the API. The vancomycin release from batch A5, which was also produced by spray drying, was characterised by an initial burst phase, due to the vancomycine HCl present on the microparticle surface that is released immediately, followed by a slow controlled release phase, due to the release of the internal vancomycin HCl.

Table 7. *Vancomycine MICs for the Staphylococcus aureus strains with different sensitivities, according to the guidelines of the US Center for Disease Control and Prevention.*

***Staphylococcus aureus* classification**	**Vancomycin MIC** (μg/mL)
Susceptible	4-8
Intermediate	8-16
Resistant	16-32

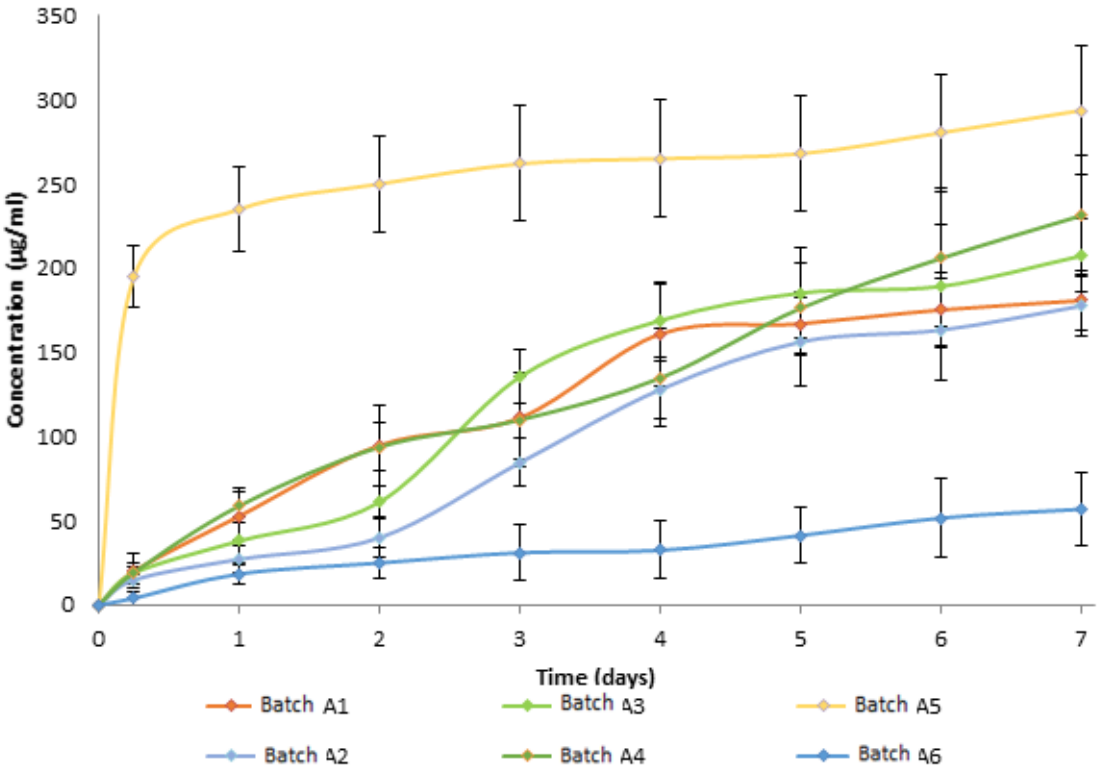

Figure 61. *Release profile of vancomycin HCl from the microparticles system for batches A1-A6 (n = 3).*

Batch A6, which was obtained by the solvent evaporation method, showed an extremely slow release profile of vancomycin HCl. In particular, over the first 24 h was circa 30% compared to the vancomycin release from the batches obtained by spray drying. This behaviour will be mainly due to the dimensions of the batch A6 microspheres, at circa 50 µm in diameter. This is 10-fold to 20-fold greater than the dimensions of the batches produced by spray drying. If we consider the release as uniform all over the surface of the single microparticles, this will be affected by the dimensions of the microparticles; the grater the average dimension of the microparticles, the lower the specific surface area, and consequently the vancomycin release. Figure 62 highlights these differences in terms of the vancomycin release between the batches obtained by the different methods and formulations.

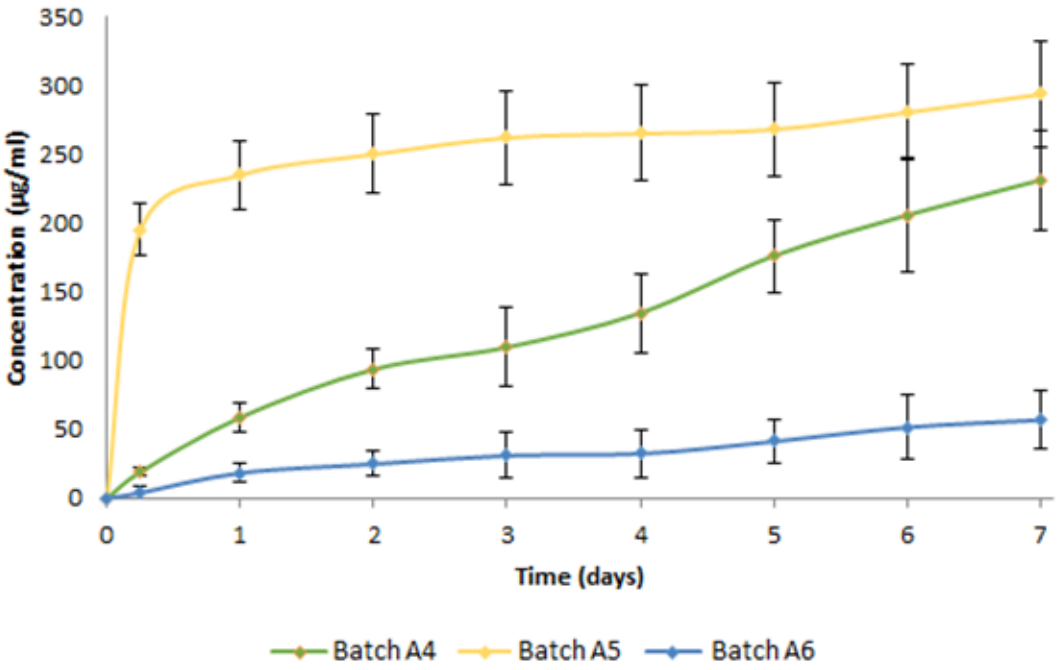

Figure 62. Vancomycin HCl release profiles from batch A4 (spray dried), batch A5 (spray dried) and batch A6 (solvent evaporated) over 7 days (n = 3).

Moreover, the *in-vitro* dissolution experiments were performed on the microparticles loaded with vancomycin HCl added as the 1% dispersion to the 20% (w/w) Poloxamer matrix hydrogel, to determine the effects of the hydrogel matrix on the release from the microparticles of the API. Three systems were tested here:

1. Batch A5 microparticles;
2. Batch A5 microparticles with 20% (w/w) Poloxamer;

3. Batch A5 microparticles with 20% (w/w) Poloxamer loaded with 1% vancomycin HCl.

These data are presented in Figure 63, as the comparison with the release of the API from the batch A5 microparticles. The release in the analysed systems were the same over the first 6 h, after which differences can be seen in the release profiles. For the batch A5 microparticle system, the release rate decreased to a lower, but constant, rate. For the formulation that contained microparticles as a 1% dispersion in the 20% (w/w) Poloxamer hydrogel matrix, the release rate was constant over the full first 24 h, after which it also decreased.

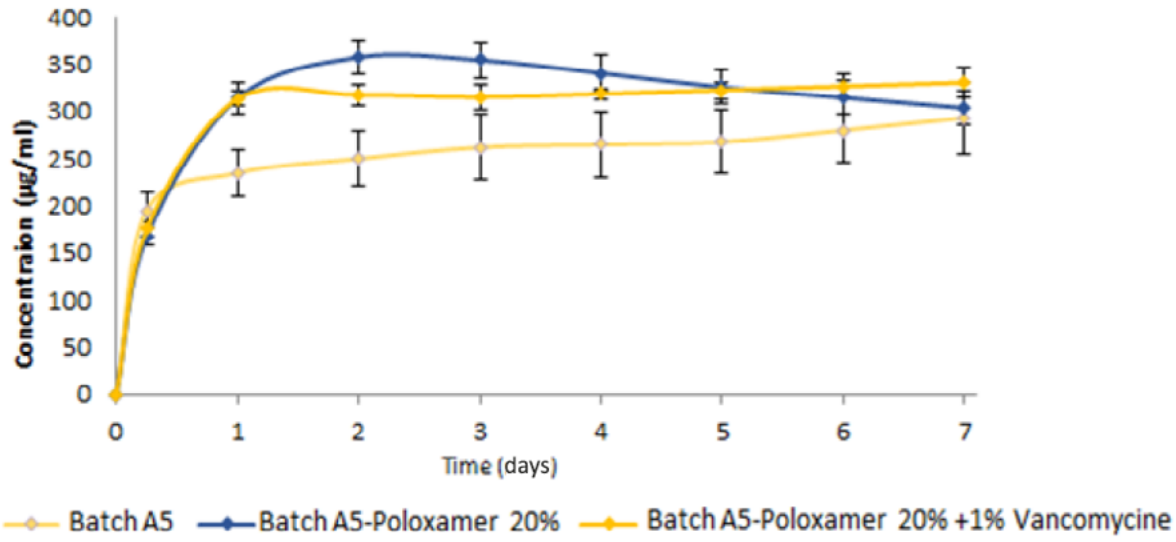

Figure 63. *Release profile for vancomycin from batch A5 microparticles, from batch A5 microparticles in the 20% (w/w) Poloxamer hydrogel matrix, and from batch A5 microparticles in the 20% (w/w) Poloxamer hydrogel matrix loaded with 1% vancomycine HCl (n = 3).*

3.6. MICROBIOLOGICAL ANALYSIS

Microbiological evaluation was performed for the 20% (w/w) Poloxamer, 20% (w/w) Poloxamer loaded with vancomycin HCl at 245 μg and 490 μg, and vancomycin HCl 30 μg as the reference (Figure 64). The inhibition diameters for each condition were expressed as means, in mm (Table 8).

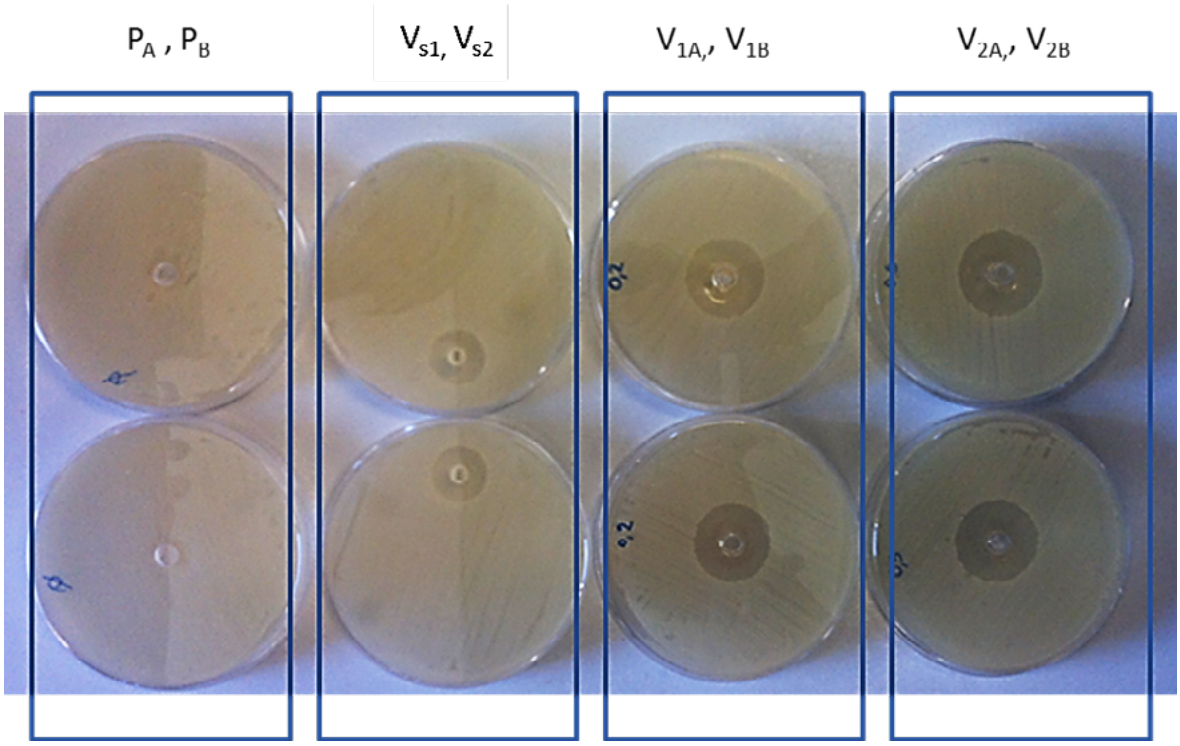

Figure 64. *Representative images of the inhibition effects after incubation at 37 °C overnight. P_A, P_B, 20% (w/w) Poloxamer; V_{S1}, V_{S2}, reference vancomycin HCl 30 μg; V_{1A}, V_{1B}, and V_{2A}, V_{2B}, 20% (w/w) Poloxamer loaded with vancomycin HCl (245 μg, 490 μg. respectively).*

Table 8. *Inhibition diameters for conditions illustrated in Figure 64.*

Plates	Condition	Inhibition diameter vs. S. *epidermidis* (mm)
P_A, P_B	20% (w/w) Poloxamer	0
V_{S1}, V_{S2}	Vancomycin HCl reference (30 µg)	19-19
V_{1A}, V_{1B}	20% (w/w) Poloxamer loaded with vancomycin HCl (245 µg)	27-27
V_{2A}, V_{2B}	20% (w/w) Poloxamer loaded with vancomycin HCl (490 µg)	27-28

From these data it can be seen that there was diffusion of the vancomycin HCl from the 20% (w/w) Poloxamer hydrogel matrix (i.e., V_{1A}, V_{1B}, 245 µg; V_{2A}, V_{2B}, 490 µg) into the growth medium. As a consequence, the bacterial growth was successfully stopped. Moreover, there was no significant difference between the two different loads of vancomycin HCl in the 20% (w/w) Poloxamer hydrogel matrix.

Further to this, the antibacterial performance was tested for the microparticle dispersion in the 20% (w/w) Poloxamer hydrogel matrix system. The batch A6 microparticles were chosen to test this antibacterial performance because of their accentuated prolonged API kinetic behaviour over the first 24 h. Two different samples were prepared here:

1. System A: 20% (w/w) Poloxamer hydrogel matrix (120 µL) with a 4 mg dispersion of batch A6 microparticles was injected into a trabecular Ti6Al4V disc. This corresponded to 540 µg vancomycine HCl

2. System B: 20% (w/w) Poloxamer hydrogel matrix (120 µL) loaded with 0.5% (w/w) vancomycin HCl with a 4 mg dispersion of batch A6 microparticles was injected into a trabecular Ti6Al4V disc. This corresponded to 1200 µg total vancomycin HCl.

Representative results are shown in Figures 65 and 66, with the full listing in Table 9.

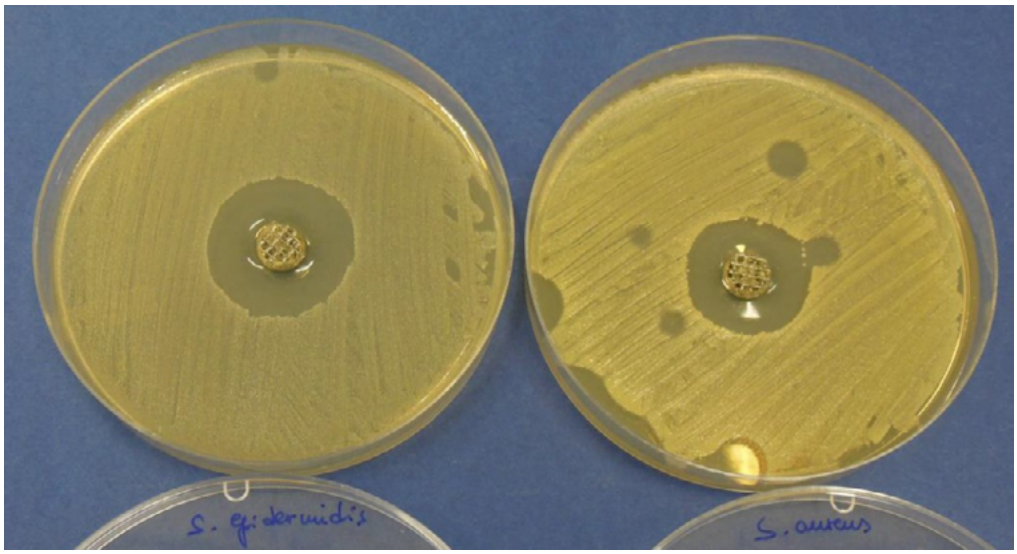

Figure 65. *Representative plates showing the diameter of inhibition of System A.*

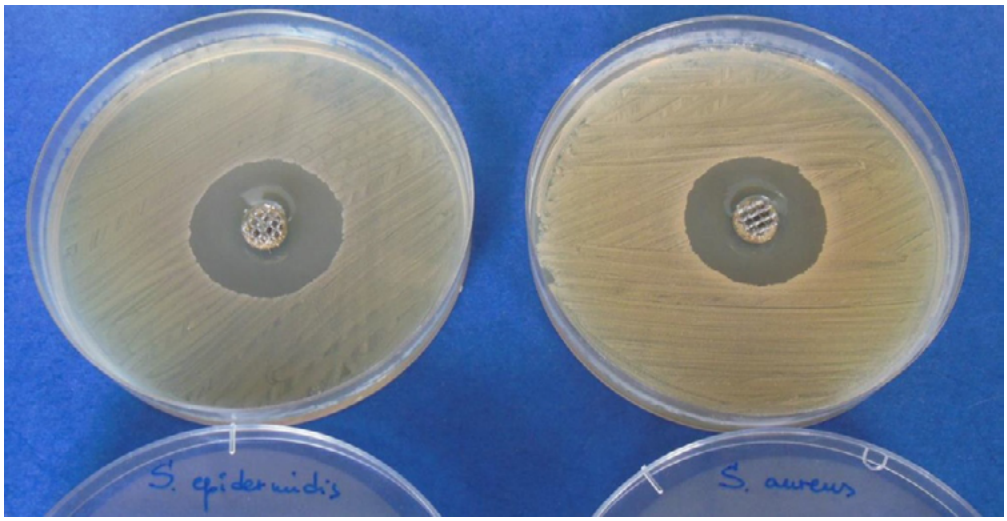

Figure 66. *Representative plates showinng the diameter of inhibition of System B.*

Table 9. *Diameter of inhibition expressed as mean in mm for MRSA and Resistant Staphylococcus epidermidis.*

System	**Diameter of inhibition vs. MRSA** (mm)	**Diameter of inhibition vs. S. *epidermidis*** (mm)
A	24	28
B	30	31

Considering the overall results from the microbiological experiments, the biphasic antibacterial system was shown to have inhibition activity on the tested bacterial strains. From the results of the mean diameters of inhibition, even when tested individually, both phases were highly efficient for the bacterial growth inhibition. In particular, taking the individual phases, the vancomycin-loaded Poloxamer hydrogel matrix and the microparticles with vancomycin show the same capacity to inhibit the bacterial growth on a prosthesis-like sample. Taking into consideration that the two phases have different loading and kinetic release of vancomycin, these results will be differently affected in some way. Indeed, it can be considered that the medium in the agar plates where the bacteria were left to grow during the night always had the same capacity for the permeation of the vancomycin, independent of the tested phase. For this reason, the mean inhibition diameters were similar for both the individual components of the antibacterial system. Thus, to understand the potentiality of the biphasic system, it has to be tested *in vivo*. At the time of writing, an *in vivo*, real time monitoring and non-invasive methodology is being set up based on bioluminescent bacteria, to investigate the antibacterial capacity of this system[86].

3.7. MATHEMATICAL MODEL

For the model to be operative, it was necessary to determinate the D_M, D_G and D_p, the local drug concentrations in the membrane, the gel, and the particles, respectively (see section 2.2.10.). For this purpose, the model was fit to experimental data according to the donor environment filled with the buffer solution containing the drug (vancomycin) at 20 mg/ mL (at 37 °C). For the sake of simplicity, all partition coefficients were set to 1.0, and φ, the particle volume fraction in the gel, was set to zero, as there were no particles. The vancomycin diffusion coefficient in the buffer (at 37 °C) was evaluated according to the Stokes Einstein equation (D_0 = 3.8 ×10^{-6} cm^2/s), while the system geometrical characteristics were: V_r (receiver volume) = 200 cm^3; L_M (membrane thickness) = 50 mm; V_G (gel volume) = 2.5 cm^3; and L_G (gel thickness) = 0.24 cm.

As can be seen from Figure 67, there is a good agreement between the best fit model (solid line) and the experimental data (circles) that were obtained during the first and second year of the project. D_M, turns out to be 2.1 ×10^{-6} cm^2/s.

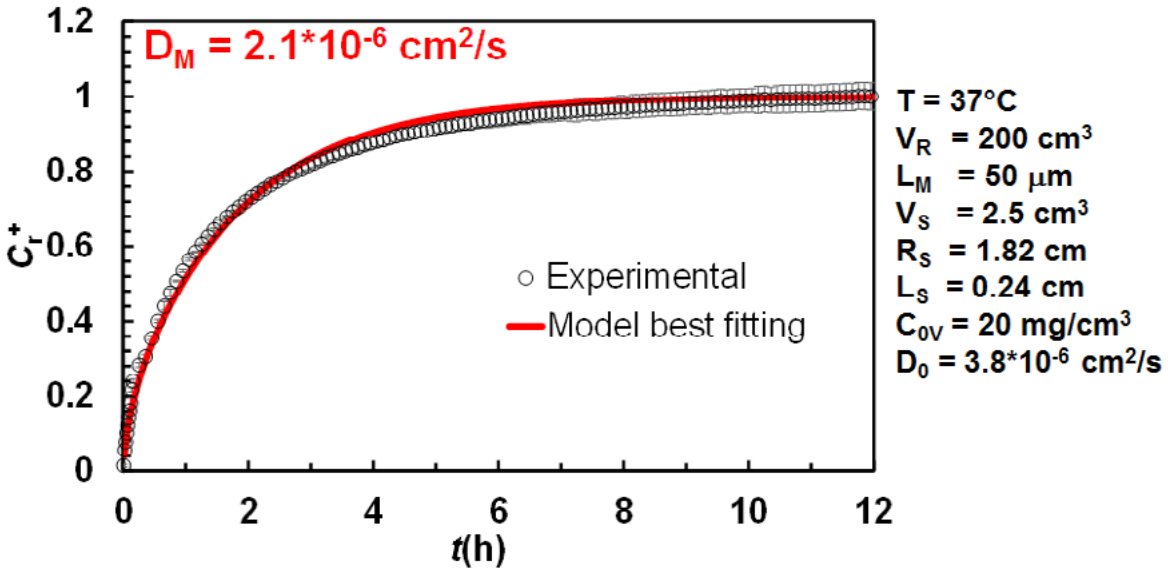

Figure 67. *Comparison between the API release kinetics as the mathematical best fit to the model versus the experimental data from an API buffer solution, to determine the D_M.*

This value of 2.1 ×10^{-6} cm^2/s for D_M is reasonable, as although this is smaller than D_0 (3.8 ×10^{-6} cm^2/s), it is not so far from D_0; i.e., the membrane did not create a very important barrier to the drug transfer in the receiver environment.

The second experimental test was devoted to the determination of the drug diffusion coefficient in the gel phase, as D_G. For this purpose, the donor environment was filled with 20% (w/w) Poloxamer hydrogel (at 37°C) that contained vancomycin at the usual concentration of 20 mg/mL. The mathematical model was fitted to the experimental data on the basis that $\varphi = 0$ (i.e., no PLGA particles), and the previously determined D_M (2.1×10^{-6} cm^2/s) (Figure 68). It can be seen that the best fit model (Figure 68, solid line) is a relatively good fit, as it always lies inside the standard deviation of the data. The resulting diffusion coefficient D_G is 1.5×10^{-6} cm^2/s. Again, this appears to be a reasonable value, as it is lower than D_0 and D_M.

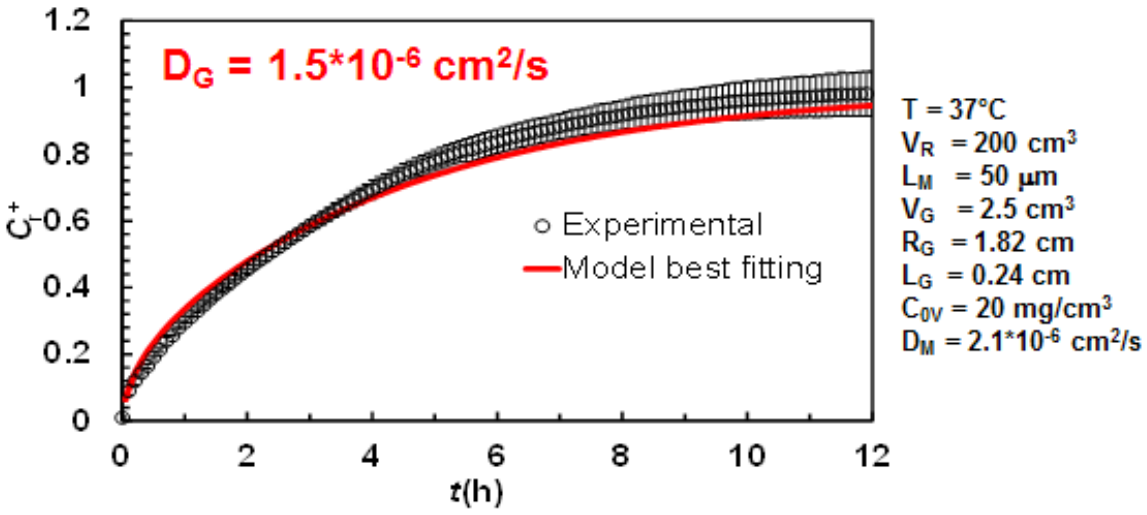

Figure 68. *Comparison between the API release kinetics as the mathematical best fit to the model versus the experimental data from an API containing Poloxamer hydrogel, to determine the D_G.*

Knowing D_0, D_M and D_G, the model was fit to the experimental data referring to the drug release from a donor environment constituted by the hydrogel containing the vancomycin-loaded PLGA particles (vancomycin, 725 mg/mL) at a volume fraction φ = of 0.04. Although the number of experimental data has to be increased, the best fit model (Figure 69, solid line) appears to correctly describe the experimental data. The only fitting parameter, D_p, is 0.7×10^{-11} cm^2/s. This very low value can be explained remembering that it accounts for all of the drug transport resistance involved in vancomycin release, including vancomycin dissolution (in the particles in its crystalline form), drug diffusion inside the particles, plus probable mass transfer resistance at the particles/ hydrogel phase interface.

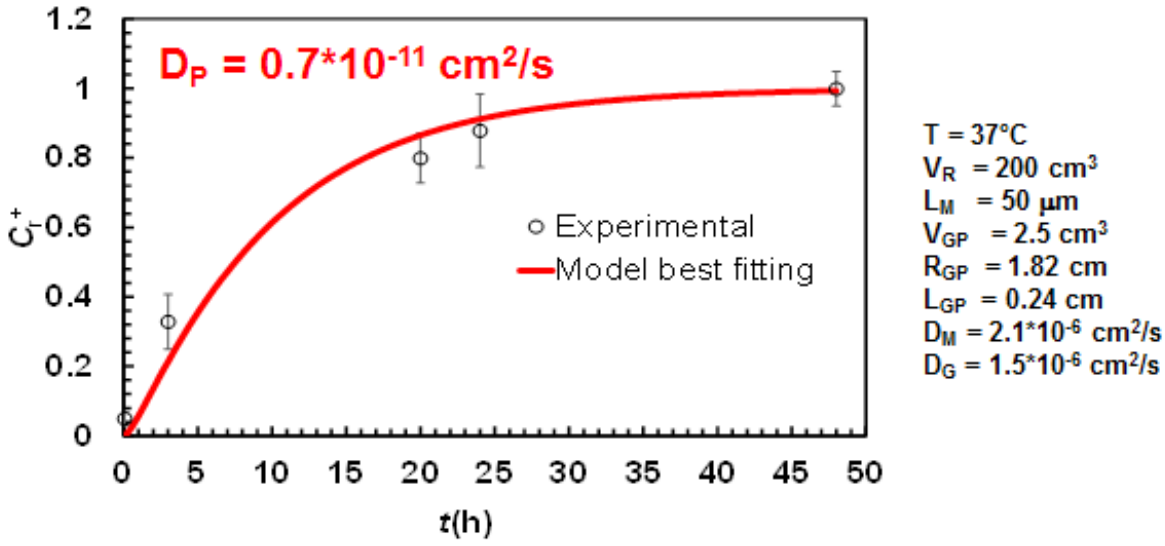

Figure 69. *Comparison between the API release kinetics as the mathematical best fit to the model versus the experimental data as the API from the PLGA microparticles loaded into the hydrogel to determinate the D_P.*

To have a deeper understanding of the studied release phenomenon, Figure 70 reports the trend in the vancomycin concentration inside the gel (C_G) at different times (6-48 h), assuming the above determined values of the various diffusion coefficients (i.e., D_M, D_G, D_p).

Correctly, C_G decreases moving from the gel bottom ($X^+ = X/L_G = 0$) to the gel/ membrane interface ($X^+ = 1$), and this decrease is more evident at the beginning of the experiment (at 6 h) while it tends to disappear after 48 h. In contrast, Figure 71 show the trend of the vancomycin concentration (C_p) inside the particles ($R^+ = r/R_p$) at the different positions in the gel (X^+), and for different times (6-48 h).

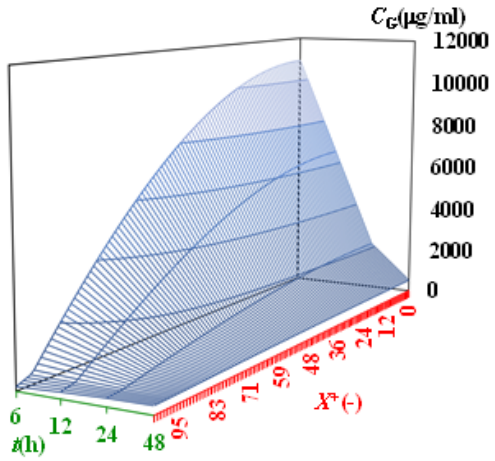

Figure 70. *Vancomycin concentration inside the hydrogel at different times.*

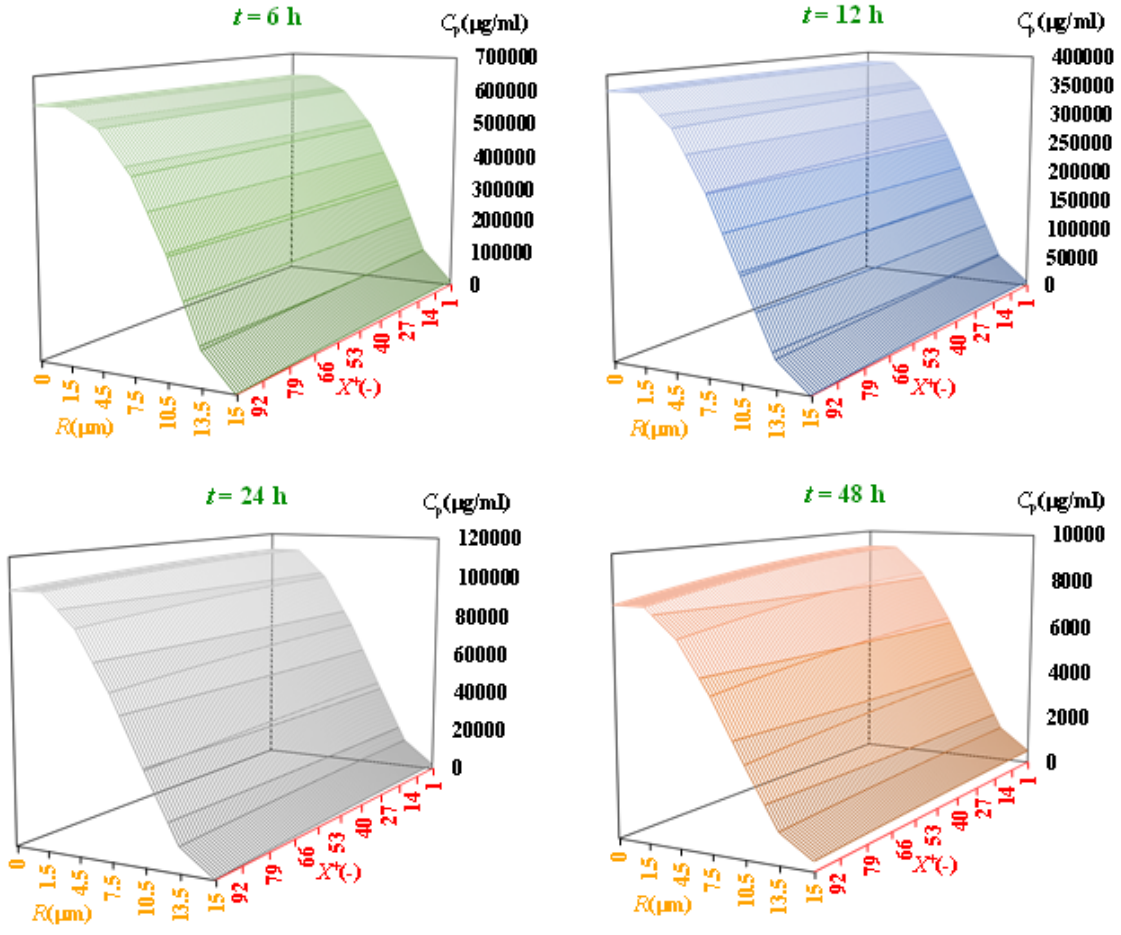

Figure 71. *Vancomycin concentration in different hydrogel positions released from particles at different times.*

It is interesting to note that the shape of the $C_p(R^+, X^+)$ surface is almost invariant with time, showing a sharp vancomycin decrease with R^+ whatever the position (X^+) in the hydrogel. At the same time, the vancomycin concentration profile inside the particles slowly decreases with particles position (X^+) in the hydrogel, whatever the time considered. The real evident effect of the elapsing time is the uniform decrease in the vancomycin concentration profile inside the particles. While after 6 h the vancomycin concentration in $R^+ = 0$ and $X^+ = 0$ is approximately 700 mg/cm^3, and after 48 h, this decreases to 20 mg/cm^3. This behaviour is probably due to the low values of D_p and φ, together with the high initial value of the vancomycin concentration in the particles.

Finally, our model was used to determine the most important parameters that rule the vancomycin release kinetics. Apart from the obvious one (i.e., vancomycin dose), the attention was focused on the PLGA particle radius (R_p) and on the Poloxamer concentration in the gel phase. Assuming the above determined values of the three diffusion coefficients (i.e., D_M, D_G, D_p), Figure 72 shows the large effect that particle radius has on the release kinetics. The R_p increase implies considerable reduction in the release kinetics with respect to the reference case of the R_p value (15 μm); i.e., that considered in this study. On the contrary, the reduction in R_p implies an increased rate of the release process.

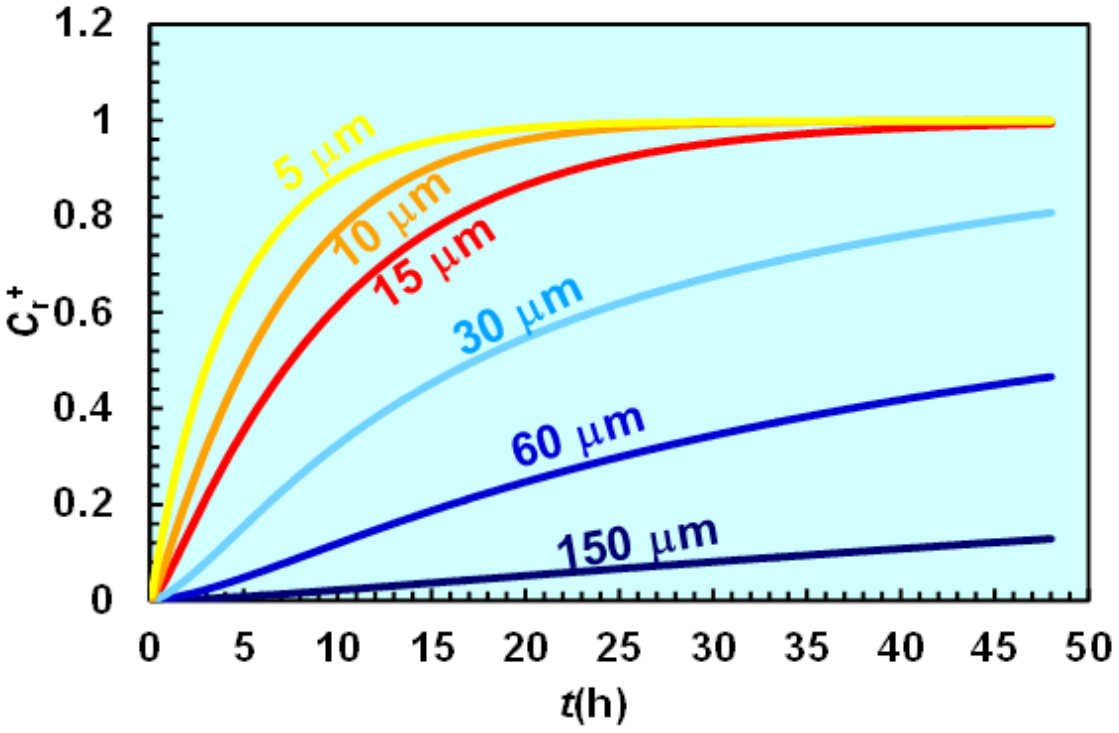

Figure 72. *Effect of the microparticles radius on the release kinetic.*

To simulate the effects of the Poloxamer volume fraction (φ_p) in the hydrogel phase, we needed to establish a relation between this parameter and the vancomycin diffusion coefficient in the hydrogel phase (D_G). For this, the Mackie and Meares [87] equation was considered:

$$D_G = D_0\left(\frac{1-\varphi_p}{1+\varphi_p}\right)^2 \quad (9).$$

Indeed, not only is this equation very simple, but it also provides a good estimation of the D_G measured with our experimental set up ($\varphi_p \approx 0.2$), as shown in Figure 73. The blue curve indicates the D_G trend predicted by Equation (9) for increasing φ_p values, while the open circles indicate the D_G value determined by the model fitting (Equations (1)-(3)) to our experimental data when $\varphi_p \approx 0.2$. For the prediction of Equation (9) to exactly coincident with the experimental D_G value, the exponent of Equation (9), was modified empirically.

This thus verifies that when the exponent is 2.3, the Equation (9) prediction allows perfect coincidence with the experimental D_G values (Figure 73, red line). The dashed lines in Figure 73 simply indicate that for φ_p <0.1, at 37 °C, the aqueous Poloxamer solution cannot form a gel).

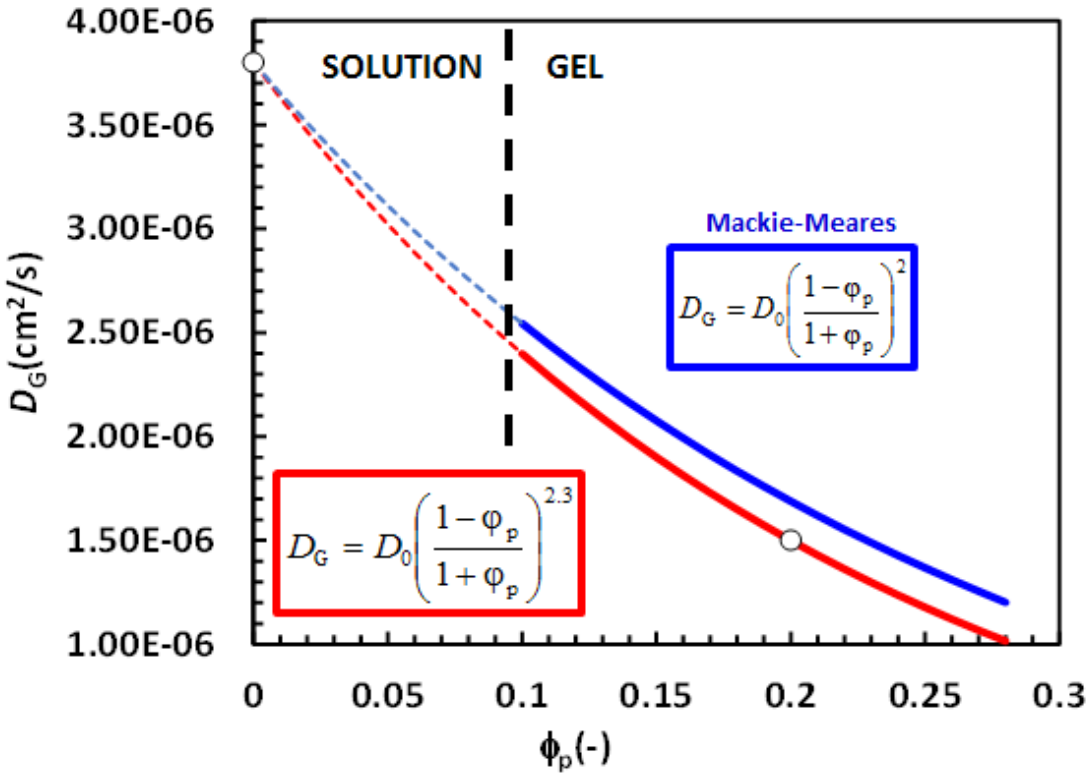

Figure 73. *Mackie and Meares equation in solution and in the hydrogel.*

Assuming this modification of the Mackie and Meares equation, Figure 74 shows the effects of the φ_p variation with respect to the reference case of $\varphi_p \approx 0.2$. It can be seen that despite the considerable φ_p variations (from pure water, $\varphi_p = 0$; to highly concentrated condition of $\varphi_p = 0.25$), the release kinetics are not gratly affected.

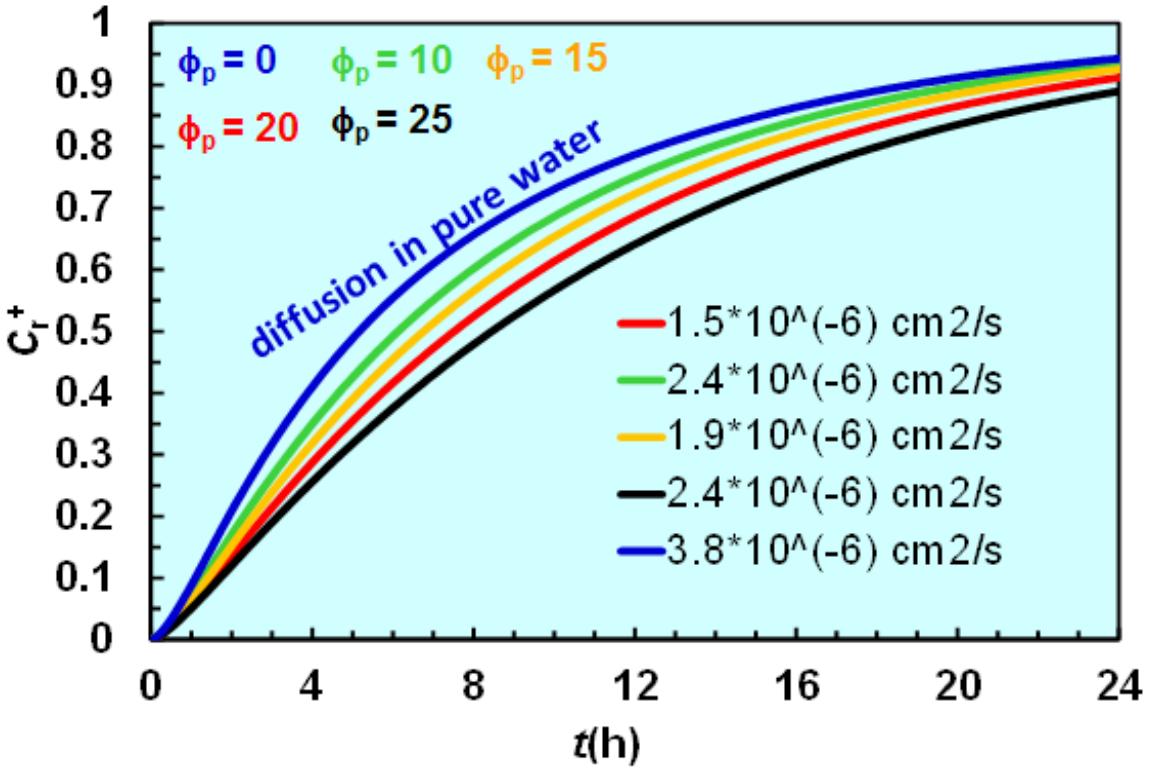

Figure 74. *Model simulation using different volume fractions (φ_p) of the polymer.*

Thus, we can conclude that the role of the gel is mainly to suspend the PLGA particles rather than to control the vancomycin diffusion. On the contrary, the particle radius is the real important parameter for the control of the release kinetics. Accordingly, it can be safely considered as an important parameter for the design and the optimisation of the vancomycin release from this system.

Finally, it is worth noting that the model can be easily implemented without renouncing its simplicity by assuming that the PLGA particle distribution is not uniform in the axial, *X*, direction.

3.8. DEPOSITION TEST

To simulate a 'real life' situation in which the biphasic system might well be used, deposition tests were performed. The parameter that had been taken in consideration was the time needed for the biphasic system to produce suitable applicability on the prosthesis surface, to to avoid its flowing and dropping from the prosthesis. Two sets of experiments were projected and were carried out in triplicate. For both the experiment sets, the starting temperature was 4 °C, as would be the case from storage conditions, while the room temperature was maintained at 21 °C.

In the first set of experiments, the time of gel formation and the prosthesis surface applicability of the deriving hydrogels were tested for 20% (w/w) Poloxamer, in comparison with 18% (w/w) Poloxamer solution. In the second set of experiments, the same Poloxamer concentrations were been tested with the addition of 1% (w/w) microparticles mixed inside the Poloxamer solution. Again it was the time and applicability that were evaluated (Table 10). These two sets of experiments were fundamental to an understanding of the validity of the rheological experiments decribed in the section 3.4.

Table 10. *The gel formation times from 4 °C to 21 °C on the prosthesis surface of the tested systems.*

Poloxamer 407 solution (%, w/w)	**Solution → gel time No microparticles** (First experiments set; min)	**Solution → gel time Microparticles (1% w/w)** (Second experiments set; min)
18	30 ±1	15-30 ±1
20	6 ±0.5	Max 7 ±1

The 18% (w/w) Poloxamer system with the microparticle dispersion was demonstrated not to be suitable, as it continued to flow and drop away from the prosthesis for an average time of 30 min, which is not an acceptable rage of time during a surgical procedure (Figure 75A). On the other hand, the best performance was obtained from the 20% (w/w) Poloxamer system combined with the 1% (w/w) microparticles, as the rheological experiments had suggested. The deposition of the biphasic system on the prosthesis surface was smooth and without any blockage caused by the biphasic system flowing through the dispenser. Passing from the

storage temperature to the room temperature, the system started to change viscoelasticity after a few minutes, a process that escalated to the mature hydrogel formation over a mean time of 7 min. This thus ensured the suitable applicability and permanence of the antibacterial layer formed on the prosthesis surface (Figure 75B-D).

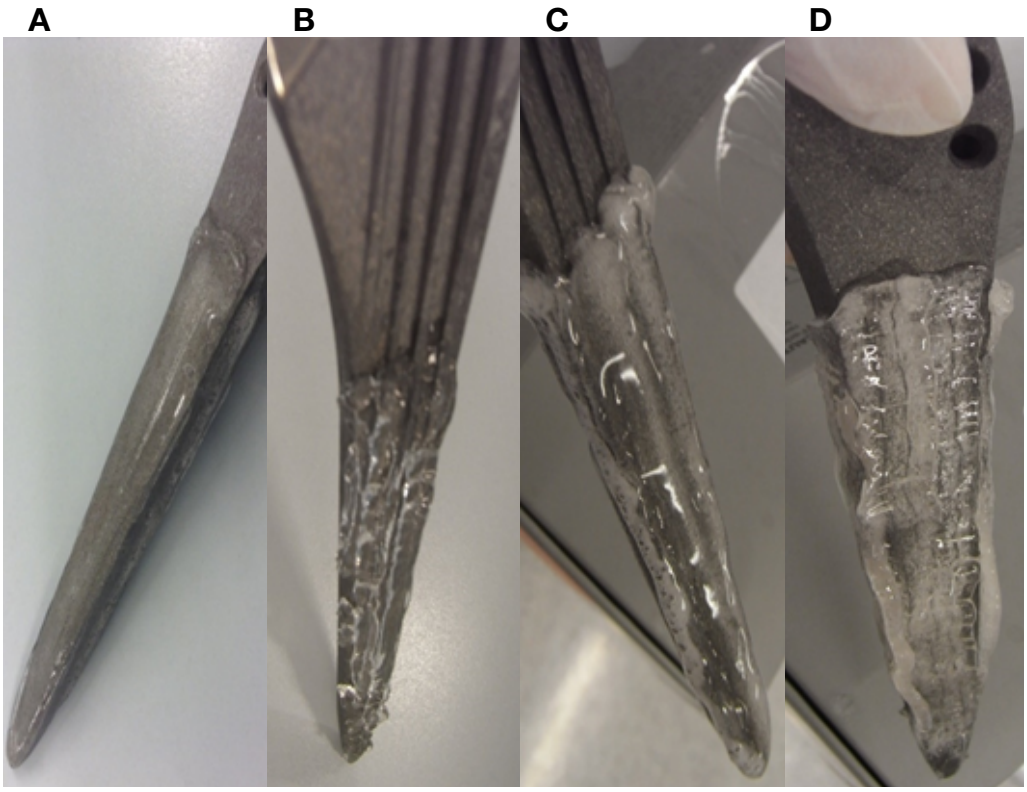

Figure 75. *Deposition after 10 min of the 18% (w/w) Poloxamer alone (A) and with 1% (w/w) microparticles (B), and of the 20% (w/w) Poloxamer alone (C) and with 1% (w/w) microparticles (D).*

CHAPTER 4:
PROJECT CONCLUSIONS

This PhD project was conducted as a collaboration between Lima Corporate, an Orthopaedic company in the Friuli-Venezia-Giulia region, and the University of Trieste, with part of project funded by the Social European Funds (FSE) Committee. The interest of Lima Corporate in the development of this research project was focused on the creation of an antibacterial system that can be used during the surgery itself, to provide improved resistance from infection from the new inserted orthopaedic implant. Moreover, the system was believed to be immediately technologically transferrable to the industry facilities without notable economic investment, and to be rapidly marketable. Thus this project was proposed to quickly become a commercial product.

To the best of our knowledge, local device strategies that provide the release *in situ* of a drug over a certain time would give the best protection for an orthopaedic implant. With this in mind, this research project was developed, oriented on the design, creation, testing and optimisation of an innovative local antibacterial system that was intended to be used to prevent and treat orthopaedic infections.

To design the best performing device, a system needed to be created that could cover a long period (as days, or even weeks) with drug release kinetics that would never go under the MIC of the most common bacteria involved in orthopaedic infections. For this reason, a biphasic system was created, and two different approaches were chosen as the most suitable for the purpose of this *in-situ* use:

1. The external phase: 20% (w/w) Poloxamer hydrogel matrix loaded with vancomycin HCl;

2. The internal phase: Microparticles of PLGA (50:50) loaded with vancomycin HCl.

All of the mechanical and biopharmaceutical tests demonstrated the efficacy of both of these approaches as single phase strategies and in combination as a biphasic system. Indeed, considering the overall microbiological data, the biphasic antibacterial system showed inhibition of the tested bacterial strains. However, due to the limitations of *in-vitro* experiments, to more deeply understand the potentiality of the biphasic system it had to be tested *in vivo*. From a mechanical point of view, the best performance system was the

20% (w/w) Poloxamer hydrogel matrix in addition to the 1% (w/w) microparticles, as the rheological experiments suggested.

For the microparticles system in particular, there were difference seen in terms of particle size and shape between the two different microparticle preparations, as those obtained by spray drying (batches 1-5) and the solvent evaporation (batch 6) technologies. Indeed, with the solvent evaporation, greater mean particle size and higher uniformity of the spherical shapes was noted with respect to the spray-dried microparticle batches.

These differences correlated with the different solvent evaporation rates in the two different production technologies. In the solvent evaporation method of batch 6, the evaporation is slower, so that the formation of the microparticles is more uniform in dimension, shape and surface. Conversely, under the operating conditions of the spray drying technique, and in particular for the dimension of the nozzle and the pressure, these resulted in the reduced mean particle diameter.

For the 20% (w/w) Poloxamer hydrogel matrix systems, the biopharmaceutical tests and mathematical modelling outcomes underlined that its role is mainly to suspend the PLGA microparticles, rather than to control the drug-diffusion process. This is of great importance, especially considering that the drug can be loaded solely in the microparticles as the solid state, giving in this way a more stable formulation. This avoids the presence of the drug in the hydrogel matrix system and thus the issues correlated to the stability in the hydrogel phase, which is itself largely made of water. On the contrary, the particle radius is the real important parameter for the control of the release kinetics. Accordingly, it can be safely considered as the main parameter for the design and the optimisation of drug release from this system.

Finally, it is worth noting that the mathematical model can be easily implemented and used in the industrial technological transfer. This feature is important to produce microparticles with the minimum quantity of the PLGA polymer to provide the desired drug release and to optimise polymer use, and thus the cost.

As another aspect of this project, the chosen Medimix injectable device was demonstrated to be a suitable mechanical method to incorporate and spread the biphasic system onto the orthopedic implant during the surgical procedure.

The future perspectives of this project are primary focused on the *in-vivo* testing[86]. At the time of writing, the *in-vivo* tests are being setting up to define the last steps before activating the industrial-scale pre-production and the regulatory affairs of the system that will permits its placing on the medical market. The *in-vivo* experimentation will involve innovative real-time monitoring and non-invasive methodology based on bioluminescent bacteria, an extremely valuable methodology to understand the potentiality of this antibacterial biphasic system[86].

If the expected results are obtained, the develop steps that following will be those of the pre-industrial scale technological transfer, performed within the Lima Corporate facilities, and the application to the Innovation Task Force meeting at the European Medicines Agency. The Innovation Task Force is dedicated to the regulatory, technical and scientific issues that arise from the development of innovative medicines, new technologies, and borderline products. These meetings are intended to facilitate the informal exchange of information and the provision of guidance in the development processes before the regulatory affairs officially take place.

REFERENCES

1. Harold E, Standring S. Gray's anatomy: the anatomical basis of clinical practice. *Elsevier Churchill Livingstone*, 3;37-38, 2005.
2. Kurtz SM, Lau KE. Future clinical and economic impact of revision total hip and knee arthroplasty. *American Journal of Bone and Joint Surgery*, 89(3);144 -151, 2007.
3. Valente M, Crucil M, Alecci M. Comparison of primary total hip replacements performed with a direct anterior approach versus the standard lateral approach: perioperative findings. *Journal of Orthopaedics and Traumatology*, 12(3);123–129, 2011.
4. Kamil E, Charles G, Helmick MD. Centers for disease control and prevention (CDC), Prevalence of doctor-diagnosed arthritis and arthritis-attributable activity limitation, United States, 2010-2012. *Morbidity and Mortality Weekly Report*, 62(44);869-873, 2013.
5. Kumar V, Abbas AK, Aster JC. Robbins Basic Pathology, 9(1); 760-780, 2013.
6. Bennell K, Hinman R. Exercise as a treatment for osteoarthritis. *Current Opinion in Rheumatology*, 17(5);634-640, 2005.
7. Weiya Z, Adrian J, Doherty M. Efficacy of topical non-steroidal anti-inflammatory drugs in the treatment of osteoarthritis: meta-analysis of randomised controlled trials. *British Medical Journal*, 329(7461);324, 2004.
8. Charles GH. American academy of orthopaedic surgeons, number of inpatient arthroplasty procedures by type, by Sex, United States, 2010/2011, 2013.
9. Mahomed NN, Barrett JA, Katz JN. Rates and outcomes of primary and revision total hip replacement in the United States medicare population. American *Journal of Bone Joint Surgery*, 85-A(1);27–32, 2003.
10. Fitzgerald JD, Orav EJ, Lee TH. Patient quality of life during the 12 months following joint replacement surgery. *Arthritis and Rheumatology,* 51(1);100–109, 2004.
11. Allyson CJ, Beaupre LA, Johnston DWC. Total joint arthroplasties: current concepts of patient outcomes after surgery. *Rheumatic Disease Clinics of North America, 33(1);71–86, 2007.*

12. Ong K, Lau E, Kurtz SM. Projections of primary and revision hip and knee arthroplasty in the United States from 2005 to 2030. *The Journal of Bone and Joint Surgery*, 89(4);780-785, 2007.

13. Callaghan JJ, Albright JC, Goetz DD. Charnley total hip arthroplasty with cement. Minimum twenty-five-year follow-up. *American Journal of Bone and Joint Surgery*, 82(4);487-497, 2000.

14. Bizot P, Nizard R, Hamadouche M. Prevention of wear and osteolysis: alumina-on-alumina bearing. *Clinical Orthopeadic Related Research*, 393; 85-93, 2001.

15. Bierbaum BE, Nairus J, Kuesis D. Ceramic-on-ceramic bearings in total hip arthroplasty. *Clinical Orthopeadic Related Research*, 405; 158-63, 2002.

16. Randeep A, Satya PB, Knight RS. Total hip arthroplasty - over 100 years of operative history. *Orthopedic Reviews*, 3(16); 72-74, 2011.

17. Johnson M, Reindl S. American academy of orthopaedic surgeons – AAOS. Online, 2014.

18. Sinha RK, Shanbhag AS, Maloney WJ, Hasselman CT, Rubash HE. Osteolysis, cause and effect, instructional course lectures. *American Academy of Orthopaedic Surgeons Press*, 47;307-320, 1998.

19. Oliphant CM. Management of orthopedic infections. *The Journal for Nurse Practitioners*, 11(10);1036-1042, 2015.

20. Kurtz SM, Lau E, Schmier J, Ong KL. Infection burden for hip and knee arthroplasty in the United States. *Journal of Arthroplasty,* 23;984–991, 2008.

21. Urquhart DM, Hanna FS, Brennan SL, Wluka AE, Leder K. Incidence and risk factors for deep surgical site infection after primary total hip arthroplasty: a systematic review. *Journal of Arthroplasty*, 25(8);1216-1222, 2009.

22. Del Pozo JL, Patel R. Clinical practice. Infection associated with prosthetic joints. *The New England Journal of Medicine*, 361(8);787–794; 2009.

23. Walls RJ, Roche SJ, O'Rourke A, McCabe JP. Surgical site infection with methicillin-resistant *Staphylococcus aureus* after primary total hip replacement. *British Journal of Bone and Joint Surgery*, 90;292–298, 2008.

24. Spyridon P, Satamatios G, Papadakis A. Biofilm and orthopaedic practice: the world of microbes in a world of implants. *Orthopaedics and Trauma*, 23(3);175-179, 2009.

25. Trampuz A, Andreas FW. Infections associated with orthopedic implants. *Current Opinion in Infection Disease,* 19(4);349-356, 2006.

26. Nathan K, Archer J. *Staphylococcus aureus* biofilms Properties, regulation and roles in human

disease. *Virulence*, 2(5);445-459, 2011.

27. Gottenbos B, Klatter F. Late hematogenous infection of subcutaneous implants in rats. *Journal of Clinical Diagnosis and Research,* 8(5);980–983, 2001.

28. Gristina AG, Naylor P, Myrvik Q. Infections from biomaterials and implants: a race for the surface. *Medical Progress Through Technology*, 14(4);205-224, 1989.

29. Bargiotas K, Wohlrab D, Sewecke JJ, Lavinge G, DeMeo PJ. Arthrodesis of the knee with a long intramedullary nail following the failure of a total knee arthroplasty as the result of infection. Surgical technique. *American Journal of Bone and Joint Surgery*, 88(3);553-558, 2007.

30. Costerton JW, Stewart PS, Greenberg EP. Bacterial biofilms: a common cause of persistent infections. *Science*, 284 (5418);1318–1322, 1999.

31. Donald RM. Biofilms: microbial life on surfaces. *Emerging Infect Disease*, 8(9);881-890, 2002.

32. Pamp SJ, Gjermansen M, Tolker NT. The biofilm matrix a sticky framework. The Biofilm Mode of Life. *Horizon Bioscience*, 4;37–69, 2007.

33. Paraje MG. Antimicrobial resistance in biofilms. *Science against microbial pathogens: communicating current research and technological advances FORMATEX*, 1;736-744, 2011.

34. Chen Y, Busscher HJ, van der Mei HC, Norde W. Statistical analysis of long-and short-range forces involved in bacterial adhesion to substratum surfaces as measured using atomic force microscopy. *Applied Environmental Microbiology,* 77(15);5065-5070, 2011.

35. Chagnot C, Zorgani MA, Astruc T, Desvaux MF. Proteinaceous determinants of surface colonization in bacteria: bacterial adhesion and biofilm formation from a protein secretion perspective. *Microbiology*, 303;1-26, 2013.

36. Stoodley P, Ehrlich GD, Baratz ME, Altman DT, Sotereanos NG. Orthopaedic biofilm infections. *Current Orthopedic Practice*, 22(6);558-563, 2011.

37. Szomolay B, Klapper I, Dockery J, Stewart PS. Adaptive responses to antimicrobial agents in biofilms. *Environmental Microbiology*, 7;1186–1191, 2005.

38. Werner E, Roe F, Bugnicourt A, Franklin MJ, Heydorn A, Molin S. Stratified growth in *Pseudomonas aeruginosa* biofilms. *Applied Environmental Microbiology*, 70(10);6188–6196, 2004.

39. Garvin KL, Konigsberg BS. Infection following total knee arthroplasty: prevention and management. *Instructional Course Lecture*, 61;411–41, 2012.

40. Sia IG, Berbari EF, Karchmer AW. Prosthetic joint infections. *Infection Disease Clinics North America,* 19(4);885–914, 2005.

41. Sendi P, Banderet F, Graber P, Zimmerli W. Clinical comparison between exogenous and haematogenous periprosthetic joint infections caused by *Staphylococcus aureus*. *Clinical Microbiology Infections*, 17(7);1098–100, 2011.

42. Parvizi J, Zmistowski B, Berbari EF, Bauer TW, Springer BD, Della Valle CJ, Garvin KL, Mont MA, Wongworawat MD, Zalavras CG. New definition for periprosthetic joint infection: from the workgroup of the musculoskeletal infection society. *Clinical Orthopedic Related Research*, 469(11);2992–2994, 2011.

43. Bedair H, Ting N, Jacovides C, Saxena A, Moric M, Parvizi J, Della Valle CJ. The mark coventry award. Diagnosis of early postoperative TKA infection using synovial fluid analysis. *Clinical Orthopedic Related Research*, 469(1);34–40, 2011.

44. Tsaras G, Maduka-Ezeh A, Berbari EF. Utility of intraoperative frozen section histopathology in the diagnosis of periprosthetic joint infection: a systematic review and meta-analysis. *American Journal of Bone and Joint Surgery*, 94(18);1700–1711, 2012.

45. Ghanem E, Antoci V, Jr, Pulido L, Joshi A, Hozack W, Parvizi J. The use of receiver operating characteristics analysis in determining erythrocyte sedimentation rate and C-reactive protein levels in diagnosing periprosthetic infection prior to revision total hip arthroplasty. *International Journal of Infects Disease*, 13(6);444–449, 2009.

46. Hayter CL, Koff MF, Potter HG. Magnetic resonance imaging of the postoperative hip. *Journal of Magnetic Resonance Imaging*, 35(5);1013–1025, 2012.

47. Zywiel MG, Stroh DA, Johnson AJ, Marker DR, Mont MA. Gram stains have limited application in the diagnosis of infected total knee arthroplasty. *International Journal of Infectious Disease*, 15(10);702–705, 2011.

48. Kim SA, Yoo SM, Hyun SH, Choi CH, Yang SY, Kim HJ, Jang BC, Suh SI, Lee JC. Global gene expression patterns and induction of innate immune response in human laryngeal epithelial cells in response to *Acinetobacter baumannii* outer membrane protein A. *Immunology and Medical Microbiology*, 54(1);45–52, 2008.

49. Deirmengian C, Kardos K, Kilmartin P, Cameron A, Schiller K, Parvizi J. Diagnosing periprosthetic joint infection: has the era of the biomarker arrived?. *Clinical Orthopaedics and Related Research*, 472(11);3254-3262, 2014.

50. Hartman MB, Fehring TK, Jordan L, Norton HJ. Periprosthetic knee sepsis. The role of irrigation and debridement. Clinical Orthopeadic Related Research, 273;113–118, 1991.

51. Aggarwal VK, Rasouli MR, Parvizi J. Periprosthetic joint infection: Current concept. *Indian Journal of Orthopaedics*, 47(1);10-17, 2013.

52. Kuzyk PR, Dhotar HS, Sternheim A, Gross AE, Safir O, Backstein D. Two-stage revision arthroplasty for management of chronic periprosthetic hip and knee infection: techniques, controversies, and outcomes. *Journal of the American Academy of Orthopaedic Surgeons*, 22(3);153-164, 2014.

53. Fitzgerald SJ, Hanssen AD. Surgical techniques for staged revision of the chronically infected total knee arthroplasty. Surgical Technology International, 21;204–211, 2012.

54. Hofmann AA, Goldberg T, Tanner AM, Kurtin SM. Treatment of infected total knee arthroplasty using an articulating spacer: 2- to 12-year experience. Clinical Orthopeadic Related Research, 430;125–131, 2005.

55. Hanssen AD, Spangehl MJ. Practical applications of antibiotic-loaded bone cement for treatment of infected joint replacements. Clinical Orthopeadic Related Research, 427;79–85. 2004.

56. Leekha S, Terrell CL, Edson RS. General principles of antimicrobial therapy. *Mayo Clinic Proceedings*, 86(2);156-167, 2011.

57. Breier AC, Brandt C, Sohr D, Geffers C, Gastmeier P. Laminar airflow ceiling size: No impact on infection rates following hip and knee prosthesis. Infection Control Hospital Epidemiology, 32(11);1097–1102, 2011.

58. Zhenyu Y, Keeney M, Goodman SB. The future of biologic coatings for orthopaedic implants. *Biomaterials*, 34(13);3174-3183, 2013.

59. Daghighi S, Sjollema J, van der Mei HC, Busscher HJ, Rochford ET. Infection resistance of degradable versus non-degradable biomaterials: an assessment of the potential mechanisms. *Biomaterials*, 34(33);8013-8017, 2013.

60. Rojo L, Barcenilla JM, Vázquez B, González R, San Román J. Intrinsically antibacterial materials based on polymeric derivatives of eugenol for biomedical applications. *Biomacromolecules,* 9(9);2530-2535, 2008.

61. Campoccia D, Montanaro L, Arciola CR. A review of the biomaterials technologies for infection-resistant surfaces. Biomaterials, 34(34);8533–8554, 2013.

62. Gallo J, Holinka M, Moucha CS. Antibacterial surface treatment for orthopaedic implants. *International Journal of Molecular Sciences*, 15(8);13849-13880, 2014.

63. Lemire JA, Harrison JJ, Turner RJ. Antimicrobial activity of metals: mechanisms, molecular targets and applications. *Nature Reviews Microbiology*, 11(6);371-384, 2013.

64. Fielding GA, Roy M, Bandyopadhyay A, Bose S. Antibacterial and biological characteristics of silver containing and strontium doped plasma sprayed hydroxyapatite coatings. *Acta Biomaterials*, 4(3);3144-3152, 2012.

65. Arenas MA, Pérez-Jorge C, Conde A. Doped TiO2 anodic layers of enhanced antibacterial properties. *Colloids and Surface B Biointerfaces*, 65(3);106-112, 2013.

66. Uhm SH, Song DH, Kwon JS, Lee SB, Han JG, Kim KN. Tailoring of antibacterial Ag nanostructures on TiO2 nanotube layers by magnetron sputtering. *Journal of Biomedicine Materials and Research,* 102(3);592-603, 2014.

67. Holinka J, Pilz M, Kubista B, Presterl E, Windhager R. Effects of selenium coating of orthopaedic implant surfaces on bacterial adherence and osteoblastic cell growth. *The* Bone and Joint Journal, 95;678–682, 2013.

68. Fei J, Liu GD, Pan CJ, Chen JY, Zhou YG, Xiao SH, Wang Y, Yu HJ. Preparation, release profiles and antibacterial properties of vancomycin-loaded Ca-P coating titanium alloy plate. *The Journal of Materials Science: Materials in Medicine*, 22;989–995, 2011.

69. Neut D, Dijkstra RJ, Thompson JI, van der Mei HC, Busscher HJ. A gentamicin-releasing coating for cementless hip prostheses-Longitudinal evaluation of efficacy using *in vitro* bio-optical imaging and its wide-spectrum antibacterial efficacy. Journal of Biomedical Material Research*,* 146(1);3220–3226, 2012.

70. Salwiczek M, Qu Y, Gardiner J, Strugnell RA, Lithgow T, McLean KM, Thissen H. Emerging rules for effective antimicrobial coatings. Trends in Biotechnology, 32;82–90, 2013.

71. Gu Y, Zhang W, Wang H, Lee WY. Chitosan surface enhances the mobility, cytoplasm spreading, and phagocytosis of macrophage. Colloids and Surface B Biointerfaces, 117;42–50, 2014.

72. Muszanska AK, Rochford ET, Gruszka A, Bastian AA, Busscher HJ, Norde W, van der Mei HC, Herrmann A. Antiadhesive polymer brush coating functionalized with antimicrobial and rgd peptides to reduce biofilm formation and enhance tissue integration. Biomacromolecules, 15(6);2019–2026, 2014.

73. Gimeno M, Pinczowski P, Pérez M, Luján L. A controlled antibiotic release system to prevent orthopedic-implant associated infections: An in vitro study. *European Journal of Pharmaceutics and Biopharmaceutics,* 96;264–271, 2015.

74. Witsø E, Persen L, Benum P, Bergh K. Release of netilmicin and vancomycin from cancellous bone. *Scandinavian Acta Orthopeadics*, 73(2);199–205, 2002.

75. Junji I, Hiroshi T, Nobuhiro K. Anti-Infectious agents against MRSA . *Molecules*, 18(1);204-24, 2013.

76. Amaral MH, Lobão P, Almeida H. Pluronic® F-127 and Pluronic lecithin organogel: main features and their applications in topical and transdermal administration of drugs, *Journal*

of Pharmacy and Pharmaceutical Sciences, 15(4);592-605, 2012.

77. Vietti B. Solubilizzazione di farmaci di classe II e di classe IV mediante polossameri. Tesi di Dottorato, Universita degli studi di Parma, 2009.

78. Makadia HK, Siegel S. Poly lactic-co-glycolic acid (PLGA) as biodegradable controlled drug delivery carrier. *Polymers,* 3;1377-1397, 2011.

79. Ming L, Rouaud O, Poncelet D. Microencapsulation by solvent evaporation: state of the art for process engineering approaches. *International Journal of Pharmaceutics*, 363(23);26-29, 2008.

80. Mikos AG, Leda Klouda l. Thermoresponsive hydrogels in biomedical applications. *European Journal of Pharmaceutics and Biopharmaceutics*, 68;34-45, 2008.

81. Kim SW, Bae YH, Jeong B. Thermosensitive sol–gel reversible hydrogels. *Advanced Drug Delivery Reviews*, 64;154-62, 2012.

82. López-Cervantes M, Naïk A, Escobar-Chávez JJ. Application of thermo-reversible Pluronic ® F-127 gels in pharmaceutical formutalions. *Journal of Pharmacy and Pharmaceutical Sciences*, 9(3);339-358, 2006.

83. Murphy J. Temperature and humidity control in surgery rooms. *Ashare Journal*, 48;18-24, 2006.

84. Lemieux P, Vinogradov S, Kabanov AV. Pluronic® block copolymers: novel functional molecules for gene therapy. *Advanced Drug Delivery Reviews*, 54;223-233, 2002.

85. Trampuz A, Andreas F. Widmer Infections associated with orthopedic implants. *Current Opinion Infection Disease*, 19(4);349-356, 2006.

86. Pribaz JR, Bernthal NMJ, Miller LS. Mouse model of chronic post-arthroplasty infection: noninvasive *in vivo* bioluminescence imaging to monitor bacterial burden for long-term study. *Orthopedic Research*, 30(3);335-340, 2012.

87. Muhr, AH, Blanshard JMV. Diffusion in gels. *Polymers*, 23;10-12, 1982.

SCIENTIFIC PUBLICATIONS AND CONFERENCE CONTRIBUTIONS

1. Dall'Acqua S, Stocchero M, Boschiero I, Schiavon M, **Golob S**, Uddin J, Voinovich D, Mammi S, Schievano E. New findings on the *in-vivo* antioxidant activity of *Curcuma longa* extract by an integrated ^{1}H-NMR and HPLC-MS metabolomic approach. *Fitoterapia*, 109;125-131, **2015.**

2. Matanović MR, Grabnar PA, Voinovich D, **Golob S**, Mijovski MB, Grabnar I. Development and preclinical pharmacokinetics of a novel subcutaneous thermoresponsive system for prolonged delivery of heparin. *International Journal of Pharmaceutics*, 496(2);583-592, **2015**.

3. Grassi M, **Golob S**, Pontelli F, Abrami M, Chiarappa G, Grassi G, Perissutti B, Voinovich D. Drug release of an antibacterical drug from a biphasic polymeric system: mathematical modeling. 4th World Conference on Physico-Chemical Methods in Drug Discovery and Development. 21-24 September; **2015.**

4. Dall'Acqua S, Perissutti B, Grabnar I, Farra R, Comar M, Agostinis C, Caristi G, **Golob S**, Voinovich D. Pharmacokinetics and immunomodulatory effect of lipophilic *Echinacea* extract formulated in softgel capsules. *European Journal of Pharmaceutics and Biopharmaceutics,* 97(Pt A);8-14, **2015.**

5. Hasa D, Perissutti B, Campisi B, Grassi M, Grabnar I, **Golob S**, Mian M, Voinovich D. Quality improvement of melt extruded laminar systems using mixture design. *European Journal of Pharmaceutical Science,* 75;169-176, **2015.**

6. Hasa D, Grassi M, Perissutti B, **Golob S**, Grabnar I, Voinovich D. Effect of composition on the release from melt extruded laminar systems by application of mixture experimental design. CESPT 2014 Slovenia Portorose 18-20 September; **2014.**

7. Zampieri D, Laurini E, Vio L, **Golob S**, Fermeglia M, Pricl S, Mamolo MG. Synthesis and receptor binding studies of some new arylcarboxamide derivatives as *Sigma*-1 ligands. *Bioorganic and Medicinal Chemistry Letters*, 24(4);1021-1025, **2014.**